JPTM

Stromal Expression of MicroRNA-21 in Advanced Colorectal Cancer Patients with Distant Metastases

Aims & Scope

The Journal of Pathology and Translational Medicine is an open venue for the rapid publication of major achievements in various fields of pathology, cytopathology, and biomedical and translational research. The Journal aims to share new insights into the molecular and cellular mechanisms of human diseases and to report major advances in both experimental and clinical medicine, with a particular emphasis on translational research. The investigations of human cells and tissues using high-dimensional biology techniques such as genomics and proteomics will be given a high priority. Articles on stem cell biology are also welcome. The categories of manuscript include original articles, review and perspective articles, case studies, brief case reports, and letters to the editor.

Subscription Information

To subscribe to this journal, please contact the Korean Society of Pathologists/the Korean Society for Cytopathology. Full text PDF files are also available at the official website (http://jpatholtm.org). *Journal of Pathology and Translational Medicine* is indexed by PubMed, PubMed Central, Scopus, KoreaMed, KoMCI, WRPIM and CrossRef. Circulation number per issue is 700.

CONTENTS

RETRACTION

Instructions for Authors for *Journal of Pathology and Translational Medicine* are available at http://jpatholtm.org/authors/authors.php

■ ORIGINAL ARTICLE ■

Aquaporin 1 Is an Independent Marker of Poor Prognosis in Lung Adenocarcinoma

Sumi Yun[1,2]* · Ping-Li Sun[3]*
Yan Jin[4] · Hyojin Kim[1]
Eunhyang Park[1] · Soo Young Park[1]
Kyuho Lee[1] · Kyoungyul Lee[5]
Jin-Haeng Chung[1]

[1]Department of Pathology, Seoul National University Bundang Hospital, Seongnam; [2]Department of Pathology, Soonchunhyang University Hospital, Seoul, Korea; [3]Department of Pathology, Second Hospital of Jilin University, Changchun; [4]Department of Pathology, Fudan University, Shanghai Cancer Center, Shanghai, China; [5]Department of Pathology, Kangwon National University Hospital, Chuncheon, Korea

Corresponding Author
Jin-Haeng Chung, MD, PhD
Department of Pathology, Seoul National University
Bundang Hospital, 82 Gumi-ro 173beon-gil,
Bundang-gu, Seongnam 13620, Korea
Tel: +82-31-787-7713
Fax: +82-31-787-4012
E-mail: chungjh@snu.ac.kr

*Sumi Yun and Ping-Li Sun contributed equally to this work.

Background: Aquaporin 1 (AQP1) overexpression has been shown to be associated with uncontrolled cell replication, invasion, migration, and tumor metastasis. We aimed to evaluate AQP1 expression in lung adenocarcinomas and to examine its association with clinicopathological features and prognostic significance. We also investigated the association between AQP1 overexpression and epithelial-mesenchymal transition (EMT) markers. **Methods:** We examined AQP1 expression in 505 cases of surgically resected lung adenocarcinomas acquired at the Seoul National University Bundang Hospital from 2003 to 2012. Expression of AQP1 and EMT-related markers, including E-cadherin and vimentin, were analyzed by immunohistochemistry and tissue microarray. **Results:** AQP1 overexpression was associated with several aggressive pathological parameters, including venous invasion, lymphatic invasion, and tumor recurrence. AQP1 overexpression tended to be associated with higher histological grade, advanced pathological stage, and anaplastic lymphoma kinase (*ALK*) translocation; however, these differences were not statistically significant. In addition, AQP1 overexpression positively correlated with loss of E-cadherin expression and acquired expression of vimentin. Lung adenocarcinoma patients with AQP1 overexpression showed shorter progression-free survival (PFS, 46.1 months vs. 56.2 months) compared to patients without AQP1 overexpression. Multivariate analysis confirmed that AQP1 overexpression was significantly associated with shorter PFS (hazard ratio, 1.429; 95% confidence interval, 1.033 to 1.977; p = .031). **Conclusions:** AQP1 overexpression was thereby concluded to be an independent factor of poor prognosis associated with shorter PFS in lung adenocarcinoma. These results suggested that AQP1 overexpression might be considered as a prognostic biomarker of lung adenocarcinoma.

Key Words: Aquaporin 1; Adenocarcinoma; Tissue array analysis; Invasion; Epithelial-mesenchymal transition

Non-small cell lung cancer (NSCLC) is one of the major causes of cancer-related deaths, and the treatment of NSCLC remains challenging. Adenocarcinoma comprises more than half of all NSCLC. Recent research has yielded a better understanding of the carcinogenesis, molecular subtypes, and prognostic factors of NSCLC, and several novel agents targeting oncogenic pathways have been introduced for the clinical treatment of NSCLC. Despite advancements in surgical treatment, selective targeted therapy, and early cancer detection, the relative long-term survival rate of NSCLC is still lower than that of other malignancies.[1-3] Therefore, a better understanding of the mechanism(s) of NSCLC tumor progression is needed, and useful prognostic

biomolecular markers for accurate prediction of the clinical outcome of NSCLC are of great clinical significance.

Aquaproin 1 (AQP1) is a member of the aquaporin family found in cell membranes, and primarily facilitates transcellular water transport. AQP1 is expressed in various tissues such as kidney, choroid plexus, and gall bladder, and has a role in various physiological and pathological processes.[4-6] Recently, several reports have revealed that AQP1 overexpression is associated with uncontrolled cell replication, invasion, migration, and metastasis in tumors.[5,7] In lung cancer, various studies have shown the preferential expression of AQP1 in adenocarcinoma, and an association between AQP1 expression and tumor cell differenti-

ation, invasion, metastasis, and poor prognosis.[8-12] However, the molecular role and mechanism of AQP1 in cancer cell invasion remains unclear.

Epithelial-mesenchymal transition (EMT) is a complex process in which epithelial cells lose cell-cell adhesions and gain migratory properties. EMT has been implicated in many aspects of cancer, such as tumor cell invasion, metastasis, drug resistance, and poor clinical outcome. The mechanism of EMT results from complex signaling pathway crosstalk between tumor cells and the tumor microenvironment. Several studies have shown that alterations in EMT-related markers are observed in lung adenocarcinoma, and these alterations enhanced tumor progression and metastasis.[13-15] Recent results have indicated that AQP1 overexpression is correlated to EMT in both colon and breast cancers,[16-18] but the correlation has not yet been investigated in lung cancer.

In the present study, we analyzed the immunohistochemical expression of AQP1 in a large series of lung adenocarcinoma specimens, and evaluated the frequency and pattern of AQP1 expression along with its association with clinicopathological factors, molecular subtypes, and patient outcome. In addition, we explored the correlation between AQP1 overexpression and alteration of the EMT-related markers E-cadherin and vimentin.

MATERIALS AND METHODS

Tissue samples and classification

Tumor samples were collected from 505 consecutive lung adenocarcinoma patients who underwent curative surgical resection at Seoul National University Bundang Hospital between May 2003 and December 2012. Clinicopathological information and follow-up data were obtained by reviewing the medical and the pathological records of the enrolled patients. Smoking history was defined as smokers who have smoked 100 cigarettes, and never-smokers who have never smoked or smoked less than 100 cigarettes in their life time. Two pathologists (S.Y. and J.-H. C) independently reviewed the hematoxylin and eosin stained slides and classified the diagnosis according to the International Association for the Study of Lung Cancer/American Thoracic Society/European Respiratory Society (IASLC/ATS/ERS) criteria and the 2015 World Health Organization (WHO) classification system.[19,20] Histological grade was based on the predominant histological subtypes as follows: grade 1, lepidic; grade 2, acinar and papillary; and grade 3, solid and micropapillary. Tumors were staged according to the American Joint Committee on Cancer, seventh staging system. Progression-free survival (PFS)

was measured from the date of surgery until disease progression or death. Overall survival (OS) was measured from the date of surgery to the time of death or last follow-up visit. The Institutional Review Board of the Seoul National University Bundang Hospital approved this study.

Tissue microarray

The most representative areas were obtained for each tumor sample and arranged for tissue microarray (TMA). Tissue cores with a diameter of 2 mm were embedded within TMA blocks, which were sectioned into series of 4-μm-thick slices and then stained with hematoxylin and eosin; immunohistochemical labeling was then performed.

Immunohistochemical staining and assessment

Immunohistochemistry for AQP1, E-cadherin, and vimentin were performed according to the antibody manufacturer's instructions. The following antibodies were used: AQP1 (B-11, 1:100, Santa Cruz Biotechnology, Santa Cruz, CA, USA), E-cadherin (SPM471, 1:150, Thermo Fisher Scientific, Carlsbad, CA, USA), and vimentin (1:100, 4A4, Zeta Corporation, Arcadia, CA, USA). AQP1 showed both apicolateral staining and complete circumferential membranous staining (Fig. 1). AQP1 overexpression was defined when ≥25% showed membranous staining with loss of polarization, as previously reported.[21] Immunohistochemical stains of E-cadherin and vimentin were scored using a semi-quantitative evaluation for each case. The intensity of staining was scored on a four-point scale as follows: 0, no staining; 1, weak staining; 2, moderate staining; and 3, strong staining. The score was based on the fraction of positive cells (1%–100%). The final score was calculated by multiplying the intensity score to the fraction score, generating a total range of 0–300. Scores of 0–100 and 101–300 were considered as negative and positive, respectively, as previously reported.[22]

Molecular characteristics

Translocation of anaplastic large cell lymphoma kinase (*ALK*) was evaluated in 440 cases by fluorescence *in situ* hybridization analysis using a probe to *ALK* (Vysis LSI ALK dual color, break-apart rearrangement probe, Abbott Molecular, Des Plaines, IL, USA); translocation was observed in 28 out of 440 cases (6.4%). Epidermal growth factor receptor (*EGFR*) mutations of exon 18 to 21 and *KRAS* mutations of codon 12 and 13 were evaluated in 484 and 413 cases using polymerase chain reaction and direct DNA sequencing, as previously described.[23] *EGFR* and *KRAS* mutations were identified in 49.0% (237/484) and 6.1%
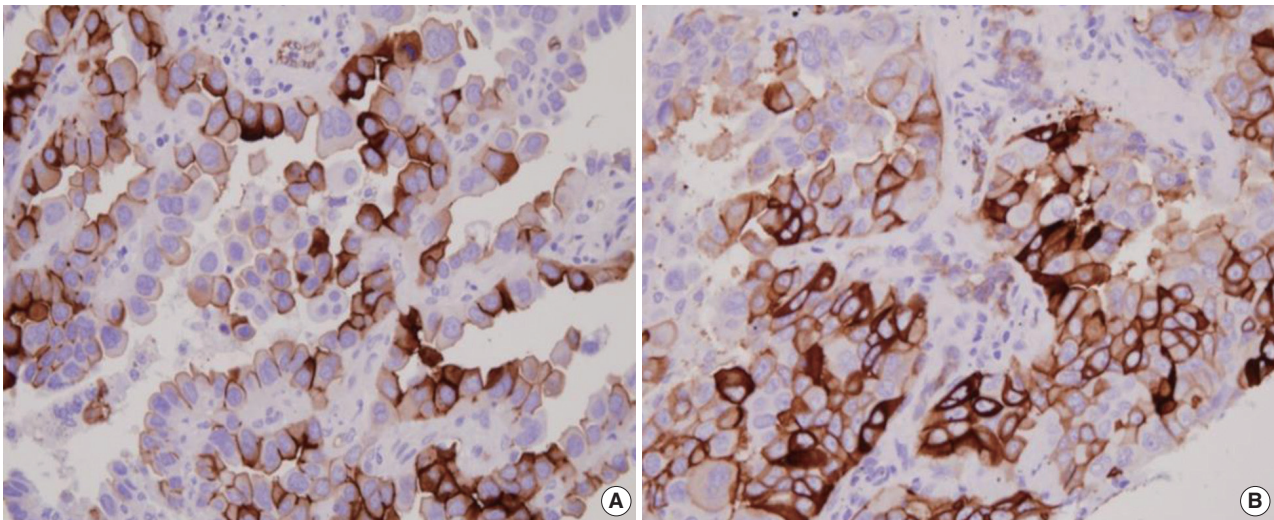
Fig. 1. Immunohistochemical expression of aquaporin 1 in lung adenocarcinomas. (A) Apicolateral pattern. (B) Circumferential membranous staining.

(25/413) of cases, respectively.

Statistical analysis

All statistical analyses were performed using SPSS ver. 18.0 (SPSS Inc., Chicago, IL, USA). The association between immunohistochemistry results and clinicopathological variables was assessed by chi-square test, Fisher exact test, or Spearman's rank correlation test. Kaplan-Meier analysis with log-rank test and multivariate cox regression analysis were performed for survival analysis. Statistical significance was defined as $p < .05$.

RESULTS

Clinicopathological characteristics

The clinicopathological characteristics of patients are summarized in Table 1. The tumor specimens in this study were from 505 lung adenocarcinoma patients, consisting of 247 male (48.9%) and 258 female (51.1%) patients. The mean age of patients was 62.9 years (range, 21 to 83 years), with 302 nonsmokers (59.8%) and 203 smokers (40.2%). With respect to tumor pathology, 274 samples (54.3%) were pathologic stage I, 93 (18.4%) were stage II, 109 (21.6%) were stage III, and 29 (5.7%) were stage IV. According to the new IASLC/ATS/ERS adenocarcinoma classification and the 2015 WHO classification, 298 (59.0%) were acinar, 83 (16.4%) were papillary, 73 (14.5%) were solid, 33 (6.5%) were lepidic, 8 (1.6%) were micropapillary, and 10 (2.0%) were invasive mucinous subtypes. Venous invasion, lymphatic invasion, and perineural invasion were observed in 25.7% (130/505), 50.1% (253/505), and 7.1%

(36/505) of samples, respectively.

AQP1 protein expression by immunohistochemistry

AQP1 expression was observed in the vascular endothelial cells and the apicolateral surfaces of hyperplastic type II pneumocytes around tumors. AQP1 was also detected in myoepithelial cells of bronchial glands and red blood cells (data not shown).

Association of AQP1 overexpression with clinicopathological features

AQP1 overexpression (Fig. 1) was detected in 20.8% of adenocarcinoma cases (105/505). Table 1 shows the association of AQP1 overexpression with clinicopathological variables. There was a significant association of AQP1 overexpression with venous invasion ($p = .035$) and lymphatic invasion ($p = .039$). The recurrence rate of patients with AQP1 overexpression was significantly higher than that of patients without AQP1 overexpression ($p = .029$). AQP1 overexpression was not associated with higher histological grade ($p = .097$), pleural invasion ($p = .131$), and other clinicopathological variables or molecular characteristics, such as *EGFR* and *KRAS* mutation and *ALK* rearrangement.

Association between AQP1 overexpression and EMT-related marker expression

In total, immunohistochemical analyses of E-cadherin and vimentin were performed for 479 and 471 cases, respectively. Loss of E-cadherin expression was observed in 201 of 479 cases (42.0%), and expression of vimentin was observed in 192 of 471 cases (40.8%). We compared the association of AQP1 over-

Table 1. Clinicopathological characteristics of AQP1 overexpression in 505 lung adenocarcinoma patients

Variable	Total	AQP1 overexpression		
		Negative	Positive	p-value
Sex				.938
Male	247	196 (79.4)	51 (20.6)	
Female	258	204 (79.1)	54 (20.9)	
Age (yr)				.092
≤60	181	136 (75.1)	45 (24.9)	
>60	324	264 (81.5)	60 (18.5)	
Smoking history				.347
Non-smoker	302	235 (77.8)	67 (22.2)	
Smoker	203	165 (81.3)	38 (18.7)	
Tumor size (cm)				.145
≤3	276	212 (76.8)	64 (23.2)	
>3	229	188 (82.1)	41 (17.9)	
Histological grade				.097
G1	34	30 (88.2)	4 (11.8)	
G2	390	312 (80.0)	78 (20.0)	
G3	81	58 (71.6)	23 (28.4)	
Acinar predominant				.368
No	207	168 (81.2)	39 (18.8)	
Yes	298	232 (77.9)	66 (22.1)	
Papillary predominant				.120
No	422	339 (78.0)	93 (22.0)	
Yes	83	71 (85.5)	12 (14.5)	
Lepidic predominant				.087
No	472	370 (78.4)	102 (21.6)	
Yes	33	30 (90.9)	3 (9.1)	
Solid predominant				.233
No	432	346 (80.1)	86 (19.9)	
Yes	73	54 (74.0)	19 (26.0)	
Others[a]				.552
No	487	387 (79.5)	100 (20.5)	
Yes	18	13 (72.2)	5 (27.8)	
Pleural invasion				.131
Absent	283	231 (81.6)	52 (18.4)	
Present	222	169 (76.1)	53 (23.9)	
Venous invasion				.035[b]
Absent	377	307 (81.4)	70 (18.6)	
Present	130	93 (72.7)	35 (27.3)	
Lymphatic invasion				.039[b]
Absent	252	209 (82.9)	43 (17.1)	
Present	253	193 (75.5)	62 (24.5)	
Perineural invasion				.290
Absent	469	369 (78.7)	100 (21.2)	
Present	36	31 (86.1)	5 (13.9)	
pTNM stage				.072
I–II	367	298 (81.2)	69 (18.8)	
III–IV	138	102 (73.9)	36 (26.1)	
Recurrence				.029[b]
No	311	256 (82.3)	55 (17.7)	
Yes	194	144 (74.2)	50 (25.8)	
Death				.130
No	415	334 (80.5)	81 (19.5)	

(continued)

Variable	Total	AQP1 overexpression		
		Negative	Positive	p-value
Yes	90	66 (73.3)	24 (26.7)	
EGFR mutation (n=484)				.583
Wild type	247	193 (78.1)	54 (21.9)	
Mutant type	237	190 (80.2)	47 (19.8)	
KRAS mutation (n=413)				.326
Wild type	388	311 (80.2)	77 (19.8)	
Mutant type	25	18 (72.0)	7 (28.0)	
ALK translocation (n=440)				.089
Wild type	412	334 (81.1)	79 (18.9)	
Mutant type	28	19 (67.9)	9 (32.1)	

Values are presented as number (%).
AQP1, aquaporin 1; EGFR, epidermal growth factor receptor; ALK, anaplastic lymphoma kinase.
[a]Invasive mucinous and micropapillary subtype; [b]Statistically significant value.

expression to expression of E-cadherin or vimentin (Table 2) and found that AQP1 overexpression was correlated with loss of E-cadherin expression (p = .011) and expression of vimentin (p < .001).

Survival analysis according to AQP1 overexpression

At the time of analysis, the median PFS was 31.0 months (range, 1 to 84 months) and the median OS was 39 months (range, 1 to 84 months). During this time, 194 patients (38.4%) suffered tumor recurrence and 90 patients (17.8%) died from cancer. Survival analysis using Kaplan-Meier and Cox proportional hazards analyses were performed to evaluate the prognostic impact of AQP1 overexpression. As shown in Fig. 2, Kaplan-Meier revealed that PFS of patients with AQP1 overexpression was significantly shorter than that of the patients without AQP1 overexpression group (p = .018). However, AQP1 overexpression had no prognostic impact on OS (p = .234). Univariate analysis indicated that larger tumor size (p < .001), higher histological grade (p = .032), pleural invasion (p < .001), venous invasion (p < .001), lymphatic invasion (p < .001), perineural invasion (p = .043), pTNM stage (p < .001), and AQP1 overexpression (46.1 months vs. 56.2 months, p = .020) were associated with shorter PFS (Fig. 2A). Multivariate cox regression analysis demonstrated AQP1 overexpression to be an independent factor indicating poor prognosis with regard to PFS in patients with lung adenocarcinoma (hazard ratio [HR], 1.429; 95% confidence interval [CI], 1.033 to 1.977; p = .031). Larger tumor size (HR, 1.797; 95% CI, 1.336 to 2.418; p < .001), pleural invasion (HR, 1.372; 95% CI, 1.007 to 1.871; p = .045), lymphatic invasion (HR, 1.547; 95% CI, 1.113 to 2.151; p = .009), and pTNM stage (HR, 2.179; 95% CI, 1.586 to 2.995; p < .001) were also independent prognostic

Table 2. Correlation between AQP1 overexpression and EMT-related proteins

Variable	Total	AQP1 overexpression		
		Negative	Positive	p-value
E-Cadherin expression (n = 479)				.011[a]
Decreased	201	147 (73.1)	54 (26.9)	
Preserved	278	230 (82.7)	48 (17.3)	
Vimentin expression (n = 471)				< .001[a]
Negative	279	238 (85.3)	41 (14.7)	
Positive	192	133 (69.3)	59 (30.7)	

Values are presented as number (%).
AQP1, aquaporin 1; EMT, epithelial-mesenchymal transition.
[a]Statistically significant value.
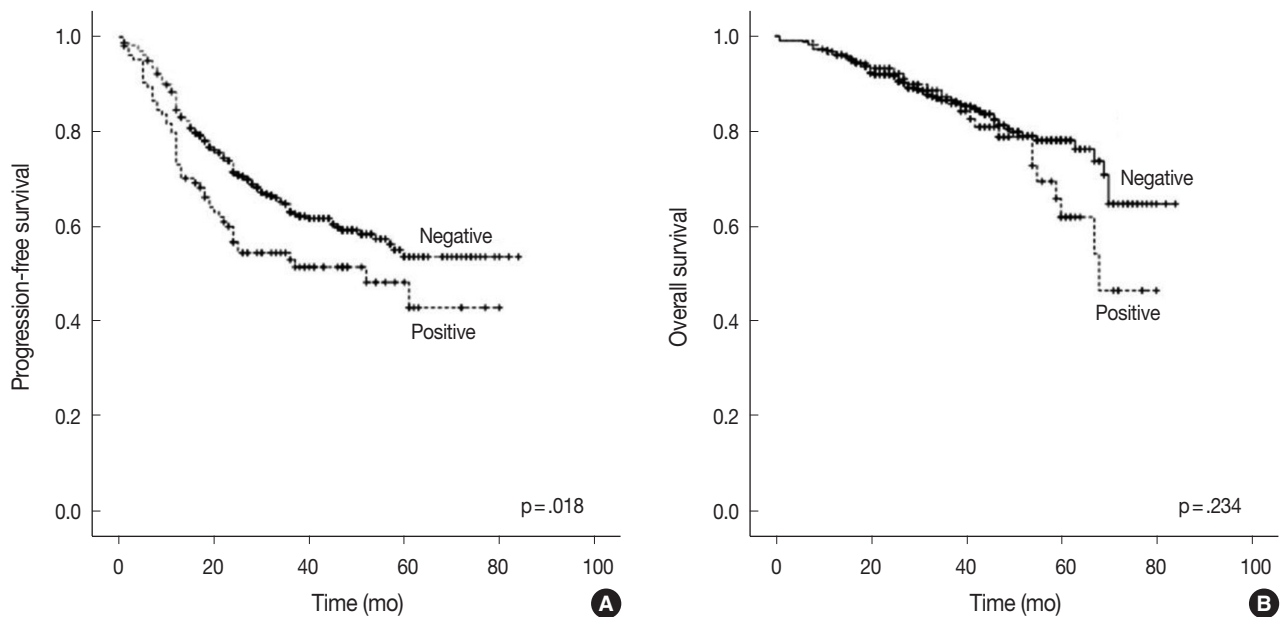
Fig. 2. Kaplan-Meier survival estimate graphs of progression-free survival (A) and overall survival (B) according to the overexpression of aquaporin 1 in lung adenocarcinoma patients.

factors associated with shorter PFS in lung adenocarcinoma. For OS, larger tumor size (p < .001), higher histological grade (p = .021), pleural invasion (p < .001), venous invasion (p < .001), lymphatic invasion (p < .001), perineural invasion (p = .001), vimentin expression (p = .045), and pTNM stage (p < .001) reached statistical significance by univariate analysis. AQP1 overexpression was not associated with OS (63.2 months vs. 70.1 months, p = .237). In multivariate analysis, larger tumor size (HR, 1.775; 95% CI, 1.137 to 2.771; p = .012), venous invasion (HR, 2.129; 95% CI, 1.352 to 3.354; p = .001), and pTNM stage (HR, 4.789; 95% CI, 3.026 to 7.578; p < .001) were statistically significant.

DISCUSSION

In the present study, we assessed the expression of AQP1 in

505 lung adenocarcinomas and evaluated the relationship between AQP1 overexpression and various clinicopathological factors and molecular characteristics, as well as the expression of EMT-related markers. Our study showed that AQP1 overexpression significantly correlated with several aggressive pathological factors and can be used as an independent prognostic factor for PFS in lung adenocarcinoma.

AQP1 is a plasma membrane channel involved in transepithelial water transport.[5,7] Recently, the functional roles of AQP1 protein expression have been studied in various cancers. Previous studies have demonstrated that AQP1 is upregulated in several cancer tissues *in vitro* and *in vivo*, and AQP1 overexpression is associated with poor prognosis.[11,13,16,17,24] Hoque *et al*.[8] reported that upregulated AQP1 in lung cancer may play a role in cancer cell proliferation by resisting apoptosis. Machida *et al*.[10]

showed that AQP1 overexpression with a loss of polarization is associated with invasive growth and poor prognosis in lung adenocarcinomas. Consistent with previous observations, our study showed that AQP1 overexpression tended to be more frequently observed in the high grade histological subtypes of adenocarcinomas although it was not statistically significant.

We also analyzed the association of AQP1 overexpression with EMT-related markers (E-cadherin and vimentin). The loss of E-cadherin and increased expression of vimentin, both hallmarks of a mesenchymal phenotype, were frequently observed in tumors with AQP1 overexpression. We hypothesized that AQP1 may participate in tumor progression through EMT (loss of E-cadherin and vimentin expression) in lung adenocarcinoma. EMT is implicated in tumor progression, invasion, metastasis, and poor prognosis in lung cancer.[6,13,25] Recently, several reports have suggested that AQP1 overexpression is associated with cancer cell invasion. AQP1 has been suggested to function as a linker molecule to promote EMT, or to stabilize the cytoskeletal complex.[8,10,26,27] Similar results were reported in various cancers including colorectal cancer, breast cancer, and brain tumors,[13,17,28] which is in line with our results. The exact biological and functional mechanism of AQP1 to promote EMT needed to be clarifiied by further studies. Of note, some studies demonstrated that tumor tissue showed intratumoral heterogeneity of AQP1 expression in brain tumor.[24,29] Thus, it is necessary to clarify the intratumoral heterogenous distribution of AQP1 overexpression in cancer and its clinical significance.

In conclusion, we demonstrated that overexpression of AQP1 was significantly associated with venous invasion, lymphatic invasion, higher pathological stage, and cancer recurrence in lung adenocarcinomas. AQP1 was also deemed an independent marker of poor prognosis with regard to PFS. In particular, increased expression of AQP1 protein was associated with the expression of vimentin and loss of E-cadherin expression, suggesting that AQP1 overexpression may be involved in tumor cell invasion through facilitating EMT.

Conflicts of Interest

No potential conflict of interest relevant to this article was reported.

REFERENCES

1. Kim JE, Kim H, Choe JY, Sun P, Jheon S, Chung JH. High expression of Sonic hedgehog signaling proteins is related to the favorable outcome, *EGFR* mutation, and lepidic predominant subtype in primary lung adenocarcinoma. Ann Surg Oncol 2013; 20 Suppl 3: S570-6.

2. Seo AN, Yang JM, Kim H, *et al*. Clinicopathologic and prognostic significance of c-MYC copy number gain in lung adenocarcinomas. Br J Cancer 2014; 110: 2688-99.

3. Pao W, Girard N. New driver mutations in non-small-cell lung cancer. Lancet Oncol 2011; 12: 175-80.

4. Cuddapah VA, Sontheimer H. Ion channels and transporters [corrected] in cancer. 2. Ion channels and the control of cancer cell migration. Am J Physiol Cell Physiol 2011; 301: C541-9.

5. Verkman AS. More than just water channels: unexpected cellular roles of aquaporins. J Cell Sci 2005; 118(Pt 15): 3225-32.

6. Wang J, Feng L, Zhu Z, *et al*. Aquaporins as diagnostic and therapeutic targets in cancer: how far we are? J Transl Med 2015; 13: 96.

7. Nico B, Ribatti D. Aquaporins in tumor growth and angiogenesis. Cancer Lett 2010; 294: 135-8.

8. Hoque MO, Soria JC, Woo J, *et al*. Aquaporin 1 is overexpressed in lung cancer and stimulates NIH-3T3 cell proliferation and anchorage-independent growth. Am J Pathol 2006; 168: 1345-53.

9. López-Campos JL, Sánchez Silva R, Gómez Izquierdo L, *et al*. Overexpression of aquaporin-1 in lung adenocarcinomas and pleural mesotheliomas. Histol Histopathol 2011; 26: 451-9.

10. Machida Y, Ueda Y, Shimasaki M, *et al*. Relationship of aquaporin 1, 3, and 5 expression in lung cancer cells to cellular differentiation, invasive growth, and metastasis potential. Hum Pathol 2011; 42: 669-78.

11. Xie Y, Wen X, Jiang Z, Fu HQ, Han H, Dai L. Aquaporin 1 and aquaporin 4 are involved in invasion of lung cancer cells. Clin Lab 2012; 58: 75-80.

12. Wei X, Dong J. Aquaporin 1 promotes the proliferation and migration of lung cancer cell *in vitro*. Oncol Rep 2015; 34: 1440-8.

13. Sato M, Shames DS, Hasegawa Y. Emerging evidence of epithelial-to-mesenchymal transition in lung carcinogenesis. Respirology 2012; 17: 1048-59.

14. Kase S, Sugio K, Yamazaki K, Okamoto T, Yano T, Sugimachi K. Expression of E-cadherin and beta-catenin in human non-small cell lung cancer and the clinical significance. Clin Cancer Res 2000; 6: 4789-96.

15. Shi Y, Wu H, Zhang M, Ding L, Meng F, Fan X. Expression of the epithelial-mesenchymal transition-related proteins and their clinical significance in lung adenocarcinoma. Diagn Pathol 2013; 8: 89.

16. Yoshida T, Hojo S, Sekine S, et al. Expression of aquaporin-1 is a poor prognostic factor for stage II and III colon cancer. Mol Clin Oncol 2013; 1: 953-8.

17. Jiang Y. Aquaporin-1 activity of plasma membrane affects HT20 colon cancer cell migration. IUBMB Life 2009; 61: 1001-9.

18. Yin T, Yu S, Xiao L, Zhang J, Liu C, Lu Y. Correlation between the expression of aquaporin 1 and hypoxia-inducible factor 1 in breast cancer tissues. J Huazhong Univ Sci Technolog Med Sci 2008; 28: 346-8.

19. Travis WD, Brambilla E, Noguchi M, et al. International Association for the Study of Lung Cancer/American Thoracic Society/European Respiratory Society international multidisciplinary classification of lung adenocarcinoma. J Thorac Oncol 2011; 6: 244-85.

20. Travis WD, Brambilla E, Burke AP, Marx A, Nicholson AG. WHO classification of tumours of the lung, pleura, thymus and heart. Lyon: IARC Press, 2015.

21. Li XQ, Yang XL, Zhang G, et al. Nuclear beta-catenin accumulation is associated with increased expression of Nanog protein and predicts poor prognosis of non-small cell lung cancer. J Transl Med 2013; 11: 114.

22. Kim H, Yoo SB, Sun P, et al. Alteration of the E-cadherin/beta-catenin complex is an independent poor prognostic factor in lung adenocarcinoma. Korean J Pathol 2013; 47: 44-51.

23. Chung JH, Choe G, Jheon S, et al. Epidermal growth factor receptor mutation and pathologic-radiologic correlation between multiple lung nodules with ground-glass opacity differentiates multicentric origin from intrapulmonary spread. J Thorac Oncol 2009; 4: 1490-5.

24. Deb P, Pal S, Dutta V, Boruah D, Chandran VM, Bhatoe HS. Correlation of expression pattern of aquaporin-1 in primary central nervous system tumors with tumor type, grade, proliferation, microvessel density, contrast-enhancement and perilesional edema. J Cancer Res Ther 2012; 8: 571-7.

25. Bartis D, Mise N, Mahida RY, Eickelberg O, Thickett DR. Epithelial-mesenchymal transition in lung development and disease: does it exist and is it important? Thorax 2014; 69: 760-5.

26. Monzani E, Bazzotti R, Perego C, La Porta CA. AQP1 is not only a water channel: it contributes to cell migration through Lin7/beta-catenin. PLoS One 2009; 4: e6167.

27. Hu J, Verkman AS. Increased migration and metastatic potential of tumor cells expressing aquaporin water channels. FASEB J 2006; 20: 1892-4.

28. Johnson MD, O'Connell M. Na-K-2Cl cotransporter and aquaporin 1 in arachnoid granulations, meningiomas, and meningiomas invading dura. Hum Pathol 2013; 44: 1118-24.

29. Oshio K, Binder DK, Liang Y, et al. Expression of the aquaporin-1 water channel in human glial tumors. Neurosurgery 2005; 56: 375-81.

■ ORIGINAL ARTICLE ■

Transformation to Small Cell Lung Cancer of Pulmonary Adenocarcinoma: Clinicopathologic Analysis of Six Cases

Soomin Ahn[1] · Soo Hyun Hwang[1]
Joungho Han[1] · Yoon-La Choi[1]
Se-Hoon Lee[2] · Jin Seok Ahn[2]
Keunchil Park[2] · Myung-Ju Ahn[2]
Woong-Yang Park[3,4]

[1]Department of Pathology and Translational Genomics, [2]Division of Hematology and Oncology, Department of Medicine, [3]Department of Molecular Cell Biology, Samsung Medical Center, Sungkyunkwan University School of Medicine, Seoul; [4]Samsung Genomic Institute, Samsung Medical Center, Seoul, Korea

Corresponding Author
Joungho Han, MD
Department of Pathology and Translational Genomics, Samsung Medical Center, Sungkyunkwan University School of Medicine, 81 Irwon-ro, Gangnam-gu, Seoul 06351, Korea
Tel: +82-2-3410-2765
Fax: +82-2-3410-0025
E-mail: hanjho@skku.edu

Background: Epidermal growth factor receptor (EGFR) tyrosine kinase inhibitors (TKIs) are considered the first line treatment for a subset of *EGFR*-mutated non-small cell lung cancer (NSCLC) patients. Although transformation to small cell lung cancer (SCLC) is one of the known mechanisms of resistance to EGFR TKIs, it is not certain whether transformation to SCLC is exclusively found as a mechanism of TKI resistance in *EGFR*-mutant tumors. **Methods:** We identified six patients with primary lung adenocarcinoma that showed transformation to SCLC on second biopsy (n = 401) during a 6-year period. Clinicopathologic information was analyzed and *EGFR* mutation results were compared between initial and second biopsy samples. **Results:** Six patients showed transformation from adenocarcinoma to SCLC, of which four were pure SCLCs and two were combined adenocarcinoma and SCLCs. Clinically, four cases were *EGFR*-mutant tumors from non-smoking females who underwent TKI treatment, and the *EGFR* mutation was retained in the transformed SCLC tumors. The remaining two adenocarcinomas were *EGFR* wild-type, and one of these patients received EGFR TKI treatment. **Conclusions:** NSCLC can acquire a neuroendocrine phenotype with or without EGFR TKI treatment.

Key Words: Lung neoplasms; Receptor, epidermal growth factor; Tyrosine kinase inhibitor; Small cell lung carcinoma; Adenocarcinoma

Currently, lung cancer is classified into two broad histological subgroups: non-small-cell lung cancer (NSCLC) and small cell lung cancer (SCLC). The distinction between these two categories is important because the treatment options differ substantially. There are different chemotherapeutic regimens for SCLC and NSCLC, and the initial response to chemotherapy is much greater for patients with SCLC than for those with NSCLC.[1,2] Currently, epidermal growth factor receptor (EGFR) tyrosine kinase inhibitors (TKIs) are considered the first-line treatment for a subset of *EGFR*-mutated NSCLC patients.[3] In many cases, however, acquired resistance emerges within a year.[4] Although the secondary T790M mutation has been well-described and reported in up to 60% of resistant samples,[5] there have been several studies proposing histological transformation from

NSCLC to SCLC as another mechanism of EGFR TKI resistance.[2,5-12] The possible explanation of this phenomenon can be the transformation of NSCLC, mostly adenocarcinoma (ADC), to high-grade neuroendocrine phenotype.[2] The other possibility can be the presence of combined histology of NSCLC and SCLC in initial samples and acquisition of different histological areas in second biopsy samples.[2] The reports showed that every transformed SCLC tumor sample retained its original *EGFR*-activating mutation,[6-11] supporting the idea that these were not independent second-primary cancers.[2] In addition, many patients with transformed SCLC tumors were female non-smokers,[6-11] which is different from the typical SCLC patient demographic.

The recent reports of transformation from NSCLC to SCLC evoke questions regarding the origin of SCLC and clinical ques-

tions. The rate of transformation to SCLC in TKI resistant tumors varied according to the study.[5,6,10] Furthermore, it is not certain whether transformation to SCLC is exclusively found as a mechanism of TKI resistance in *EGFR*-mutant tumors. Practical questions include whether repeat biopsy is indicated after EGFR TKI resistance develops following treatment initiation, especially since a good response after switching to a SCLC chemotherapy regimen in transformed SCLC tumors has been reported.[12]

Here, we report six cases of SCLC transformed from pulmonary ADC in a single institute during a 6-year period.

MATERIALS AND METHODS

Cases

During a 6-year period (2010–2015), there were a total of 2,310 diagnoses of pulmonary ADC in our institute. Of 2,310 patients, 401 patients underwent a second biopsy or resection for recurrent or metastatic tumors. Out of 401 patients, a total of six patients (1.5%) with primary lung ADC showed transformed SCLC morphology in second biopsy. Two experienced pathologists reviewed the histological slides (S.A and J.H). All patients were treated in the Department of Oncology, Samsung Medical Center (Seoul, Korea). Clinical and follow-up data were obtained through a retrospective analysis of the medical records, including age, sex, smoking history, treatment, clinical course and follow-ups. All patients were followed until March 2016 with median follow-up period of 39.2 months. The study was approved by the Institutional Review Board at Samsung Medical Center (2014-14-08610).

EGFR mutation test

DNA was extracted from sections of formalin-fixed, paraffin-embedded (FFPE) tissue that was also used for histologic diag-

nosis. Manual microdissection was performed if tumor cell percentages were less than 70% in available samples. Genomic DNA was extracted using Qiagen DNA FFPE Tissue Kit (Qiagen, Hilden, Germany) according to the manufacturer's instructions. In cases of lung ADC, routine testing for the *EGFR* mutation was performed in the pathology laboratory using peptide nucleic acid–mediated clamping polymerase chain reaction (PCR) mutation detection kit as previously described,[13] and results were retrieved from electronic medical records. For one SCLC sample, the *EGFR* mutation was detected using targeted sequencing via Illumina HiSeq 2500 (Illumina Inc., San Diego, CA, USA), which was performed for clinical trial enrollment. For the rest of SCLC samples, the *EGFR* mutation was newly evaluated using Cobas test, a real-time PCR test as previously described.[14] *EGFR* mutation results were available for all samples except for one that had no residual tumor.

Immunohistochemistry

In the current study, we used representative FFPE tissue sections for immunohistochemical staining (IHC). IHC for CD56 and thyroid transcription factor 1 (TTF-1) was performed for SCLC or combined tumors. Staining was performed on 3-μm-thick sections from each case using a biotin-avidin-peroxidase method on a BOND-MAX autostainer (Leica, Wetzlar, Germany) after retrieval with T/E buffer (CD56) or citrate buffer (TTF-1). We used primary antibodies to CD56 (1:200, Novocastra, Newcastle upon Tyne, UK) and TTF-1 (1:100, Dako, Glostrup, Denmark).

RESULTS

Sample information and histologic features

Six patients showed transformation from ADC to SCLC.

Table 1. Sample information and pathologic features of six patients showing transformation from non-small-cell lung cancer to small cell lung cancer

Case No.	Initial tumor	Sample type	Sample acquisition site	Subtype	Interval between biopsy (mo)	Transformed tumor	Sample type	Sample acquisition site	IHC TTF-1/ CD56
1	ADC	Biopsy	Lung	Acinar	37	SCLC	Biopsy	Celiac LN	–/+
2	ADC	Biopsy	Lung, brain	Acinar and papillary	21	Combined SCLC and ADC	Biopsy	Lung	–/+[a]
3	ADC	Biopsy	LN 4	Acinar	8	SCLC	Biopsy	LN 7	+/+
4	ADC	Biopsy	Lung	Acinar	5	Combined SCLC and ADC	Biopsy	Lung (same site)	+/NA
5	ADC	Resection	Lung	Acinar	31	SCLC	Biopsy	Pleura	+/+
6	ADC	Resection	Lung	Acinar and solid	50	SCLC	Biopsy	Neck LN	+/+

IHC, immunohistochemistry; TTF-1, thyroid transcription factor; ADC, adenocarcinoma; SCLC, small cell lung cancer; LN, lymph node; NA, not-applicable.
[a]CD56 was positive in only SCLC components.
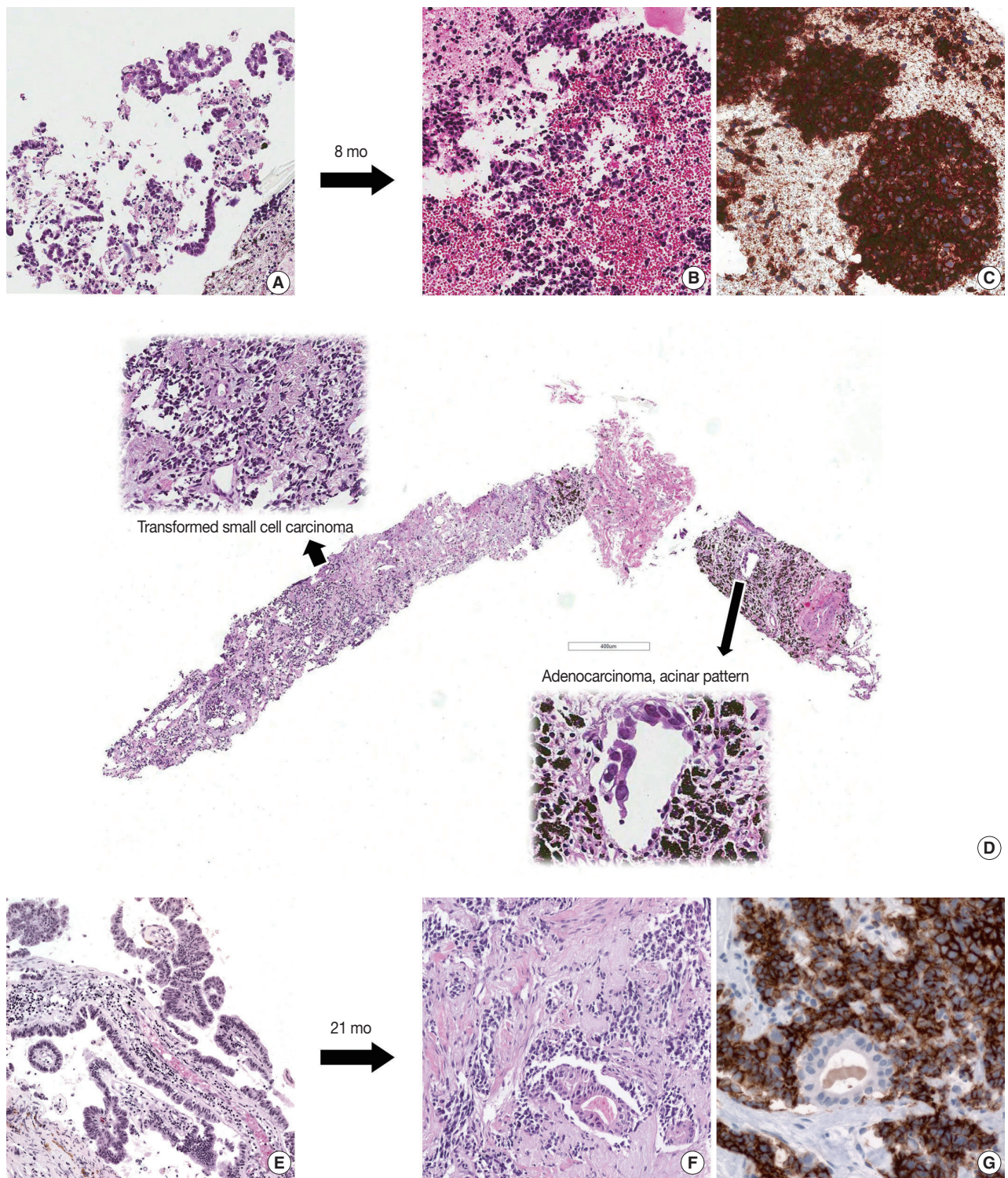
Fig. 1. Three cases showing transformation from non-small-cell lung cancer to small-cell lung cancer. (A) Initial biopsy of case 3 shows adeno-carcinoma. Second biopsy after Iressa treatment, mediastinal lymph node specimen shows small cell carcinoma (B) and tumor cells are strongly positive for CD56 (C). (D) In case 4, second biopsy after gefetinib treatment reveals combined small-cell and adenocarcinoma histology. (E) Adenocarcinoma is identified in the brain tissue of case 2 at the time of initial diagnosis. (F) Second biopsy after afatinib treatment from this patient has combined small-cell and adenocarcinoma histology. (G) CD56 is expressed in the small cell component of the tumor sample.

Sample information and pathologic features are summarized in Table 1. Of the initial samples with diagnosis of ADC, four were obtained using needle biopsy and two were surgically resected specimens. All second biopsies were obtained using needle biopsy. The histology of the six ADCs was acinar (n = 4), mixed acinar and papillary (n = 1), and mixed acinar and solid (n = 1). Of samples that showed transformation to SCLC upon second biopsy, four showed pure SCLC morphology and two showed combined ADC and SCLC morphology. In two cases, ADC components demonstrated acinar morphology (Fig. 1). For small cell components, TTF-1 was expressed in four of six cases and CD56 was expressed in all five available cases. CD56 was not expressed in ADC components.

Clinical information and EGFR status

The clinical information and *EGFR* mutation status of the six patients are summarized in Table 2. Initial treatments included complete resection and adjuvant chemotherapy for case 1 (cT2N0), palliative chemotherapy for case 2 (cT3N1M1) and case 4 (cT1N0M1), EGFR TKI for case 3 (cT2N3M1), incomplete resection and palliative chemotherapy for case 5 (cT1N0M1), and complete resection for case 6 (cT1N0). The sites of distant metastasis were as follows; brain (cases 2 and 4), pleura (case 3, 4, and 5), bone (case 4), and liver (case 4).

Of the six patients with ADC in initial biopsy, four (cases 1–4) harbored an *EGFR* mutation (L858R mutation, n = 1; exon 19 deletion, n = 3). All four, along with case 5 who had wild-type *EGFR* but was enrolled in a clinical trial of gefetinib, were treated with EGFR TKIs. Cases 1 and 3 were treated with iressa, and afatinib was also added for case 1. Case 2 was treated with afatinib only, and cases 4 and 5 were treated with gefetinib only. All five patients who underwent TKI treatment were female non-smokers (Table 2). Despite TKI treatment, all five patients showed disease progression, upon which a second biopsy was performed. The interval between initial biopsy and second biopsy ranged from 5 to 50 months with mean of 25.3 months.

After confirmation of transformation of SCLC on second biopsy, four patients received further treatment. The treatment option for two patients (cases 1 and 3) was switched to etoposide and cisplatin, and one of them (case 3) showed partial response. Case 5 died due to disease progression and the other patients were alive in the short-term follow-up period.

EGFR mutation status was compared between initial and second samples, and all pairs showed the same *EGFR* status. The original *EGFR* mutation in cases 1–4 was retained in all transformed SCLC samples, while cases 5 and 6 showed no

Table 2. Clinical information and *EGFR* status of six patients showing transformation from non-small-cell lung cancer to small cell lung cancer

Case No.	Sex	Age (yr)	Smoking history (pack years)	Tumor histology in initial sample	Clinical stage	Initial treatment	*EGFR* mutation in initial sample	Treatment related to TKI	Duration of TKI treatment before transformation (mo)	Response to TKI	Tumor histology in second biopsy sample	*EGFR* mutation in second biopsy ample	Treatment after second biopsy	Progression or recurrance	Death
1	F	57	0	ADC	T2N0	Operation, adjuvant CTx (paclitaxel/carboplatin)	L858R	Iressa, afatinib	10	PD	SCLC	L858R	CTx (etoposide/cisplatin)	F/U loss	F/U loss
2	F	54	0	ADC	T3N1M1	CTx (Alimta/cisplatin)	Del19	Afatinib	11	PD	Combined SCLC and ADC	del19	CTx (gemcitabine/cisplatin)	PR	Alive
3	F	55	0	ADC	T2N3M1	Iressa	Del19	Iressa	9	PD	SCLC	del19	CTx (etoposide /cisplatin)	PR	Alive
4	F	59	0	ADC	T1N0M1	CTx (Alimta/cisplatin)	Del19	Gefetinib	11	PD	Combined SCLC and ADC	del19	Rociletinib	PD	Alive
5	F	68	0	ADC	T1N0M1	Operation, palliative CTx (Alimta/cisplatin)	No mutation	Gefetinib	2	PD	SCLC	No mutation	No treatment[a]	PD	Dead[b]
6	M	67	35	ADC	T1N0	Operation	No mutation	No TKI	NA	PD	SCLC	No mutation	No treatment[a]	F/U loss	F/U loss

EGFR, epidermal growth factor receptor; TKI, tyrosine kinase inhibitor; F, female; ADC, adenocarcinoma; CTx, chemotherapy; PD, progressive disease; SCLC, small cell lung cancer; F/U, follow-up; PR, partial response; M, male; NA, not-applicable.
[a]No further treatment due to poor condition; [b]Dead due to disease progression.

EGFR mutation in transformed SCLC samples.

DISCUSSION

Transformation of NSCLC to SCLC was recently proposed as a mechanism of resistance to TKI therapy.[2,6] Identification of histologic transformation may be an important factor in determining a patient's treatment plan due to the differences between NSCLC and SCLC. While most reports of transformation of ADC to SCLC were identified in *EGFR* mutant patients related to TKI treatment, it is not certain whether transformation is exclusively related to *EGFR* mutation or EGFR TKI treatment.[10] Here, we report six cases of ADC which showed histologic transformation to SCLC over a 6-year period at a single institute. Similar to previous reports, four cases in our series were ADC with *EGFR* activating mutations that underwent TKI treatment and were subsequently found to have SCLC transformation on second biopsy. However, we also identified two additional cases of SCLC transformation that had no *EGFR* mutation, and one of these cases underwent initial TKI treatment.

EGFR TKIs are now being used worldwide for first-line treatment in a subset of lung cancers bearing *EGFR*-activating mutations, and they have demonstrated dramatic therapeutic efficacy.[15] However, acquired resistance through multiple mechanisms has become a major problem.[6] One of mechanism of resistance to EGFR inhibitors is the histological transformation of ADC to SCLC.[6] Although the presence of combined ADC and SCLC histology at initial diagnosis is a possibility, genomic sequencing of *EGFR* mutations shows that both the original tumor and transformed SCLC at the time of resistance share the original *EGFR*-activating mutation, thus supporting the conclusion that these were not independent tumors.[6-11] However, the small biopsy size represents only a portion of tumors, and SCLC components may become dominant at the time of disease progression. Of the six patients with initially diagnosed with ADC in our report, two were diagnosed using surgically resected samples rather than needle biopsies. For these two cases, the possibility of combined histology at the initial biopsy can be excluded. In case 6, it was difficult to distinguish between SCLC transformation and second primary SCLC considering the early stage of initial ADC.

In our series, two of six cases were *EGFR*–wild-type ADC. This suggests that transformation to SCLC is not unique to tumors bearing *EGFR* mutations, nor does it exclusively result from TKI treatment. Transformation to SCLC is also reported as a mechanism of acquired resistance to crizotinib in *ALK* rearranged lung tumors.[16] In addition, transformation to large cell neuroendocrine carcinoma was identified as an acquired resistance mechanism to EGFR TKIs and crizotinib.[17,18] Recent studies suggest that alveolar type II cells can give rise to both ADC and SCLC,[19] so *EGFR*-mutant lung cancers derived from alveolar type II cells may have the potential to transform into SCLC during the disease progression.[2] In sum, it seems that acquisition of neuroendocrine phenotype, which includes SCLC transformation, can occur in the progression of disease in both *EGFR*-mutant and *EGFR*–wild-type NSCLCs.

Second biopsies are not routinely performed for lung cancer patients when patients showed resistance to TKI treatment. Therefore, the incidence of transformation to SCLC in NSCLCs cannot be accurately calculated. An acquired TKI resistance arising from the histological transformation to SCLC has been reported to be as high as 3%.[5] In our institute, the incidence of transformation to SCLC identified in the second biopsy of total ADCs was 1.5%. Recently in our institute, there were two cases of SCLC transformation in *EGFR* mutant ADC during treatment with AZD9291, an oral irreversible EGFR TKI with selectivity for activating *EGFR* mutations and the T790M resistance mutation.[20] These cases were not included in this report. In clinical practice, identification of small cell component is important as the treatment option can be switched to etoposide and cisplatin against SCLC.[12]

In conclusion, we report six cases of lung cancer demonstrating transformation from ADC to SCLC. Four cases were *EGFR*-mutant tumors from female non-smokers who underwent TKI treatment, and the *EGFR* mutation was retained in the transformed SCLC tumors. The other two ADCs were *EGFR*–wild-type, and one of these patients received EGFR TKI treatment. The neuroendocrine phenotype can thus be acquired during ADC disease progression independent of EGFR TKI treatment.

Conflicts of Interest

No potential conflict of interest relevant to this article was reported.

REFERENCES

1. Goldstraw P, Ball D, Jett JR, *et al*. Non-small-cell lung cancer. Lancet 2011; 378: 1727-40.
2. Oser MG, Niederst MJ, Sequist LV, Engelman JA. Transformation from non-small-cell lung cancer to small-cell lung cancer: molecu-

lar drivers and cells of origin. Lancet Oncol 2015; 16: e165-72.

3. Moiseenko VM, Protsenko SA, Semenov II, *et al*. Effectiveness of gefitinib (Iressa) as first-line therapy for inoperable non-small-cell lung cancer with mutated *EGFR* gene (phase II study). Vopr Onkol 2010; 56: 20-3.

4. Engelman JA, Jänne PA. Mechanisms of acquired resistance to epidermal growth factor receptor tyrosine kinase inhibitors in non-small cell lung cancer. Clin Cancer Res 2008; 14: 2895-9.

5. Yu HA, Arcila ME, Rekhtman N, *et al*. Analysis of tumor specimens at the time of acquired resistance to EGFR-TKI therapy in 155 patients with *EGFR*-mutant lung cancers. Clin Cancer Res 2013; 19: 2240-7.

6. Sequist LV, Waltman BA, Dias-Santagata D, *et al*. Genotypic and histological evolution of lung cancers acquiring resistance to EGFR inhibitors. Sci Transl Med 2011; 3: 75ra26.

7. Zakowski MF, Ladanyi M, Kris MG; Memorial Sloan-Kettering Cancer Center Lung Cancer OncoGenome Group. *EGFR* mutations in small-cell lung cancers in patients who have never smoked. N Engl J Med 2006; 355: 213-5.

8. van Riel S, Thunnissen E, Heideman D, Smit EF, Biesma B. A patient with simultaneously appearing adenocarcinoma and small-cell lung carcinoma harbouring an identical *EGFR* exon 19 mutation. Ann Oncol 2012; 23: 3188-9.

9. Morinaga R, Okamoto I, Furuta K, *et al*. Sequential occurrence of non-small cell and small cell lung cancer with the same *EGFR* mutation. Lung Cancer 2007; 58: 411-3.

10. Norkowski E, Ghigna MR, Lacroix L, *et al*. Small-cell carcinoma in the setting of pulmonary adenocarcinoma: new insights in the era of molecular pathology. J Thorac Oncol 2013; 8: 1265-71.

11. Watanabe S, Sone T, Matsui T, *et al*. Transformation to small-cell lung cancer following treatment with EGFR tyrosine kinase inhibitors in a patient with lung adenocarcinoma. Lung Cancer 2013; 82: 370-2.

12. Kim WJ, Kim S, Choi H, *et al*. Histological transformation from non-small cell to small cell lung carcinoma after treatment with epidermal growth factor receptor-tyrosine kinase inhibitor. Thorac Cancer 2015; 6: 800-4.

13. Lee B, Han G, Kwon MJ, Han J, Choi YL. *KRAS* mutation detection in non-small cell lung cancer using a peptide nucleic acid-mediated polymerase chain reaction clamping method and comparative validation with next-generation sequencing. Korean J Pathol 2014; 48: 100-7.

14. Ahn S, Lee J, Sung JY, *et al*. Comparison of three *BRAF* mutation tests in formalin-fixed paraffin embedded clinical samples. Korean J Pathol 2013; 47: 348-54.

15. Pao W, Miller VA. Epidermal growth factor receptor mutations, small-molecule kinase inhibitors, and non-small-cell lung cancer: current knowledge and future directions. J Clin Oncol 2005; 23: 2556-68.

16. Miyamoto S, Ikushima S, Ono R, *et al*. Transformation to small-cell lung cancer as a mechanism of acquired resistance to crizotinib and alectinib. Jpn J Clin Oncol 2016; 46: 170-3.

17. Kogo M, Shimizu R, Uehara K, *et al*. Transformation to large cell neuroendocrine carcinoma as acquired resistance mechanism of EGFR tyrosine kinase inhibitor. Lung Cancer 2015; 90: 364-8.

18. Caumont C, Veillon R, Gros A, Laharanne E, Bégueret H, Merlio JP. Neuroendocrine phenotype as an acquired resistance mechanism in *ALK*-rearranged lung adenocarcinoma. Lung Cancer 2016; 92: 15-8.

19. Sutherland KD, Proost N, Brouns I, Adriaensen D, Song JY, Berns A. Cell of origin of small cell lung cancer: inactivation of Trp53 and Rb1 in distinct cell types of adult mouse lung. Cancer Cell 2011; 19: 754-64.

20. Ham JS, Kim S, Kim HK, *et al*. Two cases of small cell lung cancer transformation from *EGFR* mutant adenocarcinoma during AZD9291 treatment. J Thorac Oncol 2016; 11: e1-4.

Significance of Parafibromin Expression in Laryngeal Squamous Cell Carcinomas

Inju Cho · Mija Lee · Sharon Lim
Ran Hong

Department of Pathology, Chosun University
School of Medicine, Gwangju, Korea

Corresponding Author
Ran Hong, MD, PhD
Department of Pathology,
Chosun University School of Medicine,
309 Pilmun-daero, Dong-gu,
Gwangju 61452, Korea
Tel: +82-62-230-6356
Fax: +82-62-234-4584
E-mail: nanih@chosun.ac.kr

Background: Parafibromin is a product of the tumor suppressor gene that has been studied as a potential indicator of tumor aggressiveness in the parathyroid, breast, colorectum, and stomach. However, the clinical significance and potential function of parafibromin expression in head and neck squamous cell carcinomas remain largely unknown. The aim of this study was to evaluate the expression of parafibromin in laryngeal squamous cell carcinoma (LSCC) and to verify its potential as a biomarker of tumor behavior. **Methods:** Parafibromin expression was evaluated in 30 cases of LSCC using immunohistochemistry. The correlations between parafibromin expression and clinicopathologic parameters were investigated. **Results:** Parafibromin expression was positive in 15 cases (50%) and negative in 15 cases (50%). Tumor size and T stage showed a statistically significant inverse relationship with parafibromin expression (p = .028 and p < .001, respectively). Parafibromin expression was not associated with age, sex, lymph node metastasis, tumor differentiation, or tumor location. There was no statistically significant relationship between parafibromin expression and progression-free survival in the patients (p > .05). **Conclusions:** Our results indicate that the downregulation or loss of parafibromin expression can be employed as a novel marker of tumor progression or aggressiveness in LSCC.

Key Words: Parafibromin; Carcinoma, squamous cell; Epithelial-mesenchymal transition

Laryngeal cancer is one of the most common malignancies in the head and neck area and the 11th most common cancer worldwide, with a high mortality rate and poor prognosis. About 85%–90% of all malignant tumors in the larynx are squamous cell carcinoma.[1-3] Primary malignancies of the head and neck region other than squamous cell carcinoma are typically salivary gland tumors and neuroendocrine tumors, with rare cases of cartilaginous and soft tissue sarcomas.[1] The incidence of laryngeal squamous cell carcinoma (LSCC) has gradually increased in recent years. Invasion and metastasis are the main factors affecting a patient's overall survival and quality of life.[2] Major progress has been achieved in the treatment of laryngeal cancer. Organ-sparing protocols that combine radiation, chemotherapy, and surgery are the standard therapy for advanced laryngeal cancer.[1] Although the treatment of laryngeal cancer has been evolving, there are currently no markers for assessing prognosis or tumor behavior in LSCC. Therefore, it is worthwhile to investigate biomarkers for understanding tumor behavior and for guidance to optimal treatment.

Parafibromin is a protein encoded by the tumor suppressor gene hyperthyroidism 2 (*HRPT2*). Its mutation leads to hyper-parathyroidism-jaw-tumor syndrome, an autosomal dominant disease characterized by parathyroid adenoma or carcinoma, fibro-osseous tumors of the maxilla and mandible, renal anomalies, and uterine tumors.[4-6] The *HRPT2* gene is located on human chromosome 1q31.2, which is composed of 17 exons and spans 18.5 kb in the genome. The gene encodes a 2.7-kb transcript that is translated into a 60-kD, 531-amino acid parafibromin protein.[7,8] Along with its role as an oncosuppressor, parafibromin binds to RNA polymerase II as part of polymerase-associated factor 1 (Paf1), causing repression of β-catenin–mediated transcription and transcriptional repression of c-myc.[5,9] Zhang *et al*.[10] documented that the overexpression of parafibromin results in anti-proliferative properties through the inhibition of colony formation and cellular proliferation and induces cell cycle arrest in the G1 phase.

Various non-morphological techniques including reverse transcriptase polymerase chain reaction and northern and western blotting have suggested that parafibromin is ubiquitously expressed.[11]

Immunohistochemically, a high expression of parafibromin has been found in hepatocytes, renal cortex tubules, cells at the base

of the gastric glands, and the pars intermedia of the hypophysis.[11] Hyperparathyroidism-jaw-tumors-syndrome and sporadic parathyroid carcinoma show loss of nuclear immunoreactivity of parafibromin.[12] Selvarajan *et al*.[13] showed inverse correlations between parafibromin expression and tumor size, pathologic stage, and lymphovascular invasion of breast carcinomas. Subsequent investigations have suggested that down-regulated parafibromin expression is involved in tumor pathogenesis, growth, invasion, and metastasis and might be a novel biomarker indicating a poor prognosis in gastric and colorectal carcinomas.[14,15] Zhang *et al*.[5] demonstrated that the down-regulated expression of parafibromin protein might have a negative impact on apoptosis and suppressing cell cycle progression, proliferation, migration, invasion, and the epithelial mesenchymal transition (EMT), suggesting its important role in the pathogenesis, differentiation, and metastasis of head and neck squamous cell carcinoma (HN-SCC). Parafibromin has recently been shown to be expressed in squamous cell carcinoma of the head and neck.[5] However, research on the relationships between parafibromin and clinicopathologic parameters in LSCC has been limited. The purpose of our study was to investigate the expression of parafibromin in LSCC and to identify its clinicopathologic significance.

MATERIALS AND METHODS

Patient and tissue samples

This study was composed of 30 cases of LSCC patients who underwent surgery with/without neck dissection at the Department of Otorhinolaryngology at Chosun University Hospital (Gwangju, South Korea) from January 2003 to December 2008. Twenty cases of total laryngectomy, seven cases of partial laryngectomy, and three cases of cordectomy were included. For comparative analysis, 10 cases with normal mucosal tissue of the larynx were also included.

Histopathological evaluation

For each case, the clinical records and tissue slides were retrospectively re-evaluated by two pathologists (I.C. and R.H.). The examined tissues were prepared in 10% neutral formalin fixation, paraffin-embedded, and sectioned in 4–5 μm thickness. Hematoxylin and eosin–stained sections were examined using a light microscope (Olympus BX51, Olympus Corporation, Tokyo, Japan). We re-evaluated the histological diagnosis, tumor size, T stage, and lymph node metastasis. Tumor staging was evaluated according to the 2005 World Health Organization Classification of Head and Neck Tumors. For immunohisto-

chemical (IHC) analysis, a representative area of the tumor was selected, and slides were prepared.

IHC evaluation

IHC study was performed according to the manufacturer's instruction. For IHC analysis of parafibromin, formalin-fixed and paraffin-embedded blocks were sectioned at 4 μm thickness and mounted on precoated glass slides, which were then deparaffinized in xylene. Endogenous peroxidase was blocked with a blocking reagent (sodium chloride-citrate, Ventana Medical Systems, Tucson, AZ, USA). The IHC analysis of parafibromin (1:50, sc-33638, rabbit polyclonal, Santa Cruz Biotechnology Inc., Santa Cruz, CA, USA) was carried out using the NexES autoimmunostainer (Ventana Medical Systems), and immunolocalization was performed using the mouse ImmunoCruz Staining System (sc2050, Santa Cruz Biotechnology Inc.). The slides with the primary antibody were incubated for 32 minutes (1:50, parafibromin). For the secondary detection method, the UltraviewUniversal DAB detection kit (cat. No. 760500, Ventana Medical Systems) was used. Slides were then counterstained with hematoxylin (cat. No. 7602021, Ventana Medical Systems). Scoring was performed by two pathologists, and nuclear stain-

Table 1. Clinical and histopathologic features of the patients

Clinical and histological feature	No. of patients (%)
Age, mean (yr)	66.5
Gender	
Male	28 (93.3)
Female	2 (6.7)
Tumor location	
Localized[a]	14 (47)
Transglottic	16 (53)
Tumor differentiation	
Well differentiated	12 (40.0)
Moderately differentiated	16 (53.3)
Poorly differentiated	2 (6.7)
Tumor size (cm)	
< 1	5 (16.7)
1 to < 2	9 (30)
2 to < 3	9 (30)
3 to < 4	3 (10)
≥ 4	4 (13.3)
T stage	
1	9 (30)
2	4 (13.3)
3	9 (30)
4	8 (26.7)
Lymph node metastasis	
Absent	17 (56.7)
Present	13 (43.3)

[a]Tumors localized to supraglottis, glottis or subglottis.

ing was interpreted as positive for parafibromin. The expression positivity was graded and counted. The staining intensity score was graded as 1, weak; 2, intermediate; and 3, strong. The percentage of tumor cells with positive expression and the staining intensity grade were multiplied to obtain a final score. Of 30 cases, 11 were scored as 0, 15 were scored as > 100 (range, 115 to 260), and four were scored between 0 and 100. Statistical analyses were performed based on a two-tier system of the parafibromin-positive group and -negative group (positive, > 100; negative, ≤ 100).

Statistical analysis

Statistical evaluation was carried out using the SPSS ver. 21 (IBM Co., Armonk, NY, USA). The chi-square test and Fisher exact test were used to demonstrate the correlations between parafibromin expression and clinicopathologic characteristics. Survival analysis was performed using Kaplan-Meier survival graphs and the log-rank test. A p-value < .05 was considered to be statistically significant.

RESULTS

Clinical and pathological parameters

The clinicopathologic characteristics of the patients are summarized in Table 1. The mean age was 66.5 years (range, 47 to 81 years), and the male to female ratio was 13.2:1, showing a male predominance. Tumors localized in the supraglottic, glottic, or subglottic regions composed 47% (n=14) of the group, and transglottic tumors were found in 53% of patients (n=16). The tumors had a size < 2 cm in 14 cases (46.7%) and a size ≥ 2 cm in 16 cases (53.3%). The tumor stage was T1 in nine cases (30.0%) and T2, 3, or 4 in 21 cases (70.0%). Lymph node metastasis was present in 43.3% of the cases (n=13).

The relationships between parafibromin expression and clinicopathologic parameters

Among the 30 cases, parafibromin expression was positive in 15 cases (50%) and negative in 15 cases (50%) (Fig. 1A–D, Table 2). Among cases with positive parafibromin nuclear staining,

Table 2. The relationships between parafibromin expression and clinicopathologic parameters

Clinicopathologic parameter	Parafibromin expression		p-value
	Negative (n=15, 50%)	Positive (n=15, 50%)	
Tumor location			
Localized[a]	4	10	.066
Transglottic	11	5	
Tumor differentiation			.583
Well differentiated	7	5	
Moderately differentiated	7	9	
Poorly differentiated	1	1	
Tumor size (cm)			
0–0.9	0	5	.04[b]
1.0–1.9	4	5	
2.0–2.9	5	4	
3.0–3.9	2	1	
≥4.0	4	0	
Tumor size (cm)[c]			
<2	4	10	.028[b]
≥2	11	5	
T stage			.015[b]
T1	0	9	
T2	4	0	
T3	6	3	
T4	5	3	
T stage[d]			
T1	0	9	<.001[b]
T2, 3, and 4	15	6	
Lymph node metastasis			
Absent	8	9	.713
Present	7	6	

[a]Tumors localized to supraglottis, glottis, or subglottis; [b]Indicates p<0.05; [c]Subdivided tumor size; [d]Subdivided T stage.

a subset of cases showed parafibromin immunoreactivity at the periphery of the tumor cell nest (Fig. 1C). There was a statistically significant inverse relationship between parafibromin expression and T stage (p = .015). Interestingly, when we subdivided T stage into a T1 group and a T2, 3, or 4 group, the loss of parafibromin expression was associated with the latter (p < .001) (Table 2). Tumor size and parafibromin expression were also inversely correlated (p = .028) (Table 2). Parafibromin expression was not associated with other clinicopathologic factors such as age, sex, lymph node metastasis, tumor differentiation, or tumor location (Table 2). The follow-up periods of LSCC patients ranged from 2 to 136 months (median, 23 months). During the follow-up period, there was no disease-specific death among the patients. Eight patients experienced distant metastasis or recurrence of the cancer, and progression-free survival (PFS) ranged from 2 to 136 months (median, 21.5 months). The survival curve using the Kaplan-Meier method indicated no statistically significant relationship between parafibromin expression and PFS in the patients (p > .05) (Fig. 2).

DISCUSSION

Parafibromin is a protein product of the tumor suppressor gene that has been studied as a potential indicator of tumor aggressiveness in many organs, notably the parathyroid, breast, colorectum, and stomach.[13-16] However, the clinical significance and potential function of parafibromin expression in HNSCC have remained largely unknown. One study by Zhang et al.[5] investigated the role of parafibromin expression in tumorigenesis and the progression of HNSCC, along with its value as a prognostic marker. The overall 5-year survival rate of HNSCC is about 40%–50%, despite advancements in therapy.[5] The prognosis of laryngeal cancer varies considerably according to the anatomical site of origin. For example, glottic cancer has a better prognosis than supraglottic and subglottic cancer.[17] Until now, prevention and early diagnosis with function-preserving treatment have been
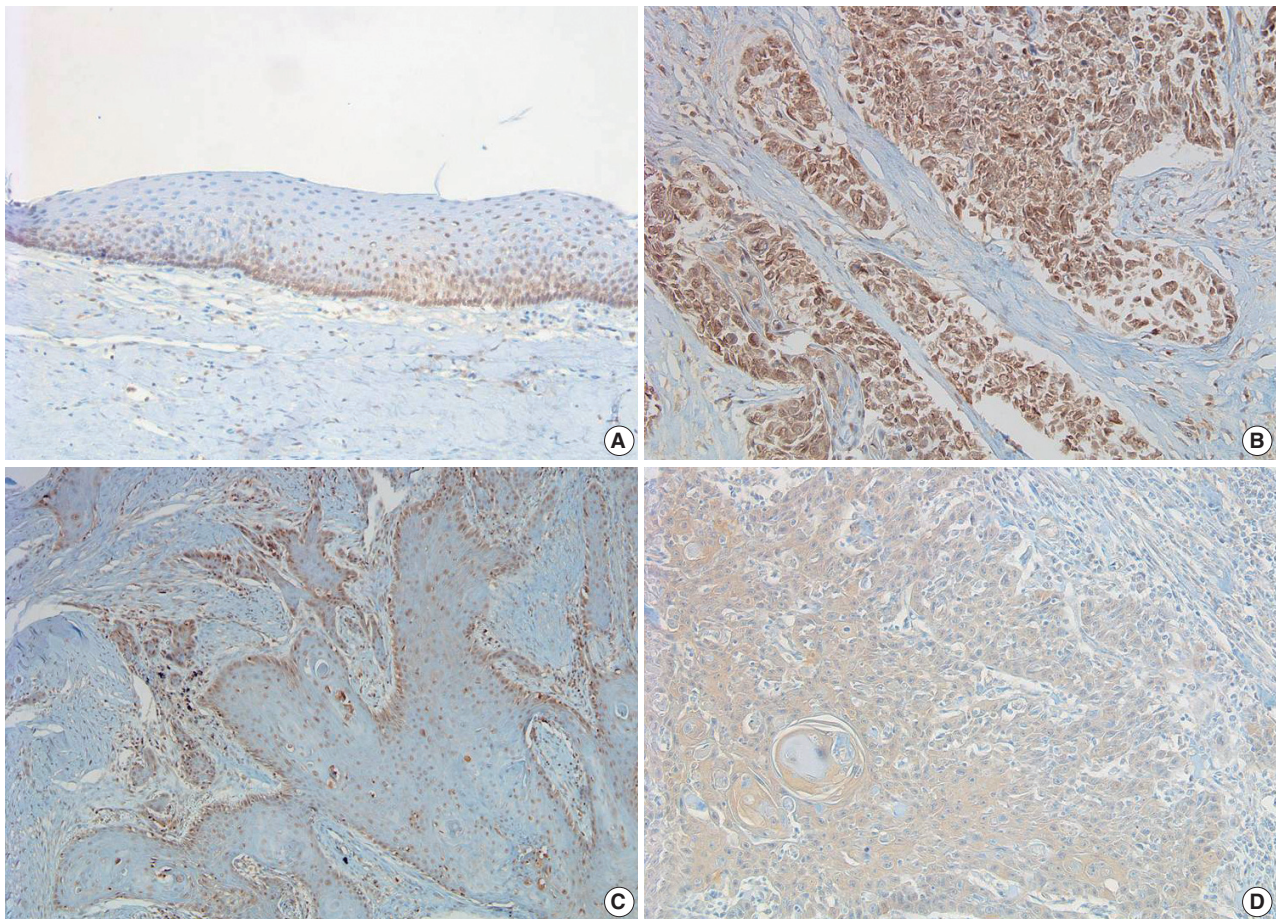
Fig. 1. Parafibromin expression in squamous cell carcinoma of the larynx. (A) Parafibromin expressed in the basal layer of normal laryngeal mucosa. (B) Parafibromin-positive staining is expressed in the nuclei of tumor cells. (C) Occasionally, parafibromin positivity is observed in the periphery of the tumor nest. (D) Representative image of parafibromin-negative staining.
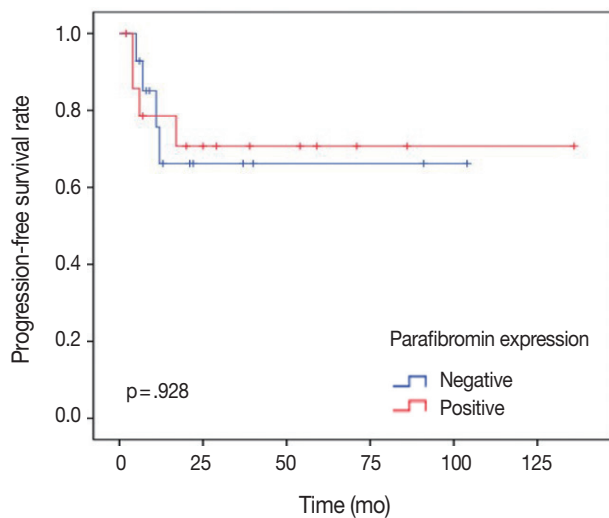
Fig. 2. Kaplan-Meier curves of progression-free survival in laryngeal squamous cell carcinoma patients according to parafibromin expression status. There is no statistically significant relationship between parafibromin expression and the progression-free survival of the patients (p > .05).

considered to be the most effective approach.[3] The aim of this study was to evaluate the expression of parafibromin in LSCC and verify its potential as a biomarker of tumor behavior. We evaluated the relationships between parafibromin staining and clinicopathologic parameters. Our results demonstrated that parafibromin expression has an inverse correlation with T stage and tumor size, indicating that downregulation or loss of parafibromin expression is involved in tumor progression or aggressiveness. Our results are in line with other studies on parafibromin expression in different organs. Zheng *et al.*[14] observed that tumor size, depth of invasion, lymph node metastasis, clinicopathologic staging, and poor prognosis were inversely correlated with parafibromin in colorectal carcinomas. Zheng *et al.*[15] also reported parafibromin expression to be associated with tumor size, depth of invasion, lymph node metastasis, lymphatic invasion, International Union against Cancer staging, and Lauren's classification in gastric carcinomas. Selvarajan *et al.*[13] observed that parafibromin expression was inversely correlated with tumor size in 163 cases of breast carcinomas.

Recent research on HNSCC conducted by Zhang *et al.*[5] showed that parafibromin expression was negatively correlated with lymph node metastasis and TNM staging but positively correlated with human papillomavirus positivity. However, other clinicopathological characteristic such as tumor status were not associated with parafibromin expression. Our results in LSCC revealed that parafibromin expression was inversely correlated with T stage (T1 or T2, 3, and 4) (p < .05). Stage T1 involves tu-

mor limited to one subsite of origin with normal vocal cord mobility. A T stage of 2, 3, or 4 involves tumor invading adjacent subsites of origin with impaired vocal cord mobility.

In addition to tumor size and volume, which are encompassed by the T stage, advanced stage disease with vocal cord fixation might be a significant parameter of tumor aggressiveness. These results also explain the role of parafibromin expression in invasion, migration, and EMT. *In vitro* experiments have documented that parafibromin overexpression suppressed the migration and invasion of transfected cells by upregulating E-cadherin expression and downregulating the expression of matrix metalloproteinase (MMP)-2, MMP-9, and Slug.[5] Thus, the loss or downregulation of parafibromin might promote invasion and migration by upregulating Snail, Slug, Zeb1, and Zep2 during EMT. However, unlike in other studies, we did not find significant relationship between parafibromin expression and lymph node metastasis or PFS. Considering our small sample size, this might not represent characteristics of LSCC but rather reflect the limited number of cases. This is a preliminary evaluation that requires support from additional studies based on larger groups with extended follow-up periods and clinicopathologic parameters.

Here, we analyzed parafibromin expression and clinicopathologic features in laryngeal cancer, revealing positive links between loss of parafibromin and tumor size and T stage. Our results suggest that parafibromin expression can be employed as a novel marker of tumor aggressiveness in LSCC. Based on this data, we suggest that parafibromin can be used to guide the individualized treatment of laryngeal cancer.

REFERENCES

1. Genden EM, Ferlito A, Silver CE, *et al*. Evolution of the management of laryngeal cancer. Oral Oncol 2007; 43: 431-9.
2. Li L, Wang J, Gao L, Gong L. Expression of paxillin in laryngeal squamous cell carcinoma and its prognostic value. Int J Clin Exp Pathol 2015; 8: 9232-9.
3. Marioni G, Marchese-Ragona R, Cartei G, Marchese F, Staffieri A.

Current opinion in diagnosis and treatment of laryngeal carcinoma. Cancer Treat Rev 2006; 32: 504-15.

4. Karaarslan S, Yaman B, Ozturk H, Kumbaraci BS. Parafibromin staining characteristics in urothelial carcinomas and relationship with prognostic parameters. J Pathol Transl Med 2015; 49: 389-95.

5. Zhang Z, Yang XF, Huang KQ, et al. The clinicopathological significances and biological functions of parafibromin expression in head and neck squamous cell carcinomas. Tumour Biol 2015; 36: 9487-97.

6. Newey PJ, Bowl MR, Thakker RV. Parafibromin: functional insights. J Intern Med 2009; 266: 84-98.

7. Carpten JD, Robbins CM, Villablanca A, et al. HRPT2, encoding parafibromin, is mutated in hyperparathyroidism-jaw tumor syndrome. Nat Genet 2002; 32: 676-80.

8. Wang PF, Tan MH, Zhang C, Morreau H, Teh BT. HRPT2, a tumor suppressor gene for hyperparathyroidism-jaw tumor syndrome. Horm Metab Res 2005; 37: 380-3.

9. Yart A, Gstaiger M, Wirbelauer C, et al. The HRPT2 tumor suppressor gene product parafibromin associates with human PAF1 and RNA polymerase II. Mol Cell Biol 2005; 25: 5052-60.

10. Zhang C, Kong D, Tan MH, et al. Parafibromin inhibits cancer cell growth and causes G1 phase arrest. Biochem Biophys Res Commun 2006; 350: 17-24.

11. Porzionato A, Macchi V, Barzon L, et al. Immunohistochemical as-

sessment of parafibromin in mouse and human tissues. J Anat 2006; 209: 817-27.

12. Gill AJ, Clarkson A, Gimm O, et al. Loss of nuclear expression of parafibromin distinguishes parathyroid carcinomas and hyperparathyroidism-jaw tumor (HPT-JT) syndrome-related adenomas from sporadic parathyroid adenomas and hyperplasias. Am J Surg Pathol 2006; 30: 1140-9.

13. Selvarajan S, Sii LH, Lee A, et al. Parafibromin expression in breast cancer: a novel marker for prognostication? J Clin Pathol 2008; 61: 64-7.

14. Zheng HC, Wei ZL, Xu XY, et al. Parafibromin expression is an independent prognostic factor for colorectal carcinomas. Hum Pathol 2011; 42: 1089-102.

15. Zheng HC, Takahashi H, Li XH, et al. Downregulated parafibromin expression is a promising marker for pathogenesis, invasion, metastasis and prognosis of gastric carcinomas. Virchows Arch 2008; 452: 147-55.

16. Howell VM, Haven CJ, Kahnoski K, et al. HRPT2 mutations are associated with malignancy in sporadic parathyroid tumours. J Med Genet 2003; 40: 657-63.

17. Licitra L, Bernier J, Grandi C, et al. Cancer of the larynx. Crit Rev Oncol Hematol 2003; 47: 65-80.

■ ORIGINAL ARTICLE ■

Stromal Expression of MicroRNA-21 in Advanced Colorectal Cancer Patients with Distant Metastases

Kyu Sang Lee[1] · Soo Kyung Nam[1]
Jiwon Koh[2] · Duck-Woo Kim[3]
Sung-Bum Kang[3] · Gheeyoung Choe[1,2]
Woo Ho Kim[2] · Hye Seung Lee[1]

[1]Department of Pathology, Seoul National
University Bundang Hospital, Seongnam;
[2]Department of Pathology, Seoul National
University College of Medicine, Seoul;
[3]Department of Surgery, Seoul National
University Bundang Hospital, Seongnam, Korea

Corresponding Author
Hye Seung Lee, PhD
Department of Pathology, Seoul National University
Bundang Hospital, 82 Gumi-ro 173beon-gil,
Bundang-gu, Seongnam 13620, Korea
Tel: +82-31-787-7714
Fax: +82-31-787-4012
E-mail: hye2@snu.ac.kr

Background: The aim of this study was to determine the regional heterogeneity and clinicopathological significance of microRNA-21 (miR-21) in advanced colorectal cancer (CRC) patients with distant metastasis. **Methods:** miR-21 expression was investigated by using locked nucleic acid–fluorescence *in situ* hybridization in the center and periphery of the primary cancer and in distant metastasis from 170 patients with advanced CRC. In addition, α-smooth muscle actin and desmin were evaluated to identify cancer-associated fibroblasts (CAFs) by using immunohistochemistry. **Results:** The miR-21 signal was observed in the cancer stroma. The expression of miR-21 (a score of 1–4) in the center and periphery of the primary cancer and in distant metastasis was observed in specimens from 133 (78.2%), 105 (61.8%), and 91 (53.5%) patients, respectively. miR-21 expression was heterogeneous in advanced CRC. Discordance between miR-21 expression in the center of the primary cancer and either the periphery of the primary cancer or distant metastasis was 31.7% or 44.7%, respectively. miR-21 stromal expression in the periphery of the primary cancer was significantly associated with a better prognosis (p = .004). miR-21 expression was significantly associated with CAFs in the center of the primary cancer (p = .001) and distant metastases (p = .041). **Conclusions:** miR-21 expression is observed in cancer stroma related to the CAF quantity and frequently presents regional heterogeneity in CRC. Our findings indicate that the role of miR-21 in predicting prognosis may be controversial but provide a new perspective of miR-21 level measurement in cancer specimens.

Key Words: Colorectal neoplasms; MicroRNA-21; Neoplasm metastasis; Genetic heterogeneity

MicroRNAs (miRNAs) are small (18–25 nucleotides), endogenous, non-coding RNAs that act as post-transcriptional modulators of all cellular processes, including proliferation, differentiation, and apoptosis.[1] Alterations in miRNA expression are associated with the deregulation of oncogenes and tumor suppressor genes.[2] The discovery that miRNA expression is deregulated in cancer suggests the potential of miRNA as biomarkers for cancer.[3] Therefore, targeting miRNAs is regarded as a potential therapeutic strategy and may be a promising diagnostic tool.

MiRNA-21 (miR-21) is consistently upregulated in various cancers, including the colon, stomach, lung, and breast cancer.[4-7] Previous studies proved that miR-21 expression correlates with carcinogenesis.[8-11] Some studies indicated that miR-21 expression is closely associated with poor prognosis in various cancers.[4,12,13] In colorectal cancer (CRC), miR-21 functions as an onco-miRNA due to its key roles in proliferation, invasion, and metastasis.[10,14] Although the mechanisms underlying the regulation of miR-21

in CRC remain to be defined, miR-21 can promote tumorigenesis in CRC. Some studies reported that plasma miR-21 is a potential noninvasive biomarker for early detection and prognosis of CRC.[15-17] Additionally, miR-21 expression is greatly increased in chemotherapy-resistant CRC cells.[18,19] Recent reports suggest that increased expression of miR-21 predicts poor prognosis in patients with CRC.[20-22] However, these results were restricted to patients with stage II CRC.[21-24] Thus, the prognostic value of miR-21 alterations in patients with advanced CRC presenting metastases is controversial.

We previously evaluated cancer-associated fibroblasts (CAFs) in advanced CRC with synchronous or metachronous distant metastases.[25] CAFs facilitate the communication between tumor cells and the tumor microenvironment. In addition, they regulate tumor invasion and metastasis.[26,27] Interestingly, most studies reported that miR-21 was predominantly observed in CAFs, not in cancer cells.[21,22,24] These findings point to a dynamic malignant

role of CAFs through miR-21 expression in CRC. Nevertheless, the correlation between miR-21 and CAF status is yet to be demonstrated in CRC.

Recently, systemic chemotherapy and targeted therapy have been used in patients with advanced CRC, increasing patient survival.[28] Despite advances in medicine, some patients with CRC respond poorly.[29] Although the reasons for drug resistance are not fully understood, they may be related to the presence of tumor heterogeneity.[30-32] Previous reports indicated that regional heterogeneity of miRNA expression is observed in various cancer types.[33-35] Therefore, variation of miR-21 expression between the primary tumor and metastatic sites needs to be elucidated in patients with advanced CRC.

The aim of this study was to evaluate the clinical significance of miR-21 and analyze its heterogeneity in patients with advanced CRC presenting metastases. Additionally, we analyzed the correlation between CAFs and miR-21 status.

MATERIALS AND METHODS

Patients and samples

To evaluate the clinicopathological significance and heterogeneity of miR-21 status, 170 patients with advanced CRC presenting synchronous or metachronous metastases who had undergone surgical resection at Seoul National University Bundang Hospital between May 2003 and December 2009 were enrolled. The clinicopathological characteristics were obtained from the patients' medical records and pathology reports. Follow-up information, including patient's outcome and the interval between the date of surgical resection and death was collected. Data from patients lost to follow-up or those who had died from causes other than CRC were censored.

Ethical statement

All samples were obtained from surgically resected tumors examined pathologically at the Department of Pathology, Seoul National University Bundang Hospital. All samples and medical record data were anonymized before use in this study and the participants did not provide written informed consent. The use of medical record data and tissue samples for this study was approved by the Institutional Review Board of Seoul National University Bundang Hospital (reference No. B-1109/136-302).

Tissue array method

Surgically resected primary CRC specimens were formalin-fixed and paraffin-embedded (FFPE). For each case, representa-tive areas of the donor blocks were obtained and rearranged into new recipient blocks (Superbiochips Laboratories, Seoul, Korea). A single core was 2 mm in diameter and those containing > 20% tumor cells were considered valid cores.

miRNA *in situ* hybridization

Tissue microarray slides were processed by using locked nucleic acid (LNA)–fluorescence *in situ* hybridization (FISH) oligonucleotide probes for miR-21 and U6, both labeled with fluorescein at the 5'-end, according to the protocol described in the preparation protocol. After deparaffinization, the slides were incubated with proteinase-K and endogenous peroxidase was blocked with 3% H_2O_2. Next, the slides were incubated with hybridization mix containing 1 nM LNA U6 snRNA probe (Exiqon, Vedbaek, Denmark) and 20 nM doubled-DIG LNA miR-21 probe (Exiqon) in ThermoBrite (Abbott Laboratories, Abbott Park, IL, USA) for 1 hour at 50°C. Next, the slides were incubated in blocking solution and antifluorescein–horseradish peroxidase antibody (1:125, PerkinElmer, Shelton, CT, USA) for 1 hour. The signals were then amplified using Tyramide Signal Amplification (TSA-plus FITC, 1:50, PerkinElmer) for 10 minutes at room temperature. After incubation, the slides were mounted directly with SlowFade Gold antifade reagent with DAPI (Invitrogen, Carlsbad, CA, USA). All steps beginning with hybridization were performed in the dark.

The experimental data were interpreted according to the instructions in the RNAscope FFPE Assay Kit (Advanced Cell Diagnostics, Hayward, CA, USA): no staining observed at $40\times$ magnification (score of 0); difficult to see at $40\times$ magnification (score of 1); difficult to see at $20\times$ magnification, but detectable staining at $40\times$ magnification (score of 2); difficult to see at $10\times$ magnification, but detectable staining at $20\times$ magnification (score of 3); and detectable staining at $10\times$ magnification (score of 4). A score of 1–4 indicates miR-21 overexpression (Fig. 1).

Immunohistochemistry

Array slides were labeled by immunohistochemistry using antibodies for smooth muscle actin (SMA; 1:1,000, Neomarkers, Fremont, CA, USA) and desmin (1:300, Dako, Glostrup, Denmark) after a microwave antigen retrieval procedure, except for SMA. The staining procedures were carried out using the ultra-View Universal DAB Kit (Ventana Medical Systems, Tucson, AZ, USA) and an automated stainer (BenchMark XT, Ventana Medical Systems), according to the manufacturer's instructions.
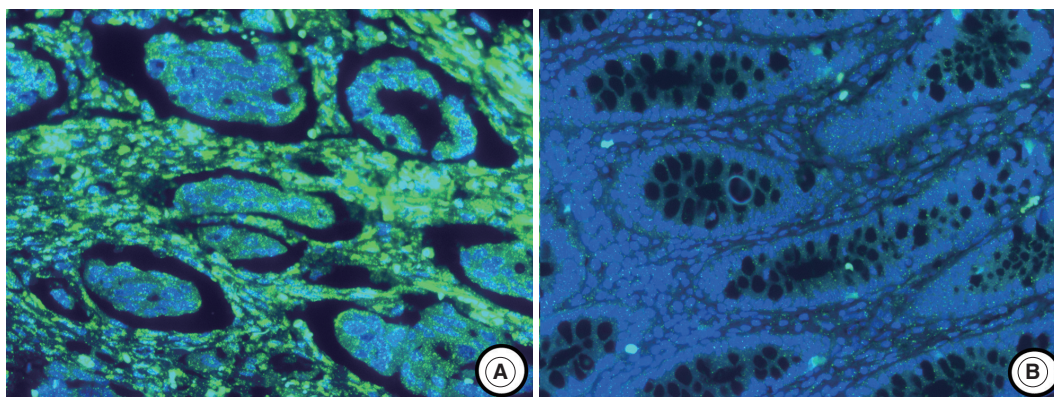
Fig. 1. MicroRNA-21 (miR-21) staining using locked nucleic acid–based *in situ* hybridization in colorectal cancer. (A) miR-21 expression is observed in cancer stromal tissue. (B) No miR-21 expression is observed in normal colonic mucosa.

Table 1. Heterogeneity of miR-21 expression with respect to tumor location in advanced CRC

miR-21 expression		Center		Total
		Negative	Positive	
Periphery	Negative	24 (14.1)	41 (24.1)	170 (100)
	Positive	13 (7.6)	92 (54.1)	
Distant metastasis	Negative	20 (11.8)	59 (34.7)	170 (100)
	Positive	17 (10.0)	74 (43.5)	

Values are presented as number (%). p-values are calculated by using chi-square test or Fisher exact test.
miR-21, microRNA-21; CRC, colorectal cancer.

Calculation of CAFs using digital pathology

CRC cells were considered as internal negative controls. Intestinal muscular layer or medium- to large-sized vessels were considered as internal positive controls for desmin and SMA. Samples showing inappropriate staining in internal negative or positive controls were considered non-informative and were excluded from the analysis. Slides were scanned using an Aperio ScanScopeH CS instrument (Aperio Technologies Inc., Vista, CA, USA) at $20 \times$ magnification. Because desmin-positive muscularis mucosa and propria are positive for SMA staining, the area of CAFs (mm^2) was calculated by subtracting the areas of desmin staining from that of SMA staining (SMA-desmin).

Microsatellite instability

Microsatellite instability (MSI) was assessed in 160 CRC cases with available tissue. MSI results were generated by comparing the allelic profiles of five microsatellite markers (BAT-26, BAT-25, D5S346, D17S250, and D2S123) in the tumors and corresponding normal samples. Polymerase chain reaction products from the FFPE tissues were analyzed using an automated DNA sequencer (ABI 3731 Genetic Analyzer, Applied Biosystems, Foster City, CA, USA) according to the protocol.

Statistical analyses

The association between the clinicopathological features and miR-21 status was analyzed by using the chi-square or Fisher exact test, as appropriate. The correlation between miR-21 expression and CAFs was examined by using the Mann-Whitney test. The patients' survival was analyzed by using the Kaplan-Meier method and the log-rank test was used to determine if there were any significant differences between the survival curves. A p-value < .05 was considered statistically significant. All statistical analyses were performed using the SPSS statistics ver. 21 software (IBM Corp., Armonk, NY, USA).

RESULTS

miR-21 stromal expression and regional heterogeneity in advanced CRC patients

The miR-21 signal was predominantly observed in the stromal compartment of the cancer and the normal mucosa was negative for miR-21 (Fig. 1). The snRNA U6 signal was observed in the nucleus of all cell types. To evaluate the regional heterogeneity of miR-21 expression, we examined tissues from three sites, including the center and periphery of primary cancer as well as distant metastases for each patient with advanced CRC. In the center of primary tumors, a miR-21 FISH score of 0 was

observed in 37 (21.8%), a score of 1 in 16 (9.4%), a score of 2 in 56 (32.9%), a score of 3 in 46 (27.1%), and a score of 4 in 15 (8.8%) patients with CRC. In the periphery of primary tumors, a miR-21 FISH score of 0 was observed in 65 (38.2%), a score of 1 in 14 (8.2%), a score of 2 in 46 (27.1%), a score of 3 in 44 (25.9%), and a score of 4 in one (0.6%) patient with CRC. Additionally, in distant metastatic tumors, a miR-21 FISH score of 0 was observed in 79 (46.5%), a score of 1 in 13 (7.6%), a

score of 2 in 43 (25.3%), a score of 3 in 32 (18.8%), and a score of 4 in three (1.8%) patients with CRC. miR-21 stromal expression (a score of 1–4) in the center and periphery of primary tumor as well as in distant metastasis was observed in 133 (78.2%), 105 (61.8%), and 91 (53.5%) patients with CRC, respectively.

The heterogeneity of miR-21 status according to tumor location is shown in Table 1. Of the 170 cases, discordance between miR-21 expression in the center and periphery was noted in 54

Table 2. The association between clinicopathological parameters and expression of miR-21 in 170 advanced CRC patients with metastasis

Variable	Total	Center miR-21		p-value	Periphery miR-21		p-value	Metastasis miR-21		p-value
		Negative	Positive		Negative	Positive		Negative	Positive	
Age (yr)										
Mean	60.0	60.7	59.7	.668	60.4	59.6	.661	59.8	60.1	.875
Sex										
Male	90	21 (12.4)	69 (40.6)	.599	31 (18.2)	59 (34.7)	.281	36 (21.2)	54 (31.8)	.073
Female	80	16 (9.4)	64 (37.6)		34 (20.0)	46 (27.1)		43 (25.3)	37 (21.8)	
pT stage										
0-2	103	23 (13.5)	80 (47.1)	.825	36 (21.2)	67 (39.4)	.275	45 (26.5)	58 (34.1)	.367
3-4	67	14 (8.2)	53 (31.2)		29 (17.1)	38 (22.4)		34 (20.0)	33 (19.4)	
Differentiation										
LG	148	33 (19.4)	115 (67.6)	.662	50 (29.4)	98 (57.6)	.002	70 (41.2)	78 (49.5)	.575
HG	22	4 (2.4)	18 (10.6)		15 (8.8)	7 (4.1)		9 (5.3)	13 (7.6)	
Location of primary tumor				.299			.260			.925
Right colon	41	8 (4.7)	33 (19.4)		20 (11.8)	21 (12.4)		20 (11.8)	21 (12.4)	
Left colon	69	12 (7.1)	57 (33.5)		23 (13.5)	46 (27.1)		31 (18.2)	38 (22.4)	
Rectum	60	17 (10.0)	43 (25.3)		22 (12.9)	38 (22.4)		28 (16.5)	32 (18.8)	
LN metastasis										
Absent	31	7 (4.1)	24 (14.1)	.903	6 (3.5)	25 (14.7)	.017	15 (8.8)	16 (9.4)	.813
Present	139	30 (17.6)	109 (64.1)		59 (34.7)	80 (47.1)		64 (37.6)	75 (44.1)	
Lymphatic invasion										
Absent	55	9 (5.3)	46 (27.1)	.238	15 (8.8)	40 (23.5)	.042	28 (16.5)	27 (15.9)	.422
Present	115	28 (16.5)	87 (51.2)		50 (29.4)	65 (38.2)		51 (30.0)	64 (37.6)	
Perineural invasion										
Absent	83	19 (11.2)	64 (37.6)	.728	29 (17.1)	54 (31.8)	.388	41 (24.1)	42 (24.7)	.455
Present	87	18 (10.6)	69 (40.6)		36 (21.2)	51 (30.0)		38 (22.4)	49 (28.8)	
Venous invasion										
Absent	118	24 (14.1)	94 (55.3)	.497	42 (24.7)	76 (44.7)	.286	58 (34.1)	60 (35.3)	.291
Present	52	13 (7.6)	39 (22.9)		23 (13.5)	29 (17.1)		21 (12.4)	31 (18.2)	
Tumor border										
Expanding	12	4 (2.4)	8 (4.7)	.314	4 (2.4)	8 (4.7)	.717	6 (3.5)	6 (3.5)	.799
Infiltrative	158	33 (19.4)	125 (73.5)		61 (35.9)	97 (57.1)		73 (42.9)	85 (50.0)	
Distant metastasis										
Synchronous	110	23 (13.5)	87 (51.2)	.714	45 (26.5)	65 (38.2)	.331	52 (30.6)	58 (34.1)	.776
Metachronous	60	14 (8.2)	46 (21.7)		20 (11.8)	40 (23.5)		27 (15.9)	33 (19.4)	
pTNM stage at initial diagnosis										
I, II	20	5 (2.9)	15 (8.8)	.709	4 (2.4)	16 (9.4)	.074	9 (5.3)	11 (6.5)	.888
III, IV	150	32 (18.8)	118 (69.4)		61 (35.9)	89 (52.4)		70 (41.2)	80 (47.1)	
MSI status										
MSS/MSI-L	157	35 (21.9)	122 (76.3)	.650	59 (36.9)	98 (61.3)	.304	74 (46.3)	83 (51.9)	.069
MSI-H	3	1 (0.6)	2 (1.3)		2 (1.3)	1 (0.6)		3 (1.9)	0	

Values are presented as number (%). p-values are calculated by using chi-square test or Fisher exact test.
miR-21, microRNA-21; CRC, colorectal cancer; T, tumor; LG, low grade; HG, high grade; LN, lymph node; MSI, microsatellite instability; MSS, microsatellite stable; MSI-L, microsatellite instability–low; MSI-H, microsatellite instability–high.

cases (31.7%). Discordance between the center and distant metastasis was detected in 76 cases (44.7%). Thus, regional heterogeneity of miR-21 stromal expression was very common in patients with advanced CRC.

Clinical implications of miR-21 stromal expression in advanced CRC patients

Table 2 shows the relationships between miR-21 status and the clinicopathological parameters of patients with advanced CRC. In the periphery of primary tumor, miR-21 expression was correlated with less aggressive features, including histologic low grade differentiation (p = .002). In addition, lymphatic invasion and lymph node metastasis was frequently observed in patients with CRC negative for miR-21 (p = .042 and p = .017, respectively). There was no statistically significant correlation between the clinicopathological factors and miR-21 expression in the center of the primary tumors and distant metastatic tumors (p > .05). The expression of miR-21 in distant metastasis was different according to metastatic site (Table 3). miR-21 stromal expression was more frequently observed in lung metastasis and peritoneal seeding (p = .046).

Table 3. Expression of miR-21 in distant metastasis according to metastatic site in 170 advanced CRC patients

Site of metastasis	Total	miR-21 in metastasis		p-value
		Negative	Positive	
Liver	76	42 (24.7)	34 (20.0)	.046
Lung	37	13 (7.6)	24 (14.1)	
Seeding	37	13 (7.6)	24 (14.1)	
Distant nodes	2	0	2 (1.2)	
Ovary	18	11 (6.5)	7 (4.1)	
Total	170	79	91	

Values are presented as number (%).
miR-21, microRNA-21; CRC, colorectal cancer.

Prognostic significance of miR-21 stromal expression in advanced CRC patients

All 170 patients with advanced CRC were successfully followed up for inclusion in the survival analysis (Fig. 2). The mean follow-up time was 42 months (range, 1 to 105 months) and 73 patients (42.9%) died from cancer during the follow-up period. Kaplan-Meier analysis showed that miR-21 stromal expression in the periphery of primary tumors was significantly associated with a better prognosis (p = .004). There was no significant correlation between the patients' prognosis and miR-21 expression in the center of primary tumors and distant metastases (p = .925 and p = .863, respectively).

Correlation between miR-21 stromal expression and CAF value

The regional heterogeneous values for CAF in CRC are shown in our previous study.[25] The area occupied by CAFs was the lowest in distant metastases (median, 0.91; interquartile range [IQR], 0.68 to 1.18) than any other sites (median, 1.12; IQR, 0.88 to 1.41 in the center of primary tumors and median, 1.22; IQR, 0.96 to 1.54 in the periphery of primary tumors). Mann-Whitney test showed that miR-21 expression was significantly associated with CAFs in the center of primary tumors (p = .001) and distant metastases (p = .041). In the periphery of primary tumors, miR-21 overexpression was not correlated with CAFs (p = .102) (Fig. 3).

DISCUSSION

Many predictive and prognostic molecular markers have been suggested for CRC. However, they are not reliably accepted due to a lack of reproducibility and validation. Previous studies pro-

Fig. 2. Kaplan-Meier curves illustrating the overall survival of patients with advanced colorectal cancer in relation to microRNA-21 expression. (A) Center. (B) Periphery. (C) Distant metastasis.
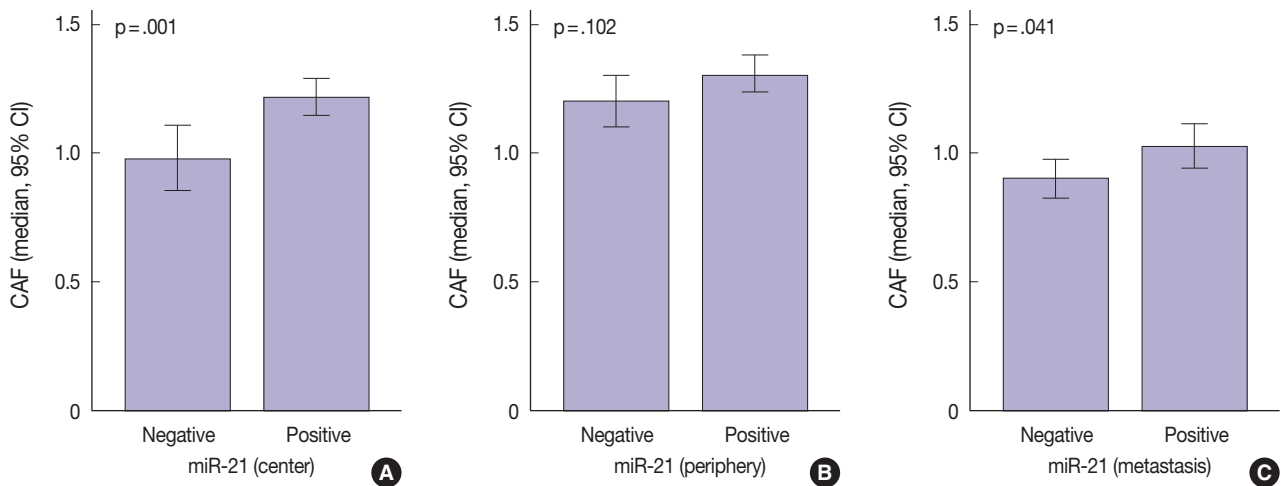
Fig. 3. Correlation between microRNA-21 (miR-21) expression and cancer associated fibroblasts (CAFs) by Mann-Whitney analysis. (A) Center. (B) Periphery. (C) Distant metastasis. CI, confidence interval.

posed that high expression of miR-21 might predict poor survival in patients with CRC.[20-24] However, elevated miR-21 level and poor prognosis correlated only in a subgroup of patients with stage II CRC.[21-24] Interestingly, our results contradict those of previous miR-21 expression studies. In our study, miR-21 expression in the periphery of primary tumors was significantly associated with a better prognosis in patients with advanced stage CRC (p = .004) (Fig. 2). Otherwise, there was no significant correlation between the prognosis and miR-21 expression in the center of primary tumors and in distant metastases (p = .925 and p = .863, respectively) (Fig. 2). This discrepancy may be explained by the fact that our cohort was largely comprised of patients with stage IV CRC (98 cases, 57.6%). They received various personalized treatments and these might reflect the statistical difference.

Bullock et al.[36] recently demonstrated that stromal miR-21 expression induced a pro-metastatic mechanism of CRC via activation of matrix metalloproteinase-2. These data highlight the importance of miR-21 deregulation in CRC metastasis. Because all patients in our study presented with advanced CRC with metastasis, miR-21 may be expressed at higher levels than that observed in previous reports. In our study, miR-21 expression in the center and periphery of primary tumors and in distant metastasis was observed in 78.2%, 61.8%, and 53.5% of the patients, respectively, whereas it was observed in 27.4% of the patients in another study.[22] Our data suggest that the lack of miR-21 expression in patients presenting with CRC with metastasis is associated with a rather poor prognosis and more frequent lymphatic invasion and lymph node metastasis (Table 2, Fig. 1), presumably because, in these patients, the metastatic mecha-

nism is controlled by other regulatory pathways. Further studies are necessary to prove that other mechanisms induce CRC metastasis, independently of miR-21. The evaluation of the prognostic value of miR-21 expression in patients with advanced CRC presenting distant metastasis might be of little importance.

Previous studies in various cancers indicated that miR-21 localizes mainly in the cancer stroma and more particularly in the stromal fibroblast-like cells.[21,22,24] This localization may be due to molecules secreted by cancer cells, which influence the microenvironment.[37-39] Meanwhile, the mechanisms of regulation of miR-21 in CAFs remain unknown. Only few studies examined the correlation between the value of CAFs and miR-21 expression.[40] Our study revealed that miR-21 expression was associated with CAF value in the center of primary tumors and distant metastases (p = .001 and p = .041, respectively) (Fig. 3). As expected, the value of CAF was greater in stroma of CRC specimens presenting miR-21 expression. Therefore, we should be careful when evaluating stromal miR-21 expression. In most previous studies, miR-21 expression was evaluated quantitatively by image analysis.[21,24,36] This method may mislead us when distinguishing miR-21 high expression from a simple increase in the number of CAFs. Thus, accurate observation should be performed to distinguish miR-21 expression from CAF increase.

To clarify miR-21 expression in CRC, being aware of the heterogeneity in miR-21 expression level is crucial because regional heterogeneity can lead to sampling bias. In recent studies, intra-tumor heterogeneity of various miRNAs was detected in colorectal, pancreatic, and breast cancer.[34,35,41] Our study indicates miR-21 regional heterogeneity, which constitutes approximately 40% of the total cohort (Table 1). Thus, a reliable assessment

of CRC miR-21 expression may include sampling of the primary tumor in several locations and metastasis.

In conclusion, we demonstrated that miR-21 is expressed in advanced CRC and that this upregulation is mainly confined to the cancer stroma. Our FISH data indicated that miR-21 expression is related to CAF value in the center of primary tumors and distant metastasis. We determined that miR-21 expression frequently presents regional heterogeneity in CRC. Such data could lead to the new perspective of miR-21 level measurement. The evaluation of miR-21 expression for the prediction of survival in patient with advanced CRC is a matter of debate.

Conflicts of Interest

No potential conflict of interest relevant to this article was reported.

REFERENCES

1. Carrington JC, Ambros V. Role of microRNAs in plant and animal development. Science 2003; 301: 336-8.

2. Zhang B, Pan X, Cobb GP, Anderson TA. microRNAs as oncogenes and tumor suppressors. Dev Biol 2007; 302: 1-12.

3. Kwak PB, Iwasaki S, Tomari Y. The microRNA pathway and cancer. Cancer Sci 2010; 101: 2309-15.

4. Chan SH, Wu CW, Li AF, Chi CW, Lin WC. miR-21 microRNA expression in human gastric carcinomas and its clinical association. Anticancer Res 2008; 28: 907-11.

5. Gabriely G, Wurdinger T, Kesari S, *et al*. MicroRNA 21 promotes glioma invasion by targeting matrix metalloproteinase regulators. Mol Cell Biol 2008; 28: 5369-80.

6. Qian B, Katsaros D, Lu L, *et al*. High miR-21 expression in breast cancer associated with poor disease-free survival in early stage disease and high TGF-beta1. Breast Cancer Res Treat 2009; 117: 131-40.

7. Markou A, Tsaroucha EG, Kaklamanis L, Fotinou M, Georgoulias V, Lianidou ES. Prognostic value of mature microRNA-21 and microRNA-205 overexpression in non-small cell lung cancer by quantitative real-time RT-PCR. Clin Chem 2008; 54: 1696-704.

8. Zhang A, Liu Y, Shen Y, Xu Y, Li X. miR-21 modulates cell apoptosis by targeting multiple genes in renal cell carcinoma. Urology 2011; 78: 474.

9. Hiyoshi Y, Kamohara H, Karashima R, *et al*. MicroRNA-21 regulates the proliferation and invasion in esophageal squamous cell carcinoma. Clin Cancer Res 2009; 15: 1915-22.

10. Asangani IA, Rasheed SA, Nikolova DA, *et al*. MicroRNA-21 (miR-21) post-transcriptionally downregulates tumor suppressor Pdcd4 and stimulates invasion, intravasation and metastasis in colorectal cancer. Oncogene 2008; 27: 2128-36.

11. Lu Z, Liu M, Stribinskis V, *et al*. MicroRNA-21 promotes cell transformation by targeting the programmed cell death 4 gene. Oncogene 2008; 27: 4373-9.

12. Mathé EA, Nguyen GH, Bowman ED, *et al*. MicroRNA expression in squamous cell carcinoma and adenocarcinoma of the esophagus: associations with survival. Clin Cancer Res 2009; 15: 6192-200.

13. Yan LX, Huang XF, Shao Q, *et al*. MicroRNA miR-21 overexpression in human breast cancer is associated with advanced clinical stage, lymph node metastasis and patient poor prognosis. RNA 2008; 14: 2348-60.

14. Yu Y, Nangia-Makker P, Farhana L, Rajendra SG, Levi E, Majumdar AP. miR-21 and miR-145 cooperation in regulation of colon cancer stem cells. Mol Cancer 2015; 14: 98.

15. Kanaan Z, Rai SN, Eichenberger MR, *et al*. Plasma miR-21: a potential diagnostic marker of colorectal cancer. Ann Surg 2012; 256: 544-51.

16. Ng EK, Chong WW, Jin H, *et al*. Differential expression of microRNAs in plasma of patients with colorectal cancer: a potential marker for colorectal cancer screening. Gut 2009; 58: 1375-81.

17. Huang Z, Huang D, Ni S, Peng Z, Sheng W, Du X. Plasma microRNAs are promising novel biomarkers for early detection of colorectal cancer. Int J Cancer 2010; 127: 118-26.

18. Yu Y, Sarkar FH, Majumdar AP. Down-regulation of miR-21 induces differentiation of chemoresistant colon cancer cells and enhances susceptibility to therapeutic regimens. Transl Oncol 2013; 6: 180-6.

19. Valeri N, Gasparini P, Braconi C, *et al*. MicroRNA-21 induces resistance to 5-fluorouracil by down-regulating human DNA MutS homolog 2 (hMSH2). Proc Natl Acad Sci U S A 2010; 107: 21098-103.

20. Xia X, Yang B, Zhai X, *et al*. Prognostic role of microRNA-21 in colorectal cancer: a meta-analysis. PLoS One 2013; 8: e80426.

21. Kjaer-Frifeldt S, Hansen TF, Nielsen BS, *et al*. The prognostic importance of miR-21 in stage II colon cancer: a population-based study. Br J Cancer 2012; 107: 1169-74.

22. Kang WK, Lee JK, Oh ST, Lee SH, Jung CK. Stromal expression of miR-21 in T3-4a colorectal cancer is an independent predictor of early tumor relapse. BMC Gastroenterol 2015; 15: 2.

23. Zhang JX, Song W, Chen ZH, *et al*. Prognostic and predictive value of a microRNA signature in stage II colon cancer: a microRNA ex-

pression analysis. Lancet Oncol 2013; 14: 1295-306.

24. Nielsen BS, Jørgensen S, Fog JU, *et al*. High levels of microRNA-21 in the stroma of colorectal cancers predict short disease-free survival in stage II colon cancer patients. Clin Exp Metastasis 2011; 28: 27-38.

25. Kwak Y, Lee HE, Kim WH, Kim DW, Kang SB, Lee HS. The clinical implication of cancer-associated microvasculature and fibroblast in advanced colorectal cancer patients with synchronous or metachronous metastases. PLoS One 2014; 9: e91811.

26. Tsujino T, Seshimo I, Yamamoto H, *et al*. Stromal myofibroblasts predict disease recurrence for colorectal cancer. Clin Cancer Res 2007; 13: 2082-90.

27. Trimboli AJ, Cantemir-Stone CZ, Li F, *et al*. Pten in stromal fibroblasts suppresses mammary epithelial tumours. Nature 2009; 461: 1084-91.

28. Knijn N, Tol J, Punt CJ. Current issues in the targeted therapy of advanced colorectal cancer. Discov Med 2010; 9: 328-36.

29. O'Connell MJ, Campbell ME, Goldberg RM, *et al*. Survival following recurrence in stage II and III colon cancer: findings from the ACCENT data set. J Clin Oncol 2008; 26: 2336-41.

30. Albanese I, Scibetta AG, Migliavacca M, *et al*. Heterogeneity within and between primary colorectal carcinomas and matched metastases as revealed by analysis of Ki-ras and p53 mutations. Biochem Biophys Res Commun 2004; 325: 784-91.

31. Park JH, Han SW, Oh DY, *et al*. Analysis of *KRAS*, *BRAF*, *PTEN*, *IGF1R*, *EGFR* intron 1 CA status in both primary tumors and paired metastases in determining benefit from cetuximab therapy in colon cancer. Cancer Chemother Pharmacol 2011; 68: 1045-55.

32. Baldus SE, Schaefer KL, Engers R, Hartleb D, Stoecklein NH, Gabbert HE. Prevalence and heterogeneity of *KRAS*, *BRAF*, and *PIK-3CA* mutations in primary colorectal adenocarcinomas and their corresponding metastases. Clin Cancer Res 2010; 16: 790-9.

33. Villegas-Ruiz V, Juárez-Méndez S, Pérez-González OA, *et al*. Heterogeneity of microRNAs expression in cervical cancer cells: overexpression of miR-196a. Int J Clin Exp Pathol 2014; 7: 1389-401.

34. Jepsen RK, Novotny GW, Klarskov LL, Christensen IJ, Riis LB, Høgdall E. Intra-tumor heterogeneity of microRNA-92a, microRNA-375 and microRNA-424 in colorectal cancer. Exp Mol Pathol 2016; 100: 125-31.

35. Raychaudhuri M, Schuster T, Buchner T, *et al*. Intratumoral heterogeneity of microRNA expression in breast cancer. J Mol Diagn 2012; 14: 376-84.

36. Bullock MD, Pickard KM, Nielsen BS, *et al*. Pleiotropic actions of miR-21 highlight the critical role of deregulated stromal microRNAs during colorectal cancer progression. Cell Death Dis 2013; 4: e684.

37. Yamamichi N, Shimomura R, Inada K, *et al*. Locked nucleic acid in situ hybridization analysis of miR-21 expression during colorectal cancer development. Clin Cancer Res 2009; 15: 4009-16.

38. Shenouda SK, Alahari SK. MicroRNA function in cancer: oncogene or a tumor suppressor? Cancer Metastasis Rev 2009; 28: 369-78.

39. Fassan M, Pizzi M, Giacomelli L, *et al*. PDCD4 nuclear loss inversely correlates with miR-21 levels in colon carcinogenesis. Virchows Arch 2011; 458: 413-9.

40. Aprelikova O, Green JE. MicroRNA regulation in cancer-associated fibroblasts. Cancer Immunol Immunother 2012; 61: 231-7.

41. Lou E, Subramanian S, Steer CJ. Pancreatic cancer: modulation of KRAS, microRNAs, and intercellular communication in the setting of tumor heterogeneity. Pancreas 2013; 42: 1218-26.

■ ORIGINAL ARTICLE ■

Detection of Tumor Multifocality Is Important for Prediction of Tumor Recurrence in Papillary Thyroid Microcarcinoma: A Retrospective Study and Meta-Analysis

Jung-Soo Pyo · Jin Hee Sohn
Guhyun Kang[1]

Department of Pathology, Kangbuk Samsung
Hospital, Sungkyunkwan University School of
Medicine, Seoul; [1]Department of Pathology, Inje
University Sanggye Paik Hospital, Inje University
College of Medicine, Seoul, Korea

Corresponding Author
Jin Hee Sohn, MD
Department of Pathology, Kangbuk Samsung
Hospital, Sungkyunkwan University School of
Medicine, 29 Saemunan-ro, Jongno-gu, Seoul
03181, Korea
Tel: +82-2-2001-2391
Fax: +82-2-2001-2398
E-mail: jhpath.sohn@samsung.com

Background: The clinicopathological characteristics and conclusive treatment modality for multifocal papillary thyroid microcarcinoma (mPTMC) have not been fully established. **Methods:** A retrospective study, systematic review, and meta-analysis were conducted to elucidate the clinicopathological significance of mPTMC. We investigated the multiplicity of 383 classical papillary thyroid microcarcinomas (PTMCs) and the clinicopathological significance of incidental mPTMCs. Correlation between tumor recurrence and multifocality in PTMCs was evaluated through a systematic review and meta-analysis. **Results:** Tumor multifocality was identified in 103 of 383 PTMCs (26.9%). On linear regression analysis, primary tumor diameter was significantly correlated with tumor number ($R^2 = 0.014$, $p = .021$) and supplemental tumor diameter ($R^2 = 0.117$, $p = .023$). Of 103 mPTMCs, 61 (59.2%) were non-incidental, with tumor detected on preoperative ultrasonography, and 42 (40.8%) were diagnosed (incidental mPTMCs) on pathological examination. Lymph node metastasis and higher tumor stage were significantly correlated with tumor multifocality. However, there was no difference in nodal metastasis or tumor stage between incidental and non-incidental mPTMCs. On meta-analysis, tumor multifocality was significantly correlated with tumor recurrence in PTMCs (odds ratio, 2.002; 95% confidence interval, 1.475 to 2.719, $p < .001$). **Conclusions:** Our results show that tumor multifocality in PTMC, regardless of manner of detection, is significantly correlated with aggressive tumor behavior.

Key Words: Papillary thyroid microcarcinoma; Multifocal; Incidental; Retrospective studies; Meta-analysis

Papillary thyroid microcarcinoma (PTMC) measuring 1 cm or less in diameter is the most common variant of papillary thyroid carcinoma (PTC). The incidence of PTMC has recently been increasing in many countries. This increase is partially attributed to the broader availability of ultrasonography (US) and computed tomography diagnostic modalities and to more frequent health screening with increased awareness of this tumor type.[1] If the primary contributor to increasing PTMC incidence is improved detection, then the proportion of late-stage and large tumors should be declining. However, the incidence of larger tumors is also increasing.[2] This pattern of increasing incidence cannot be completely explained by increased detection or more frequent health screening. Furthermore, over-diagnosis and over-treatment of PTMCs are important issues that warrant more detailed evaluation. Although PTMCs have similar molecular characteristics to PTCs larger than 1 cm (overt PTCs),[3] PTMCs generally have a better outcome profile than overt PTCs.[4,5] However, some

PTMCs demonstrate loco-regional and lymph node recurrence,[4] and diagnostic delays can result in higher rates of distant metastasis.[6]

Old age, lymph node metastasis, extrathyroidal extension, and multifocality or bilaterality are considered high risk factors of PTC.[7,8] Although the American Joint Committee on Cancer (AJCC) tumor node metastasis (TNM) classification system recommends describing tumor multifocality, TNM stage is not influenced by multifocality.[9] Furthermore, definite evaluation and treatment modalities have not been established for multifocality in PTMC. Based on American Thyroid Association (ATA) management guidelines,[7] patients with overt PTC with high risk factors are recommended to undergo total thyroidectomy with lymph node dissection.[7,10] However, no definitive treatment guidelines for PTMC with high-risk factors have been recommended. Hemithyroidectomy or subtotal thyroidectomy is generally considered adequate treatment for unifocal PTMC (uPT-

MC), while the extent of surgical resection for multifocal PTMC (mPTMC) remains controversial.[11] If incidental mPTMC is considered, the true rate of mPTMC could be higher than previously reported. The clinicopathological significance of multifocality in PTMC is not well established, and distinct treatment guidelines should be considered.

In the present study, we retrospectively investigated the clinicopathological significance and multifocality of PTMC with regard to primary tumor size. To evaluate the clinicopathological significance of incidentally detected mPTMC, the rate of incidental mPTMC and its characteristics were investigated and compared with those of non-incidental mPTMC. Recurrence of mPTMC was also evaluated through meta-analysis.

MATERIALS AND METHODS

Patients

We investigated 383 consecutive classical PTMC patients from the Department of Pathology, Kangbuk Samsung Hospital, Sungkyunkwan University School of Medicine (Seoul, Korea) from January 1, 2010 to December 31, 2011. The correlations between multifocality and clinicopathological characteristics including age, sex, tumor size, extrathyroidal extension, lymph node metastasis, pTNM stage, and US findings were evaluated by reviewing medical charts, pathology records, and glass slides and based on the seventh edition AJCC TNM classification system.[9] Patients had undergone either total thyroidectomy (n = 237) or lobectomy (including hemithyroidectomy) (n = 146) with lymph node dissection. The decisions to perform lymph node dissection and the extent of dissection were made by the surgeon based on ATA management guidelines[7] and various risk-evaluation systems.[5,9,12,13] The mean age of patients was 45.4 ± 10.4 years, the mean tumor size of the largest dominant tumor was 0.65 ± 0.20 cm, and the sex ratio (male:female) was 1:3.85. By AJCC stage grouping, there were 295 cases in stage I, 0 cases in stage II, 86 cases in stage III, and two cases in stage IV. The study protocol was approved by the Institutional Review Board (IRB) of Kangbuk Samsung Hospital (IRB No. KBC12202), who confirmed informed consents.

Definition and evaluation of tumor multifocality

Sections were cut to a thickness of 0.2 cm for postoperative pathological examination. All tumors detected during inspection were histologically examined. For evaluation of extrathyroidal extension, peritumoral parenchyma with thyroidal capsule was included. In addition, one section with normal-appearing parenchyma was included from each lobe. mPTMCs were defined as tumors with an intertumoral distance greater than 0.5 cm in the ipsilateral lobe or contralateral lobe of the primary tumor.[14] The number of tumors ranged from two to six (mean, 2.36 ± 0.70), and we designated PTMCs other than the largest tumor as supplemental tumors. Cases were subdivided into three groups based on preoperative US findings. The first group included suspicious mPTMCs, the second group included uPTMCs accompanied by benign or indeterminate nodules, and the third group included suspicious uPTMCs. Within the second and third groups, incidental mPTMCs were defined as those discovered on pathological examination, which were not detected on preoperative US. US evaluation was performed by radiologists at our institution, and results were reported according to standard criteria.

Literature search and selection criteria

Relevant articles were obtained by searching PubMed and MEDLINE databases up to January 15, 2015. Searches were performed using the keywords "papillary thyroid carcinoma" and "multifocal." The title and abstract of all searched articles were screened for exclusion. Review articles were also screened to find additional eligible studies. Search results were then scanned according to the following inclusion and exclusion criteria: (1) PTC investigated in human tissue, (2) available information regarding tumor recurrence in uPTMC and mPTMC, (3) case reports or non-original articles were excluded, and (4) non-English language publications were excluded.

Data extraction

Data from all eligible studies were extracted by two authors. The following data were extracted from each of the eligible studies: the first author's name, year of publication, number of patients analyzed, and number of patients with tumor recurrence.

Statistical analysis

Statistical analyses were conducted using SPSS ver. 18.0 software (SPSS Inc., Chicago, IL, USA). The significance of tumor multifocality and correlations with clinicopathological parameters were determined by either chi-squre test or the Fisher exact test (two-sided). The relationship between tumor multifocality and tumor size was analyzed using a two-tailed Student's t test. Linear regression analysis was conducted to investigate correlations between primary tumor size and tumor multifocality, number of tumor, and supplemental tumor size. In addition, multivariate logistic regression analysis was performed to identify the

most influential variables associated with tumor multifocality. To perform the meta-analysis, Comprehensive Meta-Analysis ver. 2 software (Biostat, Engelwood, NJ, USA) was used. Odds ratio (OR) with a 95% confidence interval (CI) was calculated by fixed-effect and random-effect models and used to evaluate the correlation between tumor multifocality and recurrence. Heterogeneity between studies was evaluated with the Q test, I^2, and p-values. Publication bias was assessed via Begg's funnel plot and Egger's test. All statistical analysis was reviewed by a statistician. The results were two-sided and were considered statistically significant when p < .05.

RESULTS

Clinicopathological features of mPTMCs

We initially investigated the correlations between tumor multifocality and clinicopathological parameters in 383 resected classical PTMCs. Tumor multifocality was noted in 103 of 383 PTMCs (26.9%), and nodal metastasis occurred at significantly higher rates in mPTMCs than in uPTMCs (p = .003). Patients who underwent total thyroidectomy showed a higher incidence of tumor multifocality than patients who underwent lobectomy (p < .001). For the 83 mPTMCs in which total thyroidectomy was undertaken, tumor bilaterality was 62.7% (52 of 83). mPTMC showed a significant correlation with higher TNM stage than uPTMC (p < .001). There were no significant differences with respect to age, sex, tumor size, or extrathyroidal extension (Table 1). On multivariate analysis, tumor multifocality was significantly correlated with lymph node metastasis (p = .002) but not age (≥45 years), sex, or extrathyroidal extension.

On preoperative US, tumor multiplicity was found in 180 cases including 54 suspicious mPTMC cases. Among suspicious mPTMCs, 41 cases were confirmed as mPTMCs (non-incidental mPTMCs) on pathological examination. For the remaining 126 suspicious uPTMCs accompanied by benign or indeterminate nodules, 20 cases were confirmed to be mPTMC (non-incidental mPTMC). Nineteen cases (three suspicious mPTMC cases and 16 non-suspicious mPTMC cases) involved incidentally found PTMCs (incidental mPTMCs) that were not identified preoperatively. In 203 cases regarded as uPTMCs on preoperative US, 23 supplemental PTMCs were incidentally discovered on pathological examination (incidental mPTMCs). In total, 103 mPTMCs (61 non-incidental and 42 incidental) of 383 PTMCs were identified (Fig. 1).

Distribution of mPTMC based on primary tumor size

The distribution of mPTMCs based on primary tumor size was investigated and is shown in Fig. 2A. The rate of mPTMC occurrence was 0%–34.4% and was shown to increase with increasing primary tumor size on linear regression analysis ($R^2 =$

Table 1. Correlation between tumor multifocality and clinicopathological features in PTMCs

Clinicopathological feature (n = 383)	Multifocal PTMC (n = 103, 26.9%)	Unifocal PTMC (n = 280, 73.1%)	p-value
Age (yr)			
<45	43 (41.7)	144 (51.4)	.093
≥45	60 (58.3)	136 (48.6)	
Gender			
Male	18 (17.5)	61 (21.8)	.355
Female	85 (82.5)	219 (78.2)	
Tumor size (cm)	0.67 ± 0.19	0.64 ± 0.20	.389
Total thyroidectomy	83 (80.6)	154 (55.0)	< .001
Lobectomy	20 (19.4)	126 (45.0)	
Extrathyroidal extension			
Present	54 (52.4)	125 (44.6)	.176
Absent	49 (47.6)	155 (55.4)	
Lymph node metastasis			
Present	52 (50.5)	95 (33.9)	.003
Absent	51 (49.5)	185 (66.1)	
Tumor stage			
I	52 (50.5)	203 (72.5)	< .001
II	0	0	
III	51 (49.5)	75 (26.8)	
IV	0	2 (0.7)	

Values are presented as number (%) or mean ± standard deviation.
PTMC, papillary thyroid microcarcinoma.
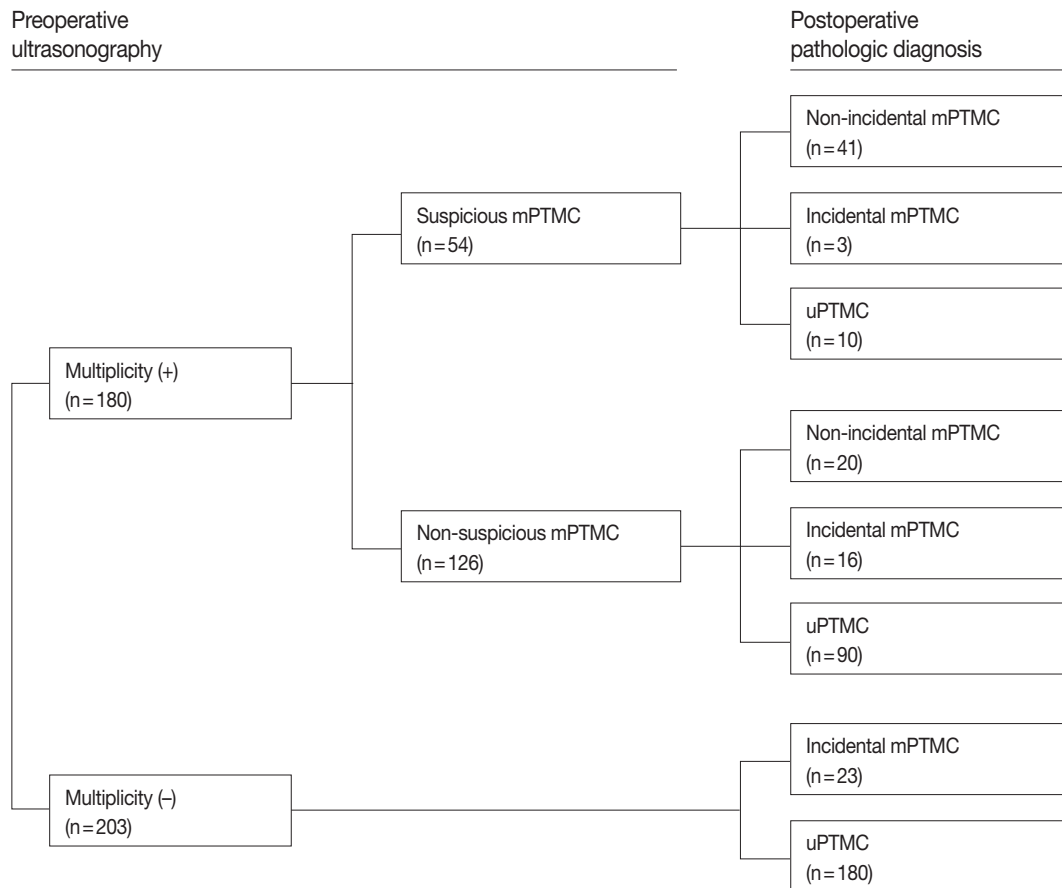
Fig. 1. Diagnostic flow in 383 patients based on preoperative ultrasonography. mPTMC, multifocal papillary thyroid microcarcinoma; uPTMC, unifocal papillary thyroid microcarcinoma.

0.519 and p = .019). PTMCs were divided with a cutoff of 0.3 cm, and the mPTMC rate was 5.9% in PTMCs smaller than 0.3 cm and 27.9% in PTMCs larger than 0.3 cm. In addition, the number of tumors and supplemental tumor size were significantly increased according to primary tumor size ($R^2 = 0.014$, p = .021 and $R^2 = 0.117$, p = .023, respectively) (Fig. 2B, C).

Lymph node metastasis in incidental and non-incidental mPTMC

Forty-two cases (40.8%) were incidentally diagnosed as mPTMC via postoperative pathological examination. To understand the significance of incidentally discovered supplemental tumors in mPTMC, we compared clinicopathological characteristics between incidental and non-incidental mPTMCs. The mean sizes of supplemental tumors were 0.23 ± 0.12 cm in incidental mPTMCs and 0.41 ± 0.17 cm in non-incidental mPTMCs. As expected, supplemental tumor size was significantly smaller in incidental mPTMCs than in non-incidental mPTMCs (p < .001), even though the largest tumor size did not differ (p = .870). The

rate of extrathyroidal extension was higher in incidental mPTMCs than in non-incidental mPTMCs (p = .016), but there was no difference in lymph node metastasis (p = .199) (Table 2).

Systematic review and meta-analysis

We performed a systematic review and meta-analysis to confirm the difference of tumor recurrence between uPTMC and mPTMC. One hundred fifty-six studies were identified through a database search and were screened (Fig. 3); 148 of these studies were excluded due to no or insufficient information (123), studies on other disease (10), case reports or non-original articles (13), and non-English-language articles (2). Eight eligible studies and 5,665 patients were included in the current meta-analysis.[15-22] Tumor multifocality was found in 1,844 of 5,665 overall PTMCs (32.6%). In the eligible studies, the rates of tumor multifocality were 24.0%–42.5%. Our meta-analysis showed significant correlation between tumor recurrence and mPTMCs in fixed-effect (OR, 2.002; 95% CI, 1.475 to 2.719; p < .001) and random-effect (OR, 2.118; 95% CI, 1.323 to 3.390; p = .002)
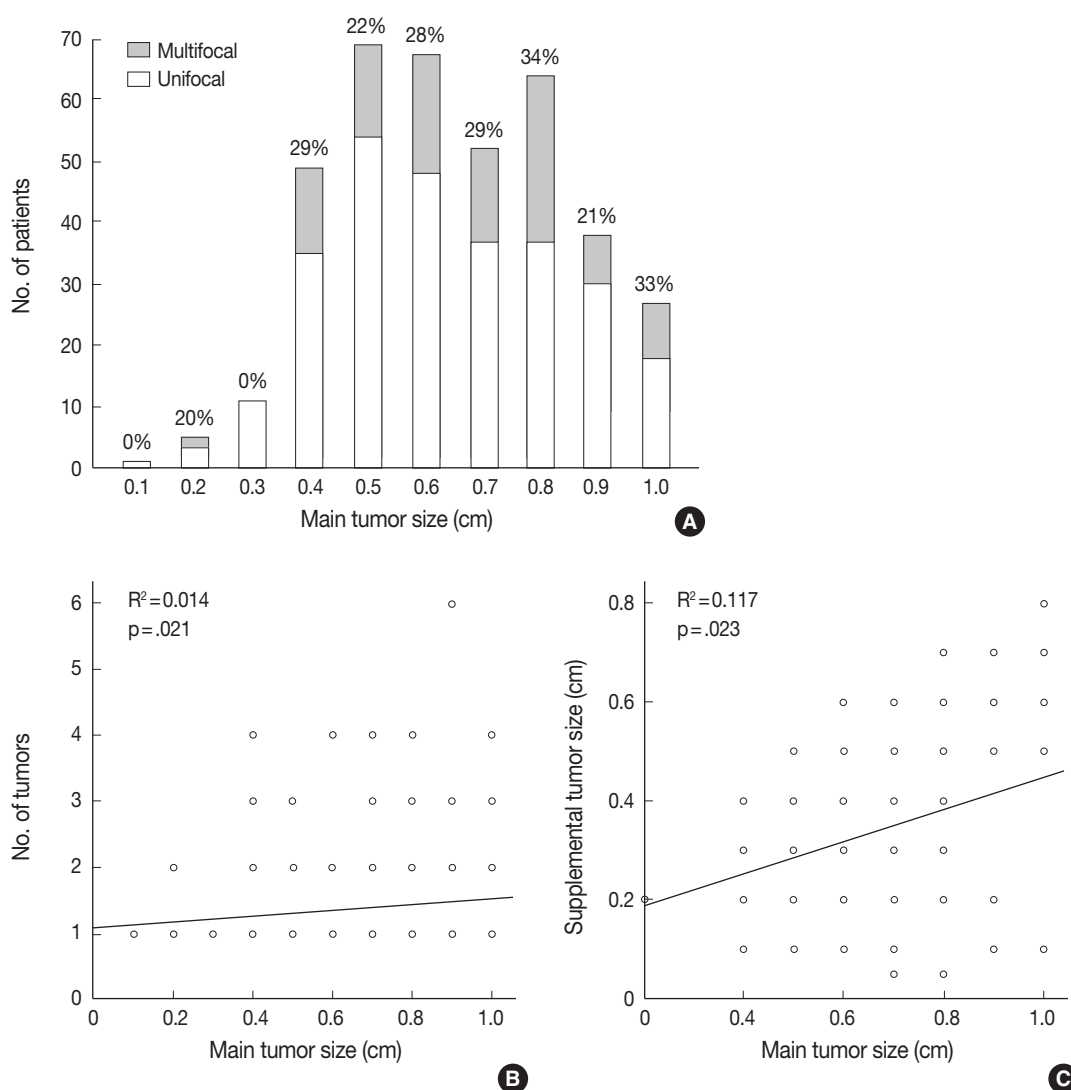
Fig. 2. Correlation between primary tumor size and multifocality in papillary thyroid microcarcinoma (PTMC). (A) Distribution of tumor multifocality based on primary tumor size in PTMC. (B) Correlation between primary tumor size and number of tumors using linear regression. (C) Correlation between primary and supplemental tumor size by linear regression.

models (Fig. 4). On sensitivity analysis, OR ranges were 1.736–2.277 and 1.907–2.417 in fixed-effect and random-effect models, respectively, and estimated ORs were not affected by eligible studies. No significant heterogeneity was identified ($I^2 = 47.4\%$, $p = .065$). There was no definite asymmetry in Begg's funnel plot (data not shown). Egger's test showed no evidence of publication bias ($p = .432$).

DISCUSSION

Multifocal PTCs are associated with loco-regional recurrence and lymph node metastasis;[10] however, the clinicopathological significance and appropriate treatment modalities for mPTMC remain unclear. In addition, little is known about the clinicopathological characteristics of incidental mPTMCs. To the best of our knowledge, this is the first report showing the clinicopathological significance of incidental mPTMCs and the correlation between tumor recurrence and mPTMCs using meta-analysis.

The incidence of PTMCs has rapidly increased in recent years.[23-25] It is debated whether PTMC is a normal finding, equivalent to disease, or a precursor of overt PTC.[23] Ito *et al.*[4] reported that the rate of PTMC enlargement without unfavorable features was 6.4% at 5 years and 15.9% at 10 years. In previous reports, distant metastasis and mortality occurred more rarely in PTMC than in overt PTC.[26,27] However, there are many reports showing that PTMCs show similar rates of extrathyroidal extension

Table 2. Analysis of clinicopathological features between incidental and non-incidental mPTMCs

Clinicopathological feature (n = 103)	mPTMCs		p-value
	Incidental (n = 42, 40.8%)	Non-incidental (n = 61, 59.2%)	
Age (yr)			
< 45	18 (42.9)	25 (41.0)	.850
≥ 45	24 (57.1)	36 (59.0)	
Gender			
Male	5 (11.9)	13 (21.3)	.217
Female	37 (88.1)	48 (78.7)	
Main tumor size (cm)	0.66±0.19	0.67±0.19	.801
Supplemental tumor size (cm)	0.23±0.12	0.41±0.17	<.001
Total thyroidectomy	29 (69.0)	54 (88.5)	.014
Lobectomy	13 (31.0)	7 (11.5)	
Extrathyroidal extension			
Present	28 (66.7)	26 (42.6)	.016
Absent	14 (33.3)	35 (57.4)	
Lymph node metastasis			
Present	18 (42.9)	34 (55.7)	.199
Absent	24 (57.1)	27 (44.3)	
Tumor stage			
I	21 (50.0)	30 (49.2)	>.999
II	0	0	
III	21 (50.0)	31 (50.8)	
IV	0	0	

Values are presented as number (%) or mean ± standard deviation.
mPTMC, multifocal papillary thyroid microcarcinoma.
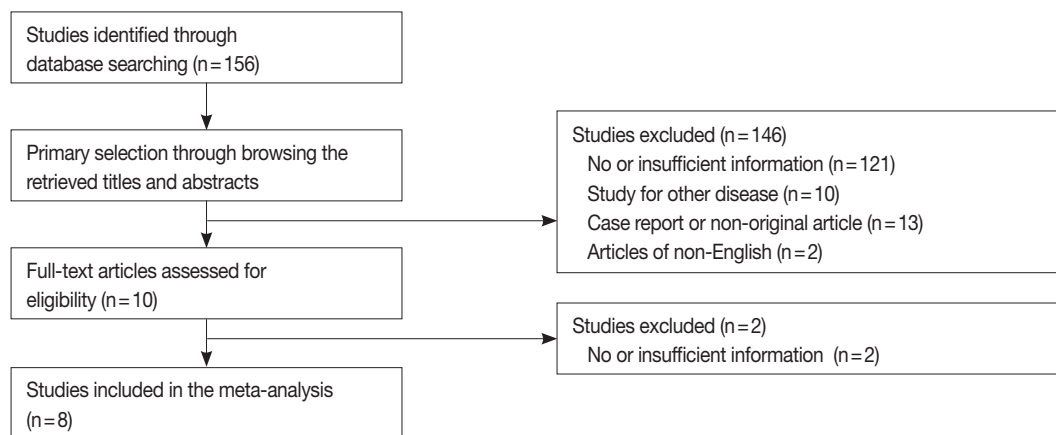
Fig. 3. Flow chart of study search and selection.

and nodal metastasis (40.3% to 64.1%).[23-25,28,29] In addition, a recent meta-analysis showed that total thyroidectomy was significantly correlated with lower recurrence and mortality rates in PTMC.[30] Patients who underwent total thyroidectomy showed a higher incidence of tumor multifocality than patients who underwent lobectomy (p < .001). In 83 mPTMCs that underwent total thyroidectomy, tumor bilaterality was 62.7% (52 of 83). Still, the unfavorable factors that can result in aggressive behavior and impact prognosis in PTMCs remain unclear.

Tumor multifocality is not considered a high-risk factor in

systems including AGES (Age, Grade, Extent, Size), AMES (Age, Distant metastasis, Extent, Size), MACIS (Distant metastasis, Age, Completeness of resection, Local invasion, Size), and GAMES (Grade, Age, Distant metastasis, Extent, Size).[6,12,13] Our data showed that tumor multifocality was significantly associated with nodal metastasis in 26.9% of total PTMCs, as in previous studies.[15,17-19] However, in the PTMCs of some previous studies, the correlation between tumor multifocality and recurrence wascontroversial.[15-22] Further cumulative prospective studies or meta-analysis should be performed to determine the clinico-

Model	Study name	Statistics for each study				Odds ratio and 95% CI
		Odds ratio	Lower limit	Upper limit	p-value	
	Baudin 1998[15]	7.781	1.647	36.758	.010	
	Chow 2003[16]	3.375	1.028	11.085	.045	
	Hay 2008[17]	2.893	1.621	5.161	.000	
	Kim 2015[18]	1.838	0.948	3.565	.072	
	Lombardi 2010[19]	11.509	1.420	93.285	.022	
	Neuhold 2011[20]	0.733	0.076	7.084	.788	
	Ross 2009[21]	1.368	0.706	2.651	.353	
	Zheng 2013[22]	0.960	0.434	2.122	.920	
Fixed		2.002	1.475	2.719	.000	
Randon		2.118	1.323	3.390	.002	

0.1 0.2 0.5 1 2 5 10
Favours A   Favours B

Fig. 4. Forest plot diagram of tumor recurrence difference between multifocal and unifocal papillary thyroid microcarcinomas.[15-22] CI, confidence interval.

pathological significance of mPTMC. Our meta-analysis showed that tumor recurrence was significantly higher in mPTMC than in uPTMC (Fig. 4). Regrettably, our data could not be included in the meta-analysis due to limitations including no recurrence cases during follow-up and short follow-up period (3 years). In addition, the current meta-analysis did not allow subgroup analysis based on positive or negative resection margins due to insufficient information provided in the eligible studies. Kuo *et al.*[31] reported that mPTMC was associated with worse survival than uPTMC but reported no difference in survival between multifocal overt PTC (> 1 cm) and mPTMC. Our results and earlier studies suggest that tumor multifocality in PTMCs, regardless of tumor size, is a useful predictive factor of aggressive tumor behavior, such as lymph node metastasis and tumor recurrence. It might be appropriate to manage patients with mPTMC differently than patients with uPTMC having no unfavorable factors.

Incidental PTMC is defined as PTMC incidentally discovered and confirmed by gross and/or microscopic examination from surgical specimens resected for the evaluation of other disease entities.[32,33] However, no clear definition for incidental mPTMC has been previously provided. In this study, we defined incidental mPTMC as supplemental tumors not detected on preoperative US that were discovered on pathological examination. Although these supplemental tumors are important for diagnosis of multifocality, the characteristics of supplemental tumors have not been previously described. In the present study, incidental mPTMCs accounted for 40.8% of the total mPTMC according to our criteria. Interestingly, incidental mPTMC was not found in PTMCs 0.3 cm or smaller. However, the lower limit of tumor size detectable on US is unclear, and more controlled and careful histological examination for entirely submitted cases is need-

ed to identify tumor multifocality. The mean size of incidentally discovered supplemental tumors was 0.27 ± 0.15 cm, which was significantly smaller than non-incidental tumors (p < .001). The supplemental tumor size of mPTMC decreased with decreasing primary tumor size (Fig. 2). The smaller size explains the lack of detection during preoperative US. However, there was no difference in nodal metastasis rate between incidental and non-incidental mPTMC. This finding suggests that tumor multifocality itself, rather than the manner of detection, is related to lymph node metastasis. In addition, the detection rate of incidental mPTMC might influence the rate of mPTMC. If these supplemental tumors are missed in pathological examination, cases are diagnosed as uPTMC and not mPTMC. Therefore, detailed examination for multiple tumors using preoperative US study and adequate postoperative pathological examination is essential in the diagnosis of PTMC.

We previously reported that evaluation of tumor multifocality based on total surface area is useful to distinguish aggressive mPTMC from less aggressive mPTMC and uPTMC.[14] On that basis, we concluded that careful detection of multifocal tumors is important despite discrepant reporting on multifocality. The discrepancies largely seem to result from different manners of pathological examination and the number of sections analyzed. Although radiological tools have improved, tumors smaller than 0.3 cm are not easily detected via radiological examination. In the present study, only four of 383 PTMCs were smaller than 0.3 cm. Among them, two cases were 0.2 cm on histological examination, after appearing larger than 0.3 cm on preoperative US. Suspicious nodules on preoperative US in the remaining two cases were confirmed as benign nodules on histological examination. Another two incidentally detected nodules (0.2 cm and 0.1 cm) were diagnosed as PTMC. Therefore, there were no sus-

picious nodules smaller than 0.3 cm reported preoperatively. In addition, it is difficult to confirm PTMC in preoperative fine-needle aspiration for tumors smaller than 0.5 cm,[34] which require thin sections in postoperative gross examination for non-detected small nodules. Because it is difficult to cut 0.2-cm-thick slices of specimens prior to fixation, thin sectioning after proper fixation is required for assessment of tumor multifocality.

In conclusion, this study demonstrates that tumor multifocality in PTMC is significantly correlated with lymph node metastasis. Our meta-analysis revealed a positive correlation between tumor multifocality and tumor recurrence in PTMC. Therefore, careful attention should be paid to detection of mPTMC, which behaves differently from uPTMC, on preoperative and postoperative examination.

Conflicts of Interest

No potential conflict of interest relevant to this article was reported.

REFERENCES

1. Mercante G, Frasoldati A, Pedroni C, *et al*. Prognostic factors affecting neck lymph node recurrence and distant metastasis in papillary microcarcinoma of the thyroid: results of a study in 445 patients. Thyroid 2009; 19: 707-16.

2. Enewold L, Zhu K, Ron E, *et al*. Rising thyroid cancer incidence in the United States by demographic and tumor characteristics, 1980-2005. Cancer Epidemiol Biomarkers Prev 2009; 18: 784-91.

3. Park YJ, Kim YA, Lee YJ, *et al*. Papillary microcarcinoma in comparison with larger papillary thyroid carcinoma in *BRAFV600E* mutation, clinicopathological features, and immunohistochemical findings. Head Neck 2010; 32: 38-45.

4. Ito Y, Miyauchi A, Inoue H, *et al*. An observational trial for papillary thyroid microcarcinoma in Japanese patients. World J Surg 2010; 34: 28-35.

5. Sugitani I, Toda K, Yamada K, Yamamoto N, Ikenaga M, Fujimoto Y. Three distinctly different kinds of papillary thyroid microcarcinoma should be recognized: our treatment strategies and outcomes. World J Surg 2010; 34: 1222-31.

6. Mazzaferri EL. Managing small thyroid cancers. JAMA 2006; 295: 2179-82.

7. American Thyroid Association (ATA) Guidelines Taskforce on Thyroid Nodules and Differentiated Thyroid Cancer, Cooper DS, Doherty GM, et al. Revised American Thyroid Association management guidelines for patients with thyroid nodules and differen-

8. Lee E, Jung W, Woo JS, *et al*. Tumor sprouting in papillary thyroid carcinoma is correlated with lymph node metastasis and recurrence. Korean J Pathol 2014; 48: 117-25.

9. Edge SB, Byrd DR, Compton CC, Fritz AG, Greene FL, Trotti A. AJCC cancer staging manual. 7th ed. New York: Springer-Verlag, 2009; 87-96.

10. Mazeh H, Samet Y, Hochstein D, *et al*. Multifocality in well-differentiated thyroid carcinomas calls for total thyroidectomy. Am J Surg 2011; 201: 770-5.

11. Dietlein M, Luyken WA, Schicha H, Larena-Avellaneda A. Incidental multifocal papillary microcarcinomas of the thyroid: is subtotal thyroidectomy combined with radioiodine ablation enough? Nucl Med Commun 2005; 26: 3-8.

12. Rodríguez-Cuevas S, Labastida-Almendaro S, Cortés-Arroyo H, López-Garza J, Barroso-Bravo S. Multifactorial analysis of survival and recurrences in differentiated thyroid cancer: comparative evaluation of usefulness of AGES, MACIS, and risk group scores in Mexican population. J Exp Clin Cancer Res 2002; 21: 79-86.

13. Voutilainen PE, Siironen P, Franssila KO, Sivula A, Haapiainen RK, Haglund CH. AMES, MACIS and TNM prognostic classifications in papillary thyroid carcinoma. Anticancer Res 2003; 23: 4283-8.

14. Pyo JS, Sohn JH, Kang G, Kim DH, Yun J. Total surface area is useful for differentiating between aggressive and favorable multifocal papillary thyroid carcinomas. Yonsei Med J 2015; 56: 355-61.

15. Baudin E, Travagli JP, Ropers J, *et al*. Microcarcinoma of the thyroid gland: the Gustave-Roussy Institute experience. Cancer 1998; 83: 553-9.

16. Chow SM, Law SC, Chan JK, Au SK, Yau S, Lau WH. Papillary microcarcinoma of the thyroid-Prognostic significance of lymph node metastasis and multifocality. Cancer 2003; 98: 31-40.

17. Hay ID, Hutchinson ME, Gonzalez-Losada T, *et al*. Papillary thyroid microcarcinoma: a study of 900 cases observed in a 60-year period. Surgery 2008; 144: 980-7.

18. Kim KJ, Kim SM, Lee YS, Chung WY, Chang HS, Park CS. Prognostic significance of tumor multifocality in papillary thyroid carcinoma and its relationship with primary tumor size: a retrospective study of 2,309 consecutive patients. Ann Surg Oncol 2015; 22: 125-31.

19. Lombardi CP, Bellantone R, De Crea C, *et al*. Papillary thyroid microcarcinoma: extrathyroidal extension, lymph node metastases, and risk factors for recurrence in a high prevalence of goiter area. World J Surg 2010; 34: 1214-21.

20. Neuhold N, Schultheis A, Hermann M, Krotla G, Koperek O, Birner P. Incidental papillary microcarcinoma of the thyroid: further evidence of a very low malignant potential: a retrospective clinico-pathological study with up to 30 years of follow-up. Ann Surg Oncol

2011; 18: 3430-6.

21. Ross DS, Litofsky D, Ain KB, *et al.* Recurrence after treatment of micropapillary thyroid cancer. Thyroid 2009; 19: 1043-8.

22. Zheng X, Wei S, Han Y, *et al.* Papillary microcarcinoma of the thyroid: clinical characteristics and *BRAFV*600E mutational status of 977 cases. Ann Surg Oncol 2013; 20: 2266-73.

23. Haymart MR, Cayo M, Chen H. Papillary thyroid microcarcinomas: big decisions for a small tumor. Ann Surg Oncol 2009; 16: 3132-9.

24. Noguchi S, Yamashita H, Uchino S, Watanabe S. Papillary microcarcinoma. World J Surg 2008; 32: 747-53.

25. Mazzaferri EL. Managing thyroid microcarcinomas. Yonsei Med J 2012; 53: 1-14.

26. Papini E, Guglielmi R, Bianchini A, *et al.* Risk of malignancy in nonpalpable thyroid nodules: predictive value of ultrasound and color-Doppler features. J Clin Endocrinol Metab 2002; 87: 1941-6.

27. Strate SM, Lee EL, Childers JH. Occult papillary carcinoma of the thyroid with distant metastases. Cancer 1984; 54: 1093-100.

28. Roh JL, Kim JM, Park CI. Central cervical nodal metastasis from papillary thyroid microcarcinoma: pattern and factors predictive of nodal metastasis. Ann Surg Oncol 2008; 15: 2482-6.

29. Cheema Y, Olson S, Elson D, Chen H. What is the biology and optimal treatment for papillary microcarcinoma of the thyroid? J Surg Res 2006; 134: 160-2.

30. Macedo FI, Mittal VK. Total thyroidectomy versus lobectomy as initial operation for small unilateral papillary thyroid carcinoma: a meta-analysis. Surg Oncol 2015; 24: 117-22.

31. Kuo SF, Lin SF, Chao TC, Hsueh C, Lin KJ, Lin JD. Prognosis of multifocal papillary thyroid carcinoma. Int J Endocrinol 2013; 2013: 809382.

32. Ito Y, Miyauchi A. Appropriate treatment for asymptomatic papillary microcarcinoma of the thyroid. Expert Opin Pharmacother 2007; 8: 3205-15.

33. Yu XM, Lloyd R, Chen H. Current treatment of papillary thyroid microcarcinoma. Adv Surg 2012; 46: 191-203.

34. Renshaw AA. Sensitivity of fine-needle aspiration for papillary carcinoma of the thyroid correlates with tumor size. Diagn Cytopathol 2011; 39: 471-4.

Morphometric Analysis of Thyroid Follicular Cells with Atypia of Undetermined Significance

Youngjin Kang · Yoo Jin Lee
Jiyoon Jung · Youngseok Lee
Nam Hee Won · Yang Seok Chae

Department of Pathology, Korea University Anam
Hospital, Seoul, Korea

Corresponding Author
Yang Seok Chae
Department of Pathology, Korea University Anam
Hospital, 73 Inchon-ro, Seongbuk-gu, Seoul 02841,
Korea
Tel: +82-2-920-5595
Fax: +82-2-920-6576
E-mail: chaeys21@korea.ac.kr

Background: Atypia of undetermined significance (AUS) is a category that encompasses a heterogeneous group of thyroid aspiration cytology. It has been reclassified into two subgroups based on the cytomorphologic features: AUS with cytologic atypia and AUS with architectural atypia. The nuclear characteristics of AUS with cytologic atypia need to be clarified by comparing to those observed in Hashimoto thyroiditis and benign follicular lesions. **Methods:** We selected 84 cases of AUS with histologic follow-up, 24 cases of Hashimoto thyroiditis, and 26 cases of benign follicular lesions. We also subcategorized the AUS group according to the follow-up biopsy results into a papillary carcinoma group and a nodular hyperplasia group. The differences in morphometric parameters, including the nuclear areas and perimeters, were compared between these groups. **Results:** The AUS group had significantly smaller nuclear areas than the Hashimoto thyroiditis group, but the nuclear perimeters were not statistically different. The AUS group also had significantly smaller nuclear areas than the benign follicular lesion group; however, the AUS group had significantly longer nuclear perimeters. The nuclear areas in the papillary carcinoma group were significantly smaller than those in the nodular hyperplasia group; however, the nuclear perimeters were not statistically different. **Conclusions:** We found the AUS group to be a heterogeneous entity, including histologic follow-up diagnoses of papillary carcinoma and nodular hyperplasia. The AUS group showed significantly greater nuclear irregularities than the other two groups. Utilizing these features, nuclear morphometry could lead to improvements in the accuracy of the subjective diagnoses made with thyroid aspiration cytology.

Key Words: Atypia of undetermined significance; Morphometric analysis; Thyroid

Thyroid fine-needle aspiration (FNA) is widely used as an effective first-line screening test to differentiate thyroid lesions[1-4] and the Bethesda System for Reporting Thyroid Cytopathology is used as a standard to interpret FNA specimens. "Atypia of undetermined significance (AUS)," known as Bethesda category III, is a category that encompasses a heterogeneous group of lesions containing follicular cells exhibiting architectural features and/or nuclear atypia that exceed expected benign changes, but are not of sufficient magnitude to justify classification into any other categories.[5]

The AUS category has some limitations. First, it is more frequently diagnosed than previously recommended (threshold of 7%).[6-8] Second, it shows a considerable intra- and inter-observer variability.[3,7,9-11] In addition, the risk of malignancy in the AUS category is not as low as previously thought;[12-14] some researchers have considered the category as "waste garbage."[7]

However, Shi *et al.*[3] considered AUS to be an indispensable category in that it increases the sensitivity and decreases the false-positive and false-negative rates of thyroid FNA cytology. It is even helpful when the criteria are only partially fulfilled, especially for cases displaying subtle cytomorphological changes or scanty suspicious cells, cases obscured by blood or inflammation, or specimens compromised by air-drying artifacts.

AUS is a heterogeneous entity and includes nuclear and/or architectural changes that do not completely meet the qualitative or quantitative criteria to be suspicious for malignancy or follicular neoplasms.[5] Based on the heterogeneity and subjective nature of this category, it has been suggested that this entity should be subcategorized into AUS with nuclear atypia and AUS with architectural atypia.[15-21] Furthermore, AUS needs to be differentiated from benign lesions (category II), including Hashimoto thyroiditis and benign follicular lesions, as these differential diagnoses have meaningful clinical significance for patient follow-up.

Computerized nuclear morphometry is an objective, reproducible, and inexpensive tool to evaluate histological features.[22,23] It has been suggested that nuclear morphometric parameters, such

as nuclear perimeters and nuclear areas, may help differentiation between various thyroid lesions.[24,25] Previous studies have revealed significant differences in nuclear areas and perimeters between benign and malignant lesions using thyroid aspiration cytology.[26,27] However, the utilization of morphometric analysis in thyroid aspiration cytology is limited in clinical research as well as routine diagnoses.[22]

The aim of this study was to determine whether there is a significant difference in the nuclear morphometry findings between borderline and benign lesions found using thyroid aspiration cytology, in specimens diagnosed as AUS, Hashimoto thyroiditis, and benign follicular lesions.

MATERIALS AND METHODS

We selected 84 cases with thyroid liquid-based preparation cytologic slides originally diagnosed as "AUS with nuclear atypia" with histologic follow-up. For comparison, we also selected 24 cases of Hashimoto thyroiditis and 26 cases of benign follicular lesions (both Bethesda category II). All selected cases were from Korea University Anam Hospital, Seoul, Korea, from 2011 to 2013. All slides were submitted to digital image analysis using ImagePro 6 software (Media Cybernetics, Bethesda, MD, USA), and we measured the morphometric parameters, including the nuclear areas and perimeters (Fig. 1). Well-preserved, non-overlapping cells were usually selected, and tight three-dimensional clusters or papillae were excluded. The average number of measured cells per case was 19 (range, 11 to 32). The differences in morphometric parameters were separately compared between the three groups. Using SPSS ver. 14.0 software (SPSS Inc., Chicago, IL, USA), the mean nuclear perimeters and areas

were compared via a Student's t test. This study was approved by the Institutional Review Board of Korea University Anam Hospital (AN15271-003).

RESULTS

The AUS group included 66 women and 18 men (mean age, 52 years), the Hashimoto thyroiditis group included 20 women and four men (mean age, 56 years), and the benign follicular lesion group included 24 women and two men (mean age, 55 years). There was no significant difference in the male:female ratio or in the mean age between groups (Table 1). The histologic diagnoses in the AUS group included conventional papillary thyroid carcinoma (n = 54), follicular variant of papillary thyroid carcinoma (n = 10), nodular hyperplasia (n = 18), and follicular neoplasm (n = 2) (Table 2, Fig. 2).

The mean nuclear area and perimeter were 19.360 ± 4.881 μm^2 (mean ± standard deviation) and 20.070 ± 3.121 µm, 27.766 ± 5.177 μm^2 and 21.112 ± 2.693 µm, and 22.264 ± 4.514 μm^2 and 18.206 ± 2.036 µm in the AUS group, Hashimoto thyroiditis group, and benign follicular lesion group, respectively (Table 3).

The nuclear areas in the AUS group were significantly smaller than those in the Hashimoto thyroiditis group (p < .001). The perimeters of the AUS group were not, however, significantly different from those of the Hashimoto thyroiditis group (p = .140). The nuclear areas in the AUS group were also significantly smaller than those in the benign follicular lesion group (p = .007), and the perimeters in the AUS group were also significantly longer than those in the benign follicular lesion group (p = .001) (Table 4).

As the AUS group showed heterogeneous follow-up biopsy

Fig. 1. Digital image analysis using ImagePro 6 software. The selected cells are marked in red.

Table 1. Mean age and sex of the selected cases

Variable	AUS	Hashimoto thyroiditis	Benign
Mean age (yr)	52	56	55
Sex			
Female	66	20	24
Male	18	4	2

AUS, atypia of undetermined significance.

Table 2. Follow-up pathologic diagnosis of cytologic slides

Pathologic diagnosis	No.
PTC	54
PTC, follicular variant	10
Nodular hyperplasia	18
Follicular neoplasm	2

PTC, papillary thyroid carcinoma.
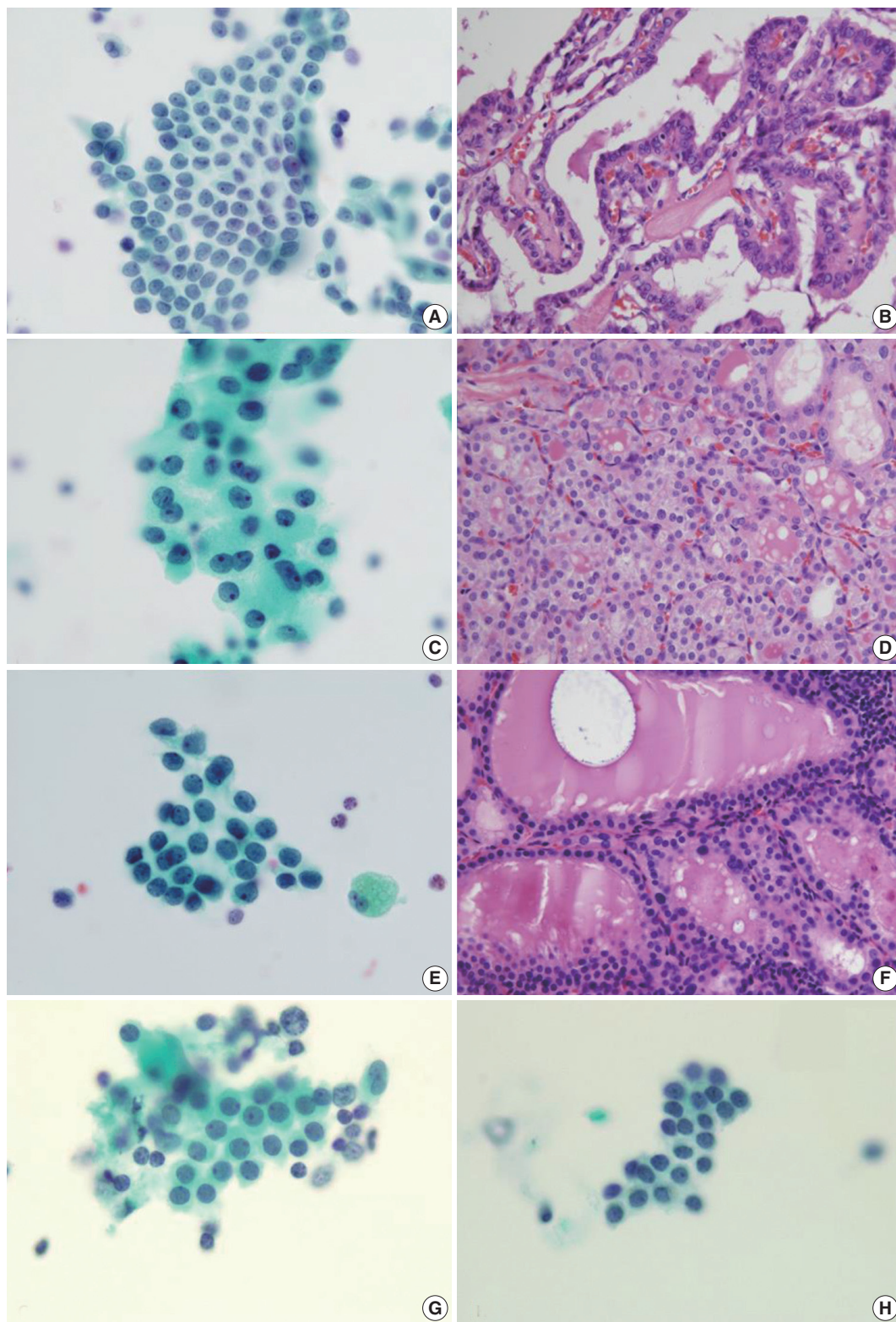
Fig. 2. (A, C, E) Cytologic slides for atypia of undetermined significance. Panels B, D, and F are the corresponding histologic findings of panels A, C, and E, respectively. Finally, images are the cytologic slides for Hashimoto thyroiditis (G) and benign follicular nodule (H), respectively. They have no corresponding histologic slides, as a surgical resection was not performed. (B) Papillary carcinoma. (D) Papillary carcinoma (follicular variant). (F) Nodular hyperplasia.

results, we subcategorized the results into a papillary carcinoma group (AUS finally diagnosed as papillary thyroid carcinoma) and a nodular hyperplasia group (AUS finally diagnosed as nodular hyperplasia). The papillary carcinoma group was composed

Table 3. Mean nuclear areas and perimeters of the three groups

Variable	AUS	Hashimoto thyroiditis	Benign
Area (μm^2)	19.360 ± 4.881	27.766 ± 5.177	22.264 ± 4.514
Perimeter (μm)	20.070 ± 3.121	21.112 ± 2.693	18.206 ± 2.036

Values are presented as mean ± standard deviation.
AUS, atypia of undetermined significance.

Table 4. Comparison of nuclear areas and perimeters between groups

Group	Two-tailed p-value	Mean differences
AUS vs. Hashimoto thyroiditis		
Area (μm^2)	< .001	–8.406
Perimeter (μm)	.140	–1.042
AUS vs. benign follicular lesions		
Area (μm^2)	.007	–2.904
Perimeter (μm)	.001	1.864
Hashimoto thyroiditis vs. benign follicular lesions		
Area (μm^2)	< .001	5.502
Perimeter (μm)	< .001	2.906

AUS, atypia of undetermined significance.

Table 5. Mean nuclear areas and perimeters in the AUS subgroups

Variable	AUS finally diagnosed as PTC	AUS finally diagnosed as nodular hyperplasia
Area (μm^2)	18.711 ± 4.283	21.562 ± 6.506
Perimeter (μm)	19.805 ± 3.113	21.147 ± 3.235

Values are presented as mean ± standard deviation.
AUS, atypia of undetermined significance; PTC, papillary thyroid carcinoma.

of cases that were diagnosed as conventional papillary carcinoma and follicular variant papillary carcinoma. Follicular neoplasm was excluded from the comparison as there were only two cases.

The mean nuclear area and perimeter in the papillary carcinoma group was $18.711 ± 4.283$ μm^2 (mean ± standard deviation) and $19.805 ± 3.113$ μm, respectively, and that in the nodular hyperplasia group was $21.562 ± 6.506$ μm^2 and $21.147 ± 3.235$ μm, respectively (Table 5).

The nuclear areas in the papillary carcinoma group were significantly smaller than those in the nodular hyperplasia group (p = .030), but the perimeters were not statistically different (p = .094). The nuclear areas in the papillary carcinoma group were also significantly smaller than those in the Hashimoto thyroiditis group (p < .001), but the perimeters were not statistically different (p = .073). Similarly, the nuclear areas in the nodular hyperplasia group were significantly smaller than those in the Hashimoto thyroiditis group (p = .001), but the perimeters were not statistically different (p = .970). The perimeters in the nodular hyperplasia group were significantly longer than those in the benign follicular lesion group (p = .001), but the nuclear areas were not statistically different (p = .674). Finally, the nuclear areas and perimeters in the papillary carcinoma group were significantly smaller and longer, respectively, than those in the benign follicular lesion group (Table 6).

DISCUSSION

FNA cytology has been widely used in the assessment of thyroid lesions. The Bethesda System for Reporting Thyroid Cytopathology has standardized the reporting of FNA cytology

Table 6. Comparison of nuclear areas and perimeters between subgroups

Subgroup	Two-tailed p-value	Mean difference
AUS finally diagnosed as PTC vs. AUS finally diagnosed as nodular hyperplasia		
Area (μm^2)	.030	–2.851
Perimeter (μm)	.094	–1.342
AUS finally diagnosed as nodular hyperplasia vs. benign follicular lesions		
Area (μm^2)	.674	–0.702
Perimeter (μm)	.001	2.941
AUS finally diagnosed as nodular hyperplasia vs. Hashimoto thyroiditis		
Area (μm^2)	.001	–6.204
Perimeter (μm)	.970	0.034
AUS finally diagnosed as PTC vs. Hashimoto thyroiditis		
Area (μm^2)	< .001	–9.055
Perimeter (μm)	.073	–1.308
AUS finally diagnosed as PTC vs. Benign follicular lesions		
Area (μm^2)	.001	–3.552
Perimeter (μm)	.018	1.599

AUS, atypia of undetermined significance; PTC, papillary thyroid carcinoma.

findings for thyroid specimens. The diagnostic categories include non-diagnostic or unsatisfactory (category I), benign (category II), AUS (category III), follicular neoplasm or suspicious for a follicular neoplasm (category IV), suspicious for malignancy (category V), and malignant (category VI). The benign category (category II) has several subcategories, including benign follicular nodules and Hashimoto thyroiditis. The criteria for AUS, however, include lesions that do not fulfill the criteria for follicular neoplasms and papillary carcinomas, predominant Hurthle cells, and sample artifacts. The AUS category thus needs to be distinguished from both benign follicular nodules and Hashimoto thyroiditis.

The AUS lesion is a heterogeneous entity, and different institutions categorize it into multiple subgroups. These subgroups include AUS with cytologic atypia and AUS with architectural atypia. Among these subgroups, AUS with cytologic atypia is thought to be associated with an increased risk of malignancy. Mathur et al.[28] subcategorized 463 cases of thyroid aspiration cytology, re-reviewed as AUS, and the subgroup with nuclear atypia was found to have a greater risk of malignancy than any other subgroup (68%), which was even greater than the overall risk of malignancy (39%). In our study, 64 out of 84 cases of AUS (76%) were found to be papillary carcinoma. Thus, the atypical nuclear features found in AUS should be evaluated thoroughly and differentiated from benign lesions, as it is critical for patient follow-up procedures.

Nevertheless, AUS is an essential, clinically significant category. Shi et al.[3] have shown that eliminating the AUS category resulted in a consistent and considerable decrease of sensitivity in detecting thyroid lesions. The sensitivity of detecting papillary carcinoma was reduced from 100% to 27% when the AUS category was eliminated. Studies have also shown that eliminating the AUS category increases the false-negative and false-positive rates.[3] Without the AUS category, up to 53% of neoplastic thyroid lesions and 37% of papillary carcinomas would be underestimated as benign, and might not be clinically re-evaluated for months or years. Lastly, up to 38% of pathologically diagnosed benign lesions would be overestimated as a follicular neoplasm or suspicious for follicular neoplasm. These findings reveal that it is important to maintain the AUS category.

In these circumstances, additional objective morphological analysis is helpful in differentiating between AUS and benign lesions. Computerized nuclear morphometry is one of the solutions, which has the advantage of being both reproducible and inexpensive.[22,23] Using nuclear morphometry, a number of parameters, such as nuclear size and shape, can be easily quantified.

The evaluation of these parameters has been documented to potentialize the diagnosis and the management of various neoplasms, including urinary bladder carcinoma,[29] skin lymphoma,[30] breast carcinoma,[31] and soft tissue sarcoma.[32] It has been suggested that nuclear morphometric parameters, such as nuclear areas and perimeters, may facilitate the differentiation between thyroid lesions.[24,25] To date, however, the use of morphometric analysis in thyroid pathology has been limited.

Quantitative studies in pathology have enabled improvements in the accuracy of subjective diagnoses made in routine practice.[26] Objective information gained through the quantification of nuclear morphological features may be useful in classifying different lesions. In thyroid follicular neoplasms, the most helpful parameters in the differential diagnosis are the nuclear parameters, including the mean nuclear area, the mean nuclear perimeter, the ratio of the largest to the smallest diameters of the nuclei, the coefficient of variation of the nuclear area, and the circular rate.[33-36] Shih et al.[34] retrospectively studied cytologic features using computerized morphometry and clinical data in 118 cases. Multivariate logistic analysis showed that the parameters significantly related to recurrence were the nucleus-to-cell ratios, variations of the nuclear area, tumor sizes, and patient age. Aiad et al.[22] retrospectively studied 48 cases of different thyroid lesions to compare their parameters, including nuclear size, shape, perimeter, and area. Most parameters related to the sizes and the shapes of the nuclei were significantly higher in follicular variant papillary carcinoma than in follicular neoplasm. Also, nuclear areas and sizes were found to be the most reliable parameters to differentiate between follicular variant papillary carcinoma and follicular adenoma. Finally, Wright et al.[27] evaluated 119 cases of FNA cytology of thyroid nodules and found significant differences in the nuclear areas and perimeters between the cases of multinodular goiters and follicular and papillary neoplasms, as well as between follicular adenomas and follicular and papillary carcinomas. These findings suggest that nuclear morphometry is useful in differentiating malignant from benign lesions.

We compared morphometric parameters, including the nuclear areas and perimeters, among groups categorized with AUS, Hashimoto thyroiditis, or benign follicular lesions. The AUS lesions showed significantly smaller nuclear areas with longer perimeters, suggesting that marked nuclear irregularity is statistically present. Most of the lesions were diagnosed as papillary carcinoma on the final histologic evaluation. However, the Bethesda System for Reporting Thyroid Cytopathology diagnostic criteria for papillary carcinoma includes enlarged nuclei.

Previous studies using conventional smear slides revealed nuclear enlargement in papillary carcinoma. Murata *et al.*[37] analyzed 39 cases of Pap-stained aspiration cytology smear specimens including nine cases of papillary carcinoma and revealed that papillary carcinomas had larger and more irregularly shaped nuclei than those of the benign groups. All selected cases in this study were liquid-based preparation cytologic slides, which may be a major cause of the smaller nuclei. Due to the inherent technical differences including alcohol fixation and the elimination of air-drying artifact cells, the nuclei may appear smaller in the liquid-based preparation specimens compared to the conventional smear specimens.

The nuclear irregularity of AUS lesions may also be a useful screening index in the routine diagnosis. In this study, the mean ratio of nuclear perimeter to nuclear area was 1.0367 in the AUS group, which was greater than the other two groups (0.76035 and 0.81773 in the Hashimoto thyroiditis group and the benign follicular group, respectively). A proper cut-off value would make the diagnosis of AUS much more objective, and thus further studies are needed to determine this proper cut-off value.

The AUS group is a heterogeneous entity, including histologic follow-up diagnoses of papillary carcinoma and nodular hyperplasia, but it is an essential category in spite of its limitations. We found that the AUS with cytologic atypia group was associated with an increased risk of malignancy, particularly due to its smaller nuclear areas and longer perimeters, indicating nuclear irregularity. Utilizing these features, nuclear morphometry would lead to improvements in the accuracy of the subjective diagnoses made using thyroid aspiration cytology. By determining a proper cut-off value, the diagnosis of AUS would be even more objective.

Conflicts of Interest

No potential conflict of interest relevant to this article was reported.

REFERENCES

1. DeMay RM. Cytopathology of false negatives preceding cervical carcinoma. Am J Obstet Gynecol 1996; 175(4 pt 2): 1110-3.
2. Greenblatt DY, Woltman T, Harter J, Starling J, Mack E, Chen H. Fine-needle aspiration optimizes surgical management in patients with thyroid cancer. Ann Surg Oncol 2006; 13: 859-63.
3. Shi Y, Ding X, Klein M, *et al*. Thyroid fine-needle aspiration with atypia of undetermined significance: a necessary or optional category? Cancer 2009; 117: 298-304.
4. Yang J, Schnadig V, Logrono R, Wasserman PG. Fine-needle aspiration of thyroid nodules: a study of 4703 patients with histologic and clinical correlations. Cancer 2007; 111: 306-15.
5. Cibas ES, Ali SZ; NCI Thyroid FNA State of the Science Conference. The Bethesda System For Reporting Thyroid Cytopathology. Am J Clin Pathol 2009; 132: 658-65.
6. Broome JT, Solorzano CC. The impact of atypia/follicular lesion of undetermined significance on the rate of malignancy in thyroid fine-needle aspiration: evaluation of the Bethesda System for Reporting Thyroid Cytopathology. Surgery 2011; 150: 1234-41.
7. Kholová I, Ludvíková M. Thyroid atypia of undetermined significance or follicular lesion of undetermined significance: an indispensable Bethesda 2010 diagnostic category or waste garbage? Acta Cytol 2014; 58: 319-29.
8. Ohori NP, Nikiforova MN, Schoedel KE, *et al*. Contribution of molecular testing to thyroid fine-needle aspiration cytology of "follicular lesion of undetermined significance/atypia of undetermined significance". Cancer Cytopathol 2010; 118: 17-23.
9. Bhasin TS, Mannan R, Manjari M, *et al*. Reproducibility of 'The Bethesda System for reporting Thyroid Cytopathology': a multicenter study with review of the literature. J Clin Diagn Res 2013; 7: 1051-4.
10. Cochand-Priollet B, Schmitt FC, Totsch M, Vielh P; European Federation of Cytology Societies Scientific Committee. The Bethesda terminology for reporting thyroid cytopathology: from theory to practice in Europe. Acta Cytol 2011; 55: 507-11.
11. Walts AE, Bose S, Fan X, *et al*. A simplified Bethesda System for reporting thyroid cytopathology using only four categories improves intra- and inter-observer diagnostic agreement and provides non-overlapping estimates of malignancy risks. Diagn Cytopathol 2012; 40 Suppl 1: E62-8.
12. Chen JC, Pace SC, Khiyami A, McHenry CR. Should atypia of undetermined significance be subclassified to better estimate risk of thyroid cancer? Am J Surg 2014; 207: 331-6.
13. Ho AS, Sarti EE, Jain KS, *et al*. Malignancy rate in thyroid nodules classified as Bethesda category III (AUS/FLUS). Thyroid 2014; 24: 832-9.
14. Park VY, Kim EK, Kwak JY, Yoon JH, Moon HJ. Malignancy risk and characteristics of thyroid nodules with two consecutive results of atypia of undetermined significance or follicular lesion of undetermined significance on cytology. Eur Radiol 2015; 25: 2601-7.
15. Horne MJ, Chhieng DC, Theoharis C, *et al*. Thyroid follicular lesion of undetermined significance: evaluation of the risk of malignancy using the two-tier sub-classification. Diagn Cytopathol 2012; 40: 410-5.

16. Nishino M, Wang HH. Should the thyroid AUS/FLUS category be further stratified by malignancy risk? Cancer Cytopathol 2014; 122: 481-3.

17. Olson MT, Clark DP, Erozan YS, Ali SZ. Spectrum of risk of malignancy in subcategories of 'atypia of undetermined significance'. Acta Cytol 2011; 55: 518-25.

18. Renshaw AA. Should "atypical follicular cells" in thyroid fine-needle aspirates be subclassified? Cancer Cytopathol 2010; 118: 186-9.

19. Renshaw AA. Subclassification of atypical cells of undetermined significance in direct smears of fine-needle aspirations of the thyroid: distinct patterns and associated risk of malignancy. Cancer Cytopathol 2011; 119: 322-7.

20. VanderLaan PA, Marqusee E, Krane JF. Usefulness of diagnostic qualifiers for thyroid fine-needle aspirations with atypia of undetermined significance. Am J Clin Pathol 2011; 136: 572-7.

21. Wu HH, Inman A, Cramer HM. Subclassification of "atypia of undetermined significance" in thyroid fine-needle aspirates. Diagn Cytopathol 2014; 42: 23-9.

22. Aiad H, Abdou A, Bashandy M, Said A, Ezz-Elarab S, Zahran A. Computerized nuclear morphometry in the diagnosis of thyroid lesions with predominant follicular pattern. Ecancermedicalscience 2009; 3: 146.

23. Hamilton PW, Allen DC. Morphometry in histopathology. J Pathol 1995; 175: 369-79.

24. Fadda G, Rabitti C, Minimo C, et al. Morphologic and planimetric diagnosis of follicular thyroid lesions on fine needle aspiration cytology. Anal Quant Cytol Histol 1995; 17: 247-56.

25. Słowińska-Klencka D, Klencki M, Sporny S, Lewiński A. Karyometric analysis in the cytologic diagnosis of thyroid lesions. Anal Quant Cytol Histol 1997; 19: 507-13.

26. Artacho-Pérula E, Roldán-Villalobos R, Blanco-García F, Blanco-Rodríguez A. Objective differential classification of thyroid lesions by nuclear quantitative assessment. Histol Histopathol 1997; 12: 425-31.

27. Wright RG, Castles H, Mortimer RH. Morphometric analysis of thyroid cell aspirates. J Clin Pathol 1987; 40: 443-5.

28. Mathur A, Najafian A, Schneider EB, Zeiger MA, Olson MT. Malignancy risk and reproducibility associated with atypia of undetermined significance on thyroid cytology. Surgery 2014; 156: 1471-6.

29. Kapur U, Antic T, Venkataraman G, et al. Validation of World Health Organization/International Society of Urologic Pathology 2004 classification schema for bladder urothelial carcinomas using quantitative nuclear morphometry: identification of predictive features using bootstrap method. Urology 2007; 70: 1028-33.

30. Lira M, Schenka AA, Magna LA, et al. Diagnostic value of combining immunostaining for CD3 and nuclear morphometry in mycosis fungoides. J Clin Pathol 2008; 61: 209-12.

31. Cui Y, Koop EA, van Diest PJ, Kandel RA, Rohan TE. Nuclear morphometric features in benign breast tissue and risk of subsequent breast cancer. Breast Cancer Res Treat 2007; 104: 103-7.

32. Kazanowska B, Jelen M, Reich A, Tarnawski W, Chybicka A. The role of nuclear morphometry in prediction of prognosis for rhabdomyosarcoma in children. Histopathology 2004; 45: 352-9.

33. Nagashima T, Suzuki M, Oshida M, et al. Morphometry in the cytologic evaluation of thyroid follicular lesions. Cancer 1998; 84: 115-8.

34. Shih SR, Chang YC, Li HY, et al. Preoperative prediction of papillary thyroid carcinoma prognosis with the assistance of computerized morphometry of cytology samples obtained by fine-needle aspiration: preliminary report. Head Neck 2013; 35: 28-34.

35. Tseleni-Balafouta S, Kavantzas N, Paraskevakou H, Davaris P. Computerized morphometric study on fine needle aspirates of cellular follicular lesions of the thyroid. Anal Quant Cytol Histol 2000; 22: 323-6.

36. Wang SL, Wu MT, Yang SF, Chan HM, Chai CY. Computerized nuclear morphometry in thyroid follicular neoplasms. Pathol Int 2005; 55: 703-6.

37. Murata S, Mochizuki K, Nakazawa T, et al. Morphological abstraction of thyroid tumor cell nuclei using morphometry with factor analysis. Microsc Res Tech 2003; 61: 457-62.

Clinical Significance of an HPV DNA Chip Test with Emphasis on HPV-16 and/or HPV-18 Detection in Korean Gynecological Patients

Min-Kyung Yeo[1,2] · Ahwon Lee[1]
Soo Young Hur[3] · Jong Sup Park[3]

[1]Department of Hospital Pathology, College of Medicine, The Catholic University of Korea, Seoul; [2]Department of Pathology, Chungnam National University School of Medicine, Daejeon; [3]Department of Obstetrics and Gynecology, Seoul St. Mary's Hospital, College of Medicine, The Catholic University of Korea, Seoul, Korea

Received: January 26, 2016
Revised: April 6, 2016
Accepted: May 9, 2016

Corresponding Author
Ahwon Lee, MD
Department of Hospital Pathology,
College of Medicine, The Catholic University
of Korea, 222 Banpo-daero, Seocho-gu,
Seoul 06591, Korea
Tel: +82-2-2258-1621
Fax: +82-2-2258-1627
E-mail: klee@catholic.ac.kr

Background: Human papillomavirus (HPV) is a major risk factor for cervical cancer. **Methods:** We evaluated the clinical significance of the HPV DNA chip genotyping assay (MyHPV chip, Mygene Co.) compared with the Hybrid Capture 2 (HC2) chemiluminescent nucleic acid hybridization kit (Digene Corp.) in 867 patients. **Results:** The concordance rate between the MyHPV chip and HC2 was 79.4% (kappa coefficient, $\kappa = 0.55$). The sensitivity and specificity of both HPV tests were very similar (approximately 85% and 50%, respectively). The addition of HPV result (either MyHPV chip or HC2) to cytology improved the sensitivity (95%, each) but reduced the specificity (approximately 30%, each) compared with the HPV test or cytology alone. Based on the MyHPV chip results, the odds ratio (OR) for ≥ high-grade squamous intraepithelial lesions (HSILs) was 9.9 in the HPV-16/18 (+) group and 3.7 in the non-16/18 high-risk (HR)-HPV (+) group. Based on the HC2 results, the OR for ≥ HSILs was 5.9 in the HR-HPV (+) group. When considering only patients with cytological diagnoses of "negative for intraepithelial lesion or malignancy" and "atypical squamous cell or atypical glandular cell," based on the MyHPV chip results, the ORs for ≥ HSILs were 6.8 and 11.7, respectively, in the HPV-16/18 (+) group. **Conclusions:** The sensitivity and specificity of the MyHPV chip test are similar to the HC2. Detecting HPV-16/18 with an HPV DNA chip test, which is commonly used in many Asian countries, is useful in assessing the risk of high-grade cervical lesions.

Key Words: Human papillomavirus; DNA chip; Hybrid capture 2; Cervical intraepithelial neoplasia; Cervical carcinoma

Human papillomavirus (HPV) is a DNA tumor virus that is an essential causative factor for cervical cancer. Persistent infection, particularly with high-risk (HR) HPV (HR-HPV) genotypes, plays a major role in the progression of precancerous cervical lesions to invasive cancer.[1] The incidence rate of high-grade cervical lesions is reported to be higher in patients infected with HPV-16 and/or HPV-18 (HPV-16/18) than in patients with other HR-HPV strains,[2-5] and HPV-16 and HPV-18 cause 71% of HPV infections in cervical cancer patients.[6,7]

Although cytology in cervical cancer screening has been successful, it has several limitations, including low sensitivity and reproducibility. Addition of HPV DNA test to the cytology test, so-called co-test, is the preferred screening method for prevention and early detection of cervical cancer according to the 2012 American Cancer Society screening guidelines.[8] For the first time, these recommendations have adopted HPV 16/18 genotyping in the management of women with positive HPV tests and negative cytology. Specifically, these women should under-

go subsequent HPV-16/18 genotyping or repeat co-testing in 12 months.[8]

The Hybrid Capture 2 (HC2) chemiluminescent nucleic acid hybridization kit (Digene Corp., Gaithersburg, MA, USA) is a frequently used method to detect HR-HPV and is approved by the United States Food and Drug Administration (U.S. FDA). The kit detects 13 HR-HPV types and reports results as either HR-HPV (+) or HR-HPV (–).

The HPV DNA chip test (MyHPV chip, Mygene Co., Seoul, Korea) identifies 15 HR and nine low-risk HPV types and is a commercial HPV DNA genotyping tool used in Korea and other Asian countries. Furthermore, the MyHPV chip kit is approved by the Korean Food and Drug Administration (K-FDA). However, no previous study has assessed the association between HPV-16/18 detected using the MyHPV chip and the risk of developing high-grade cervical lesions.

In this study, we compared the clinical performance of the MyHPV chip and HC2 tests using a histological cut-off for high-

grade squamous intraepithelial lesions (HSILs).

MATERIALS AND METHODS

Study subjects

This study was approved by the Institutional Review Board of The Catholic University of Korea, Seoul St. Mary's Hospital, and complied with the tenets of the Declaration of Helsinki. We retrospectively reviewed the pathology archive database records of 867 consecutive gynecological patients treated at Seoul St. Mary's Hospital, from January 2006 to December 2009, for whom cervical cytology and HPV test results from both the HC2 and MyHPV chip were available and confirmed by histological examination. The majority of patients were referred to our institution due to abnormal results in routine cervical examinations, and thus the patients underwent cervical cytology, HPV test (HC2 to confirm HPV infection and MyHPV chip to determine infected HPV genotype), and colposcopic examinations followed by tissue biopsy if necessary. The cervical cytology, HC2 test, and MyHPV chip tests were simultaneously performed on the same sample in most cases. Otherwise, we selected cytology that was performed within 2 weeks prior to HPV testing. We classified cervical cytology according to the 2001 Bethesda System for Reporting Cervical Cytology.[9] The diagnoses of all included patients were pathologically confirmed by biopsy, conization and/or hysterectomy within 3 months of cervical cytology and HPV testing. The patients were divided based on age as follows: ≤29 years, 178 patients (20.5%); 30–39 years, 281 patients (32.4%); 40–49 years, 243 patients (28.0%); 50–59 years, 109 patients (12.6%); and ≥60 years, 56 patients (6.5%); the mean age was 40 years.

HPV genotyping using the MyHPV chip test

The MyHPV chip test contains probes for 15 HR (HPV-16, -18, -31, -33, -35, -39, -45, -51, -52, -53, -56, -58, -59, -66, and -68) and 9 low-risk HPV types (HPV 6, 11, 34, 40, 42, 43, 44, 54, and 70). The MyHPV chip test was performed according to the manufacturer's instructions under the supervision of Dr. A. Lee (pathologist with a specialty in gynecopathology and molecular pathology). The cervical DNA was isolated from specimens and amplified using polymerase chain reaction (PCR) with consensus GP5$^+$/GP6$^+$ primers. Beta-globin was amplified as an internal control. The PCR product (5 μL) was subjected to 2.5% agarose gel electrophoresis. Twenty-four type-specific 30-mer oligonucleotide probes containing an amine group at the 5' terminus were immobilized onto a slide glass chip. The PCR products were labelled with Cy5-dUTP, denatured, mixed with hybridization solution, and incubated on the DNA chip. The hybridized HPV DNA was visualized using a DNA chip scanner (ScanArray LITE, GSI Lumonics Inc., Bedford, MA, USA).

Clearly visualized double-positive spots for a specific HPV type were considered "specific HPV-positive." Samples negative on the chip scanner but positive for the 150-bp HPV-specific band using gel electrophoresis were interpreted as "negative for 15 HR-HPV and nine low-risk HPV types but positive for other HPV types." A lack of visualized spots and samples negative for the 150-bp HPV-specific band using gel electrophoresis were considered "HPV-negative."

HC2 DNA hybridization assay

The HC2 test was performed according to the manufacturer's instructions as previously described.[10] In brief, the specimens for the HC2 test were denatured and hybridized with RNA probes to detect 13 HR-HPV types (HPV-16, -18, -31, -33, -35, -39, -45, -51, -52, -56, -58, -59, and -68) in a microplate format. These hybrids react with multiple antibody conjugates and are quantified based on an amplified chemiluminescent signal. Relative light units/positive control values ≥1.00 were considered "positive," whereas values <1.00 were considered "negative."

Statistical analysis

The concordance rates of the MyHPV chip and HC2 were evaluated using the kappa coefficient (κ) with 95% confidence intervals (CIs). The sensitivity, specificity, positive predictive value (PPV), and negative predictive value (NPV) of the MyHPV chip and HC2 for ≥HSILs were determined using standard statistical tests. The age-adjusted odds ratios (ORs) for ≥HSILs with 95% CI were evaluated for different categories of MyHPV chip and HC2 results with a binary logistic regression using the SPSS ver. 22.0 software (IBM Co., Armonk, NY, USA). To analyze the MyHPV chip results, patients with single or multiple samples positive for 15 HR genotypes were categorized as HR-HPV (+). Patients with HPV-16 (+) and/or HPV-18 (+) were categorized as HPV-16/18 (+), irrespective of the presence of any other HPV genotypes. Patients with HPV-16 (–) and HPV-18 (–), 13 other HR-HPV (+) with or without low-risk HPV (+) or "HPV-other types" (+) were categorized as non-16/18 HR-HPV (+). Patients with low-risk HPV (+), "HPV-other types" (+) or HPV (–) were categorized as HR-HPV (-). In cases of multiple infections, patients were classified based on the HPV genotypes associated with a higher risk of invasive cancer. For example, a patient with HPV-16 (+) and HPV-31 (+)

was allocated to the HPV-16/18 (+) group.

RESULTS

HPV, cytology, and histology test results

Among 867 patients, 575 (66.3%) were HR-HPV (+) according to the MyHPV chip test, 540 (62.3%) were HR-HPV (+) according to the HC2 test, and 545 (62.9%) were classified as atypical squamous cells of undetermined significance (ASCUS) or worse (≥ASCUS) cytology. The following cytological diagnoses were made for 867 patients: 322 patients were negative for intraepithelial lesion or malignancy (NILM), 138 patients exhibited ASCUS, six patients exhibited atypical glandular cells (AGC), 30 patients exhibited atypical squamous cells for which HSILs (ASC-H) cannot be excluded, 183 patients exhibited low-grade squamous intraepithelial lesions (LSILs), 123 patients exhibited HSILs, including carcinoma *in situ*, and 65 patients

exhibited invasive cancer, including squamous cell carcinoma and adenocarcinoma (Table 1). The overall prevalence rates of histology confirmed HSIL or worse (≥HSIL) according to the cytological diagnosis of NILM, ASCUS, LSIL, ASC-H, HSIL, and invasive cancer were 12.4%, 25.4%, 24.0%, 60.0%, 83.7%, and 98.4%, respectively. The overall prevalence rates of ≥HSIL according to the MyHPV chip test for HPV-16/18 (+), non-16/18 HR-HPV (+), and HR-HPV (–) were 58.1%, 36.0%, and 13.0%, respectively. The overall prevalence rates of ≥HSIL according to the HC2 test for HR-HPV (+) and HR-HPV (-) were 48.3% and 13.5%, respectively (Tables 1, 2).

Clinical performance of the cytology, the MyHPV chip and the HC2

The concordance rate between the MyHPV chip test and the HC2 test was 79.4% (688/867), with a κ-value of 0.551 (Table 3). Among 272 cases with HPV-16/18 (+) based on the MyHPV

Table 1. Histology results according to cytology, HPV DNA chip results,[a] and HC2 results

Histology	Cervicitis (n=241)	LSIL (n=321)	HSIL (n=210)	Cancer (n=95)	Total (n=867)
Cytology					
NILM	161 (66.8)	121 (37.7)	29 (13.8)	11 (11.6)	322
ASCUS	28 (11.6)	75 (23.4)	31 (14.8)	4 (4.2)	138
ASC-H	3 (1.2)	9 (2.8)	14 (6.7)	4 (4.2)	30
AGC	5 (2.1)	0 (0)	1 (0.5)	0 (0)	6
LSIL	39 (16.2)	100 (31.2)	42 (20)	2 (2.1)	183
HSIL	4 (1.7)	16 (5.0)	86 (41.0)	17 (17.9)	123
Cancer	1 (0.4)	0 (0)	7 (3.3)	57 (60.0)	65
HPV DNA chip					
HR-HPV (–)	133 (55.2)	121 (37.7)	27 (12.9)	11 (11.6)	292
Non-16/18 HR-HPV (+)	67 (27.8)	127 (39.6)	84 (40.0)	25 (26.3)	303
HPV-16/18 (+)	41 (17.0)	73 (22.7)	99 (47.1)	59 (62.1)	272
HPV HC2					
HR-HPV (–)	155 (64.3)	128 (39.9)	28 (13.3)	16 (16.8)	327
HR-HPV (+)	86 (35.7)	193 (60.1)	182 (86.7)	79 (83.2)	540

HPV, human papillomavirus; HC2, Hybrid Capture 2; LSIL, low-grade squamous intraepithelial lesion; HSIL, high-grade squamous intraepithelial lesion; NILM, negative for intraepithelial lesion or malignancy; ASCUS, atypical squamous cells of undetermined significance; ASC-H, atypical squamous cells cannot exclude HSIL; AGC, atypical glandular cells; HR, high-risk.
[a]HPV-HR (–) includes HPV (–) or low-risk HPV (+) or "HPV-other types" (+); non-16/18 HR-HPV (+) includes HPV-16 (–) and HPV-18 (–), 13 other HR-HPV (+) with or without low-risk HPV (+) or "HPV-other types" (+); HPV-16/18 (+) includes HPV-16 (+) and/or HPV-18 (+), with or without any other HPV genotypes present.

Table 2. Age-adjusted odds ratio for ≥HSIL histology in each HPV group

	Total	≥ HSIL	Odds ratio	95% CI	p-value
HPV DNA chip[a]					
HR-HPV (–)	292	38 (13.0)			
Non-16/18 HR-HPV (+)	303	109 (36.0)	3.739	2.448–5.709	.000
HPV-16/18 (+)	272	158 (58.1)	9.874	6.418–15.190	.000
HPV HC2					
HR-HPV (–)	327	44 (13.5)			
HR-HPV (+)	540	261 (48.3)	5.914	4.102–8.527	.000

≥HSIL, high-grade squamous intraepithelial lesion or worse; HPV, human papillomavirus; CI, confidence interval; HR, high-risk.
[a]HPV-HR (–) includes HPV (–) or low-risk HPV (+) or "HPV-other types" (+); non-16/18 HR-HPV (+) includes HPV-16 (–) and HPV-18 (–), 13 other HR-HPV (+) with or without low-risk HPV (+) or "HPV-other types" (+); HPV-16/18 (+) includes HPV-16 (+) and/or HPV-18 (+), with or without any other HPV genotypes present.

chip test, 229 cases (84.2%) were also HR-HPV (+) based on HC2 test. The sensitivity, specificity, PPV, and NPV of the cytology, HC2 and MyHPV chip for ≥HSIL histology were evaluated and found similar among the tests (Table 4). The clinical performance of cytology and HC2 as well as cytology and the MyHPV chip were then evaluated (Table 4). The addition of either HPV test (HC2 or HPV DNA) to cytology for detecting ≥ HSIL histology improved the sensitivity and NPV, but reduced the specificity and PPV compared with the HPV test or cytology alone.

Table 3. Comparison between HPV DNA chip results[a] and HC2 results

HC2	HPV DNA chip			Total
	Negative	Non-16/18 HR-HPV (+)	HPV-16/18 (+)	
Negative	220 (75.3)	64 (21.1)	43 (15.8)	327
Positive	72 (24.7)	239 (78.9)	229 (84.2)	540
Total	292	303	272	867

HPV, human papillomavirus; HC2, Hybrid Capture 2; HR, high-risk.
[a]HR-HPV (–) includes HPV (–) or low-risk HPV (+) or "HPV-other types"(+); non-16/18 HR-HPV (+) includes HPV-16 (–) and HPV-18 (–), 13 other HR-HPV (+) with or without low-risk HPV (+) or "HPV-other types" (+); HPV-16/18 (+) includes HPV-16 (+) and/or HPV-18 (+), with or without any other HPV genotypes present.

ORs for ≥HSILs according to the MyHPV chip and HC2 results

We calculated the ORs for ≥HSILs based on the MyHPV chip and HC2 results. The MyHPV chip results were categorized as HPV-16/18 (+), non-16/18 HR-HPV (+), and HR-HPV (–) groups. The age-adjusted ORs for ≥HSIL were 9.9 (95% CI, 6.4 to 15.2) in the HPV-16/18 (+) group and 3.7 (95% CI, 2.4 to 5.7) in the non-16/18 HR-HPV (+) group. Based on HC2 results, the age-adjusted OR for ≥HSIL was 5.9 (95% CI, 4.1 to 8.5) in the HR-HPV (+) group (Table 2). A further subgroup analysis was performed among patients with cytological diagnoses of "NILM" and "atypical squamous cells (ASC) or AGC" (Table 5). Regarding the cytology of "NILM" patients, based on MyHPV chip results, the age-adjusted OR for ≥HSIL in the HPV-16/18 (+) group was 6.8 (95% CI, 2.1 to 21.6), but the OR for ≥HSIL in the non-16/18 HR-HPV (+) group did not significantly differ from the OR in the HR-HPV (–) group. Based on the HC2 results, the age-adjusted OR for ≥HSIL was 5.9 (95% CI, 2.9 to 12.2) in the HR-HPV (+) group (Table 5). Regarding the cytology of "ASC or AGC" patients, based on the MyHPV chip results, the age-adjusted OR for ≥HSIL was 11.7 (95% CI, 4.1 to 33.5) in the HPV-16/18 (+) group, but the OR for ≥HSIL in the

Table 4. Clinical performance of cytology, HPV DNA chip test, and HC2 test

	Cytology	HPV DNA chip	HC2	Cytology+HC2	Cytology+HPV DNA chip
Sensitivity	0.869	0.875	0.856	0.954	0.951
Specificity	0.502	0.452	0.504	0.379	0.304
PPV	0.486	0.464	0.483	0.455	0.426
NPV	0.876	0.87	0.865	0.938	0.919

HPV, human papillomavirus; HC2, Hybrid Capture 2; PPV, positive predictive value; NPV, negative predictive value.

Table 5. Age-adjusted odds ratio for ≥HSIL histology in each HPV group exhibiting "NILM" and "ASC or AGC" cytology

Cytology	HPV test	Total	≥HSIL	Odds ratio	95% CI	p-value
NILM	HPV DNA chip					
	HR-HPV (–)	186	15 (8.1)			
	Non-16/18 HR-HPV (+)	69	7 (10.1)	2.119	0.642–6.995	.217
	HPV-16/18 (+)	67	18 (26.9)	6.756	2.114–21.588	.000
	HPV HC2					
	HR-HPV (–)	227	14 (6.2)			
	HR-HPV (+)	95	26 (27.4)	5.894	2.852–12.180	.000
ASC or AGC	HPV DNA chip[a]					
	HR-HPV (–)	52	6 (11.5)			
	Non-16/18 HR-HPV (+)	59	13 (22.0)	2.454	0.819–7.353	.190
	HPV-16/18 (+)	63	35 (55.6)	11.715	4.101–33.463	.000
	HPV HC2					
	HR-HPV (–)	50	8 (16.0)			
	HR-HPV (+)	124	46 (37.1)	2.988	1.269–7.039	.012

≥HSIL, high-grade squamous intraepithelial lesion or worse; HPV, human papillomavirus; NILM, negative for intraepithelial lesion or malignancy; ASC, atypical squamous cells; AGC, atypical glandular cells; CI, confidence interval; HR, high-risk; HC2, Hybrid Capture 2.
[a]HR-HPV (–) includes HPV (–) or low-risk HPV (+) or "HPV-other types" (+); non-16/18 HR-HPV (+) includes HPV-16 (–) and HPV-18 (–), 13 other HR-HPV (+) with or without low-risk HPV (+) or "HPV-other types" (+); HPV-16/18 (+) includes HPV-16 (+) and/or HPV-18 (+), with or without any other HPV genotypes present.

non-16/18 HR-HPV (+) group did not significantly differ from the OR in the HR-HPV (−) group. Based on the HC2 results, the age-adjusted OR for ≥HSIL was 3.0 (95% CI, 1.3 to 7.0) in the HR-HPV (+) group (Table 5).

DISCUSSION

HPV-16 and HPV-18 are the main carcinogenic HPV genotypes associated with cervical cancer and are responsible for 55%–60% and 10%–15% of invasive cancers, respectively. Non-16/18 HR-HPV genotypes are associated with 25%–35% of invasive cancers.[1,7,11] Because the importance of HPV-16 and HPV-18 in cervical pathology has been sufficiently demonstrated, the updated U.S screening guidelines for the early detection of cervical cancer and its precursors recommend co-testing (cytology in combination with HR-HPV testing) over cytology alone and integrated HPV-16/18 genotyping for the management of patients whose HPV test was positive and cytology negative.[8] Recently, interim guidelines stating that primary HR-HPV testing for cervical cancer screening can be considered an alternative to current U.S cervical cancer screening methods have been published.[12]

In many Asian countries, including Korea, the HPV DNA chip test and PCR-based HPV detection kits as well as the HC2 test are commonly used in clinical settings because the sensitivity and specificity of the HPV DNA chip test and PCR-based HPV detection kits are comparable to the HC2 test for the detection of HSIL or worse disease.[13] The concordance rate between the HPV DNA chip and the HC2 test was previously reported to be 88% (κ = 0.61).[14] In our study, the concordance rate was 79.4% (688/867), with a κ-value of 0.55. The HPV DNA chip exhibits concordance rates ranging from 61.5% and 91.1% compared with DNA sequencing.[15,16] The wide range of concordance rates for the HPV DNA chip compared with other assays may result from different viral detection thresholds and cross-reactivity. The sensitivity of the HC2 method is approximately 5,000 copies of the HPV genome.[17] The PCR-amplification HPV DNA chip method is subject to a minimum signal detection level, which is the scanner signal:background noise ratio limit at low viral loads, approximately 100 to 1,000 copies.[18] Additionally, a simple primer set targeting the HPV MY09 region and sequence similarities between the 24 probes of the HPV DNA chip may lead to cross-reactivity that contributes to discordance.[16,19] In this study, the clinical performance of the MyHPV chip was comparable to HC2 for detecting HSILs or worse. The sensitivity and specificity of both HPV tests and cytology were very similar (approximately 85% and 50%, respectively). Adding the HPV test (MyHPV chip or HC2) to cytology exhibited excellent sensitivity (95%, each) but low specificity (approximately 30%, each). Furthermore, we demonstrated that patients who were HPV-16/18 (+) according to the MyHPV chip were at a higher risk of lesions graded HSIL or worse than patients who were non-16/18 HR-HPV (+) (OR 9.9 vs. 3.7). Among cytology "NILM" and "ASC or AGC" subgroups, the ORs were 5.9 and 3.0, respectively, for patients HR-HPV (+) based on HC2 test, compared with HR-HPV (−) patients. Conversely, patients who tested HR-16/18 positive using the MyHPV chip showed much higher ORs (6.8 and 11.7, respectively). According to these results, clinicians need to refer patients who are HPV-16/18 (+) according to HPV genotyping for immediate colposcopy instead of follow up, even when the cytology test is negative or ambiguous.

We found that patients who were non-16/18 HR-HPV (+) according to the MyHPV chip showed higher risk for ≥HSILs than patients with HR-HPV (−) (OR, 3.7). However, in the subgroup study of cytology "NILM" and "ASC or AGC," the OR for ≥HSILs in the non-16/18 HR-HPV (+) group did not significantly differ from the HR-HPV (−) group, probably due to the small subgroup population.

The limitations of our study include its retrospective design and that it was conducted at a single institution. Additionally, our patients were primarily referred from local clinics and previously diagnosed as "abnormal" based on local cervical cytology. The overall prevalence rates of ≥HSIL in NILM (12.4%) and ASCUS (25.4%) patients were higher than those reported in a previous study.[4] We hypothesize the cytology may have been under sampled because clinicians tend to forego subsequent extensive sampling if previously diagnosed.

In conclusion, the sensitivity and specificity of the HPV DNA chip test are similar to the HC2 test, and detecting HPV 16/18 with a HPV DNA chip is useful for predicting high-grade cervical lesions. Therefore, the HPV DNA chip genotyping method, which is commonly used in many Asian countries as an HPV DNA test, may be useful in assessing the risk of high-grade cervical lesions.

REFERENCES

1. Walboomers JM, Jacobs MV, Manos MM, et al. Human papillomavirus is a necessary cause of invasive cervical cancer worldwide. J Pathol 1999; 189: 12-9.

2. Castle PE, Solomon D, Schiffman M, Wheeler CM. Human papillomavirus type 16 infections and 2-year absolute risk of cervical precancer in women with equivocal or mild cytologic abnormalities. J Natl Cancer Inst 2005; 97: 1066-71.

3. Khan MJ, Castle PE, Lorincz AT, et al. The elevated 10-year risk of cervical precancer and cancer in women with human papillomavirus (HPV) type 16 or 18 and the possible utility of type-specific HPV testing in clinical practice. J Natl Cancer Inst 2005; 97: 1072-9.

4. Stoler MH, Wright TC Jr, Sharma A, et al. High-risk human papillomavirus testing in women with ASC-US cytology: results from the ATHENA HPV study. Am J Clin Pathol 2011; 135: 468-75.

5. Wright TC Jr, Stoler MH, Sharma A, et al. Evaluation of HPV-16 and HPV-18 genotyping for the triage of women with high-risk HPV+ cytology-negative results. Am J Clin Pathol 2011; 136: 578-86.

6. Bosch FX, Burchell AN, Schiffman M, et al. Epidemiology and natural history of human papillomavirus infections and type-specific implications in cervical neoplasia. Vaccine 2008; 26 Suppl 10: K1-16.

7. de Sanjose S, Quint WG, Alemany L, et al. Human papillomavirus genotype attribution in invasive cervical cancer: a retrospective cross-sectional worldwide study. Lancet Oncol 2010; 11: 1048-56.

8. Saslow D, Solomon D, Lawson HW, et al. American Cancer Society, American Society for Colposcopy and Cervical Pathology, and American Society for Clinical Pathology screening guidelines for the prevention and early detection of cervical cancer. Am J Clin Pathol 2012; 137: 516-42.

9. Solomon D, Davey D, Kurman R, et al. The 2001 Bethesda System: terminology for reporting results of cervical cytology. JAMA 2002; 287: 2114-9.

10. Terry G, Ho L, Londesborough P, Cuzick J, Mielzynska-Lohnas I, Lorincz A. Detection of high-risk HPV types by the Hybrid Capture 2 test. J Med Virol 2001; 65: 155-62.

11. Muñoz N, Bosch FX, de Sanjosé S, et al. Epidemiologic classification of human papillomavirus types associated with cervical cancer. N Engl J Med 2003; 348: 518-27.

12. Huh WK, Ault KA, Chelmow D, et al. Use of primary high-risk human papillomavirus testing for cervical cancer screening: interim clinical guidance. Obstet Gynecol 2015; 125: 330-7.

13. Lee JK, Hong JH, Kang S, et al. Practice guidelines for the early detection of cervical cancer in Korea: Korean Society of Gynecologic Oncology and the Korean Society for Cytopathology 2012 edition. J Gynecol Oncol 2013; 24: 186-203.

14. Kang WD, Kim CH, Cho MK, et al. Comparison of the hybrid capture II assay with the human papillomavirus DNA chip test for the detection of high-grade cervical lesions. Int J Gynecol Cancer 2009; 19: 924-8.

15. Choi YD, Jung WW, Nam JH, Choi HS, Park CS. Detection of HPV genotypes in cervical lesions by the HPV DNA Chip and sequencing. Gynecol Oncol 2005; 98: 369-75.

16. Park S, Kang Y, Kim DG, Kim EC, Park SS, Seong MW. Comparison of the analytical and clinical performances of Abbott RealTime High Risk HPV, Hybrid Capture 2, and DNA Chip assays in gynecology patients. Diagn Microbiol Infect Dis 2013; 76: 432-6.

17. Brink AA, Snijders PJ, Meijer CJ. HPV detection methods. Dis Markers 2007; 23: 273-81.

18. Um TH, Lee EH, Chi HS, Kim JW, Hong YJ, Cha YJ. Comparison of HPV genotyping assays and Hybrid Capture 2 for detection of high-risk HPV in cervical specimens. Ann Clin Lab Sci 2011; 41: 48-55.

19. Cho EJ, Do JH, Kim YS, Bae S, Ahn WS. Evaluation of a liquid bead array system for high-risk human papillomavirus detection and genotyping in comparison with Hybrid Capture II, DNA chip and sequencing methods. J Med Microbiol 2011; 60 (Pt 2): 162-71.

Isolated Mass-Forming IgG4-Related Cholangitis as an Initial Clinical Presentation of Systemic IgG4-Related Disease

Seokhwi Kim · Hyunsik Bae
Misun Choi · Binnari Kim
Jin Seok Heo[1] · **Ho Seong Kim**[2]
Seung Hee Choi[3] · **Kee-Taek Jang**

Departments of Pathology and Translational
Genomics, [1]Surgery, [2]Nuclear Medicine,
and [3]Radiology, Samsung Medical Center,
Sungkyunkwan University School of Medicine,
Seoul, Korea

Corresponding Author
Kee-Taek Jang, MD
Department of Pathology and Translational
Genomics, Samsung Medical Center,
Sungkyunkwan University School of Medicine,
81 Irwon-ro, Gangnam-gu, Seoul 06351, Korea
Tel: +82-2-3410-2763
Fax: +82-2-3410-0025
E-mail: kt12.jang@samsung.com

IgG4-related disease (IgG4-RD) may involve multiple organs. Although it usually presents as diffuse organ involvement, localized mass-forming lesions have been occasionally encountered in pancreas. However, the same pattern has been seldom reported in biliary tract. A 61-year-old male showed a hilar bile duct mass with multiple enlarged lymph nodes in imaging studies and he underwent trisectionectomy under impression of cholangiocarcinoma. Gross examination revealed a mass-like lesion around hilar bile duct. Histopathologically, dense lymphoplasmacytic infiltration and storiform fibrosis were identified without evidence of malignancy. Immunohistochemical stain demonstrated rich IgG4-positive plasma cell infiltration. Follow-up imaging studies disclosed multiple enlarged lymph nodes with involvement of pancreas and perisplenic soft tissue. The lesions have been significantly reduced after steroid treatment, which suggests multi-organ involvement of systemic IgG4-RD. Here, we report an unusual localized mass-forming IgG4-related cholangitis as an initial presentation of IgG4-RD, which was biliary manifestation of systemic IgG4-related autoimmune disease.

Key Words: IgG4-related disease; Bile ducts; Mass-forming; Cholangiocarcinoma

IgG4-related disease (IgG4-RD) may involve multiple organs including pancreas, head and neck region, kidney, lung, retroperitoneum, and lymph node.[1] Histologically, it is characterized by lymphoplasmacytic infiltration, storiform fibrosis and/or obliterative phlebitis with IgG4 immunohistochemical reactivity in plasma cells.[2] In addition to histologic findings, serum IgG4 level is often elevated in patients with IgG4-RD.[3,4] It is not difficult to diagnose IgG4-RD if an involved organ shows diffuse enlargement with an elevated serum IgG4 level. However, it may not be easy to suspect IgG4-RD if the lesion presents as a localized mass-forming lesion rather than diffuse organ involvement. Although localized mass-forming IgG4-related autoimmune pancreatitis has been reported occasionally,[5-7] such manifestation in biliary tract has seldom been described in the literature. In addition, most reported biliary cases had simultaneous segmental involvement of bile duct wall as well as mass-forming lesions.[8-10] Here, we report a case of localized mass-forming IgG4-related cholangitis, which mimicked hilar cholangio-carcinoma and later progressed to multi-organ involving IgG4-related systemic autoimmune disease, with review of relevant literatures.

CASE REPORT

A 61-year-old male, who had a past medical history of diabetes, coronary artery bypass surgery and idiopathic pulmonary disease, was admitted for the control of his blood sugar level. He complained of general weakness, easy fatigability, and weight loss of 3 kg for 10 days. Laboratory test results were within normal range except for elevated aspartate aminotransferase (100 U/L), alanine transaminase (114 U/L), and alkaline phosphatase (397 U/L). Although serum tumor markers were within normal limits (α-fetoprotein, 2 ng/mL; carcinoembryonic antigen, 1.56 ng/mL; carbohydrate antigen 19-9, 13.71 U/mL), additional tests for malignancy was conducted due to his weight loss. The magnetic resonance cholangiopancreatography disclosed a mass le-

sion at hilar bile duct. Magnetic resonance imaging (MRI) revealed a 2.1-cm-sized relatively well-demarcated mass at bifurcation of the left hepatic duct. The mass showed high signal intensity in diffusion restriction image and low intensity in apparent diffusion coefficient (ADC) map image, suggestive of type IV hilar cholangiocarcinoma with periductal invasion into underlying hepatic parenchyma (Fig. 1A, B). Since the patient had type 3 variation of intrahepatic bile duct-prior branching of right posterior Glisson pedicle which made the mass to be located apart from the right posterior duct, the lesion was considered to be resectable. Preoperative evaluation of positron emission tomography (PET) showed multiple enlarged lymph nodes in left axillary, common hepatic, portocaval, and aortocaval areas. Ultrasonography-guided biopsy of the axillary lymph node was performed; however, malignant cell was not identified, suggesting a reactive change rather than metastasis. Clinicians decided to perform surgery with an impression of hilar cholangiocarcinoma. A firm mass was detected at upper hilar level during the operation. Invasion to the left portal vein was suspected and the mass was also close to the right portal vein. Left trisectionectomy was performed for curative resection.

The resected specimen revealed a white firm mass-like lesion, measuring 2.5×2.0×1.3 cm, at bifurcation of the left intrahepatic bile duct (Fig. 1C). Histologic examination showed an extensive infiltration of lymphocytes and plasma cells (Fig. 2A). Storiform fibrosis was noted with a few foci of obliterative phlebitis (Fig. 2B). Immunohistochemical staining for IgG and IgG4 showed numerous IgG- and IgG4-immunoreactive plasma cells (Fig. 2C, D). The IgG4+ plasma cells were identified up to 53 cells per high-power field. IgG4+/IgG plasma cell ratio was 0.42. According to the consensus statement on the pathology of IgG4-RD, the lesion was diagnosed as "histologically highly suggestive of IgG4-RD."[2]

Following the pathologic diagnosis of IgG4-RD, laboratory tests for serum IgG level was performed and it was within upper normal range in postoperative day 12 (1,522 mg/dL; refer-
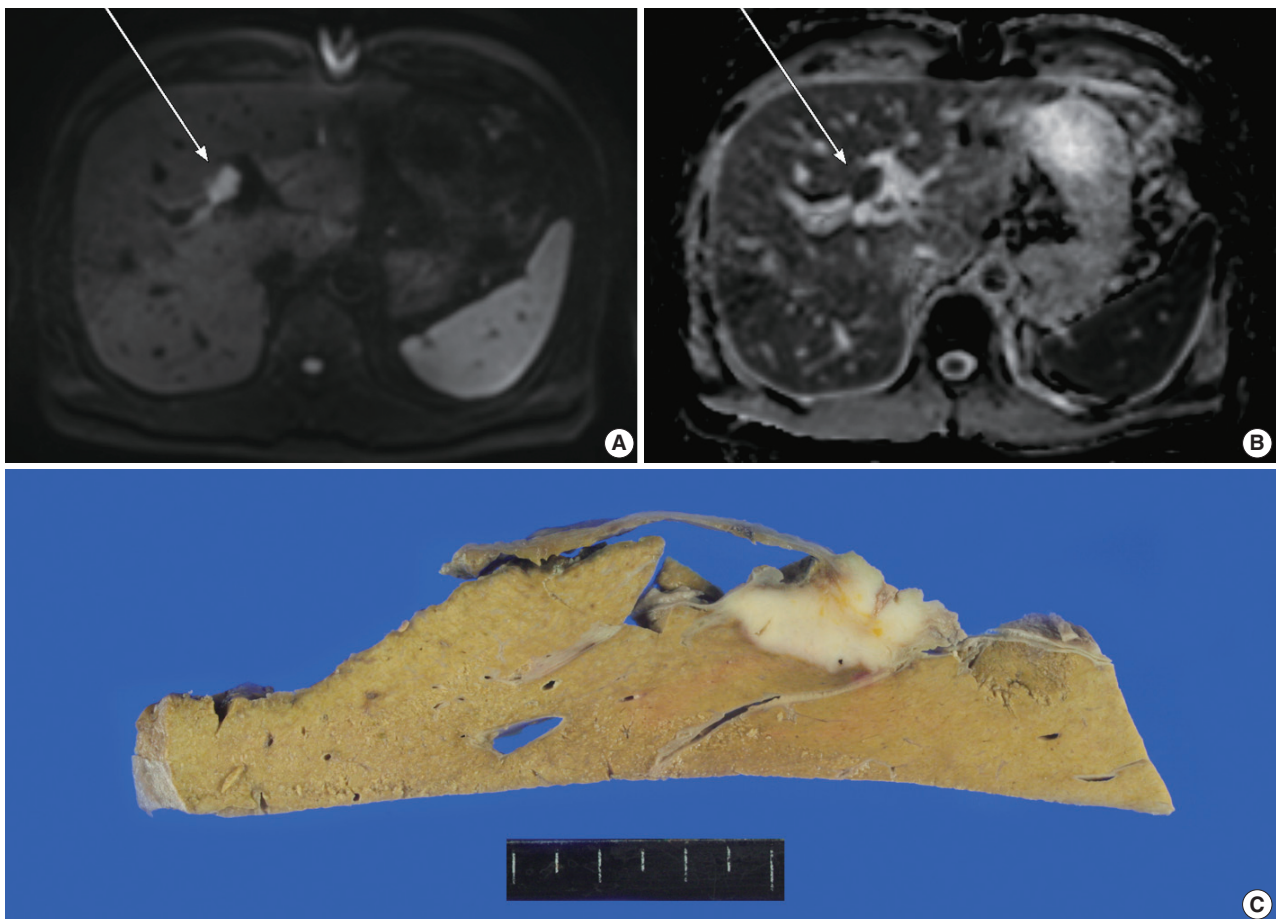
Fig. 1. Magnetic resonance imaging reveals an enhancing mass lesion which has high signal intensity on diffusion restriction phase (A) and low intensity on apparent diffusion coefficient map phase (B), suspicious for malignancy. (C) The cut section of hilar bile duct shows a relatively well-demarcated mass-forming lesion with a hepatic parenchymal invasion.

ence range, 700 to 1,600 mg/dL). All subclasses of IgG were elevated: IgG1, 1,070 mg/dL (reference range, 341 to 894 mg/dL); IgG2, 694 mg/dL (reference range, 171 to 632 mg/dL); IgG3, 134 mg/dL (reference range, 11.5 to 105.3 mg/dL); and IgG4, 257 mg/dL (reference range, 2.4 to 121.0 mg/dL). Thorough investigation for involvement of other organs by IgG4-RD was done, but it failed to identify any additional abnormality. The patient did not receive corticosteroid treatment because no residual lesion was left after the resection and also because he was diabetic.

After a year, follow-up PET scan revealed an increased fluorodeoxyglucose (FDG) uptake in the biliary trees of right liver, pancreas, and perisplenic soft tissue as well as hypermetabolic lymphadenopathy involving supraclavicular, mediastinal, pulmonary hilar, subcarinal and left abdominal paraaortic lymph nodes, suggestive of progression to extrabiliary multi-organ IgG4-related autoimmune disease (Fig. 3A). Serum IgG level had also increased to 3,677 mg/dL, more than twice as high as the initial value. Fluorescent antinuclear antibody test showed 4+ result. The patient started to take prednisone once a day. However, computed tomography (CT) images after prednisone treatment for 6 months revealed subpleural consolidations and en-

largement of mediastinal lymph nodes. As prednisone treatment was continued, the extent of subpleural consolidations diminished on the follow-up CT images. A year persistent treatment markedly decreased FDG uptake in bilateral supraclavicular, left axilla, mediastinal, subcarinal, pulmonary hilar, and retroperitoneal left paraaortic lymph nodes on PET scan, reflecting the patient's multi-organ IgG4-RD response to the steroid (Fig. 3B).

This study was approved by the Institutional Review Board of the Samsung Medical Center (IRB No. 2015-10-203).

DISCUSSION

IgG4-RD was originally recognized in pancreas as autoimmune pancreatitis.[11] Concomitant extrapancreatic manifestation is not uncommon in bile duct, lymph node, salivary glands, gastric mucosa, and kidney.[1,3,12] Solitary organ involvement without pancreatitis has also been reported.[1,3,4] IgG4-RD tends to present as diffuse lesion in the involved organs, especially in pancreas and biliary tract.[13] Localized mass-forming autoimmune pancreatitis had frequently been misdiagnosed as malignancy and had resulted in unnecessary surgical resections.[6,7] In contrast, mass-forming IgG4-related cholangitis is far less common and
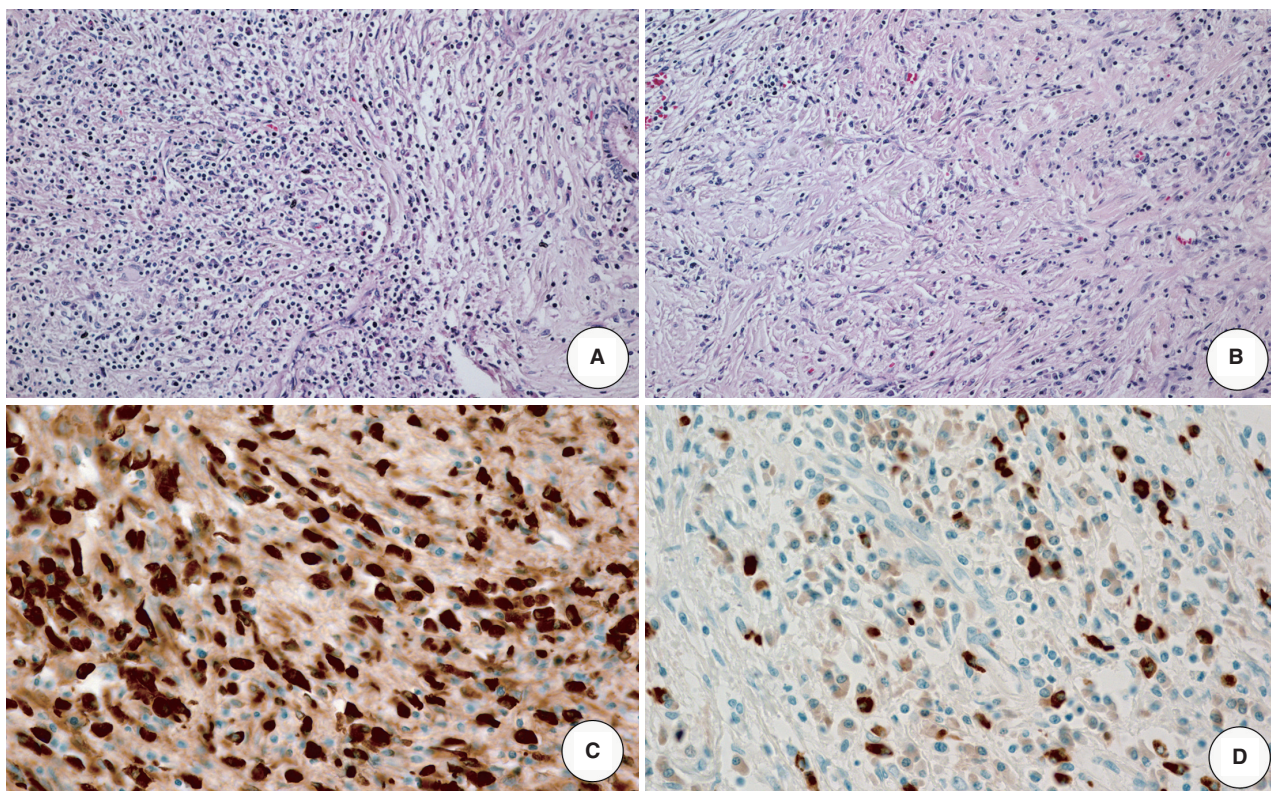
Fig. 2. Histologic examination reveals dense infiltration of lymphocytes and plasma cells (A) and storiform fibrosis (B). Both IgG-immunopositive (C) and IgG4-immunopositive (D) plasma cells are identified by immunohistochemical staining.
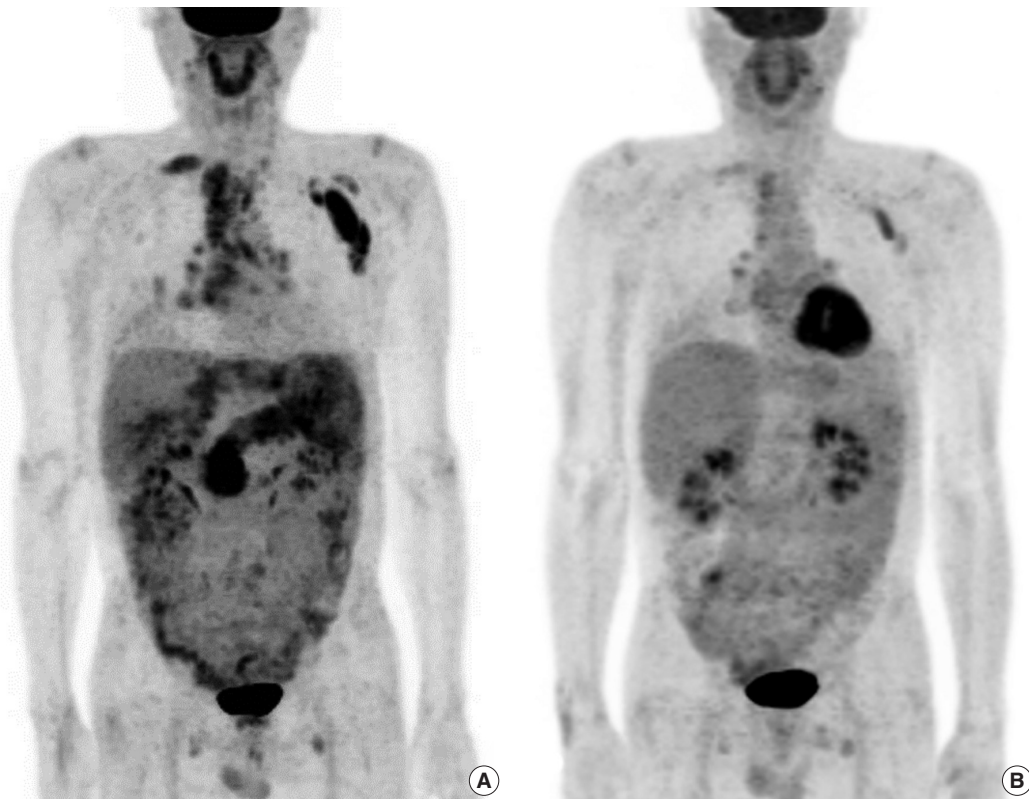
Fig. 3. (A) Fluorodeoxyglucose (FDG) positron emission tomography–computed tomography, maximum intensity projection image show hypermetabolic lesions involving bilateral supraclavicular, left axillar, mediastinal, pulmonary hilar and retroperitoneal lymph nodes, right liver biliary tract, pancreas, and perisplenic area. (B) After steroid treatment, markedly decreased FDG uptake is noted although uptakes in some lymph nodes are still seen.

Table 1. Clinicopathological findings of previously reported cases of mass-forming IgG4-related cholangitis

Reference	Sex	Age (yr)	Specimen type	Site	Symptom	Radiologic finding	IgG4 count (/HPF)	Sequence of biliary manifestation	Other manifestations	Serum IgG4/IgG	Follow-up
Present case	M	61	Resection	Hilum	Fatigue, weight loss	Localized mass	45	Initial	Pancreas, pleura, LN, perisplenic soft tissue	257 /1,522	Response on steroids
Deshpande et al.[8]	M	68	Biopsy	Liver and IBD	Jaundice	Vague mass with alternate narrowing and dilatation of IBD	37	Initial	Salivary gland, retroperitoneum	4,160 /3,580	Response on steroids
	F	42	Resection	Hilum	Hepatic hilar mass	NA	140	Secondary	Pancreas	NA	No steroid use
Hamano et al.[10]	F	50	Biopsy	CBD	Abdominal pain, jaundice	Mass with long CBD narrowing	NA	Initial	No	122 /1,711	Response on steroids
Zen et al.[9]	M	59	Resection	IBD	NA	Mass with irregular stricture	+++[a]	Initial	No	NA	NA
	M	79	Resection	IBD	NA	Mass with irregular stricture	+++[a]	Initial	No	NA	NA
	M	56	Resection	IBD	NA	Mass with irregular stricture	+++[a]	Initial	LN	NA	NA
	M	64	Resection	IBD	NA	Mass with irregular stricture	+++[a]	Initial	LN	NA	NA
	M	67	Resection	Left HD	NA	Mass with irregular stricture	+++[a]	Initial	No	NA	NA

HPF, high power field; M, male; LN, lymph node; IBD, intrahepatic bile duct; F, female; NA, not available; CBD, common bile duct; HD, hepatic duct.
[a]The number of IgG4-immunopositive plasma cells is not counted; semiquantitative score is used instead.

most reported cases were identified as long segment smooth narrowing of the bile ducts.[14] Table 1 summarizes clinical, radiological and pathologic characteristics of localized mass-forming IgG4-related cholangitis cases that have been reported to date. Besides our case, all except one presented as hilar or intrahepatic mass accompanied by biliary stricture.[8-10] Since these lesions had often been misdiagnosed as cholangiocarcinoma, many patients had undergone unnecessary resection of liver. IgG4-RD could be diagnosed only after histopathologic examination of the resected specimen, which showed numerous IgG4+ plasma cell infiltrates.[9,15,16]

The case presented here clearly showed a mass lesion in both imaging studies and resected specimen without accompanying biliary stricture. Radiologists also had no doubt that the lesion was malignancy since it was not only a well-defined isolated mass but also it had characteristic features of malignant lesion in many imaging modalities; arterial phase of CT revealed enhancement and the lesion showed high signal intensity on diffusion restriction phase and low intensity on ADC map phase of MRI. Furthermore, the patient lost 3 kg of his weight for 10 days, a suspicious sign of malignancy. Multiple enlarged lymph nodes in our case were also regarded as metastasis from cholangiocarcinoma until the aspiration biopsy proved otherwise. Despite the negative result of aspiration biopsy of the lymph node, hilar cholangiocarcinoma was still suspected, considering the result as false-negative. However, a possibility of nodal manifestation of IgG4-RD should have been considered in this case because systemic nodal metastasis is an unusual finding for cholangiocarcinoma.[17]

Clinical diagnostic criteria to aid detection of IgG4-related sclerosing cholangitis were suggested by a Japanese group.[18] The criteria included four items: (1) characteristic biliary imaging findings, (2) elevation of serum IgG4, (3) coexistence of other IgG4-related disease, and (4) histopathological features. To make definite diagnosis, thorough investigation of clinical, radiologic, laboratory and histopathologic examination is essential; however, all of these examinations are not always performed. Although there are some radiologic characteristics which help distinguish IgG4-related cholangitis from primary sclerosing cholangitis, it is still difficult to exclude hilar cholangiocarcinoma by image alone. Likewise, serum IgG4 level alone is not helpful since its sensitivity and specificity are not high.[19] Some of IgG4-related cholangitis cases showed only minimally elevated serum IgG4 level.[10] Histologic confirmation is necessary for definite diagnosis in this regard. Biopsy seems to be superior to brush cytology because some cases revealed false-positive atypical cells in brush cytology but resection specimen consisted of IgG4+ plasma cells and fibrosis only.[20] Both quantity and quality of the biopsy are crucial for representing the entire lesion and immunohistochemical staining for IgG and IgG4 is required for an accurate diagnosis.

In summary, we report an unusual case of localized mass-forming IgG4-related cholangitis that mimicked hilar cholangiocarcinoma in the initial diagnostic approach. Since isolated mass-forming IgG4-RD without biliary stricture is extremely rare, exclusion of malignancy can be difficult without histopathologic confirmation. Also, the IgG4-related cholangitis in this patient later progressed to the most extensive form of systemic disease reported to date. Although IgG4-related cholangitis is rare, it should be considered in differential diagnosis of a solitary mass in the biliary tree that mimics cholangiocarcinoma, especially when it is accompanied by any evidence of systemic manifestation, including multiple lymphadenopathy and suspicious extrapancreatic organ involvement.

Conflicts of Interest

No potential conflict of interest relevant to this article was reported.

REFERENCES

1. Zen Y, Nakanuma Y. IgG4-related disease: a cross-sectional study of 114 cases. Am J Surg Pathol 2010; 34: 1812-9.

2. Deshpande V, Zen Y, Chan JK, *et al*. Consensus statement on the pathology of IgG4-related disease. Mod Pathol 2012; 25: 1181-92.

3. Stone JH, Zen Y, Deshpande V. IgG4-related disease. N Engl J Med 2012; 366: 539-51.

4. Mahajan VS, Mattoo H, Deshpande V, Pillai SS, Stone JH. IgG4-related disease. Annu Rev Pathol 2014; 9: 315-47.

5. Chang WI, Kim BJ, Lee JK, *et al*. The clinical and radiological characteristics of focal mass-forming autoimmune pancreatitis: comparison with chronic pancreatitis and pancreatic cancer. Pancreas 2009; 38: 401-8.

6. Matsumoto I, Shinzeki M, Toyama H, *et al*. A focal mass-forming autoimmune pancreatitis mimicking pancreatic cancer with obstruction of the main pancreatic duct. J Gastrointest Surg 2011; 15: 2296-8.

7. Naitoh I, Nakazawa T, Hayashi K, *et al*. Clinical differences between mass-forming autoimmune pancreatitis and pancreatic cancer. Scand J Gastroenterol 2012; 47: 607-13.

8. Deshpande V, Sainani NI, Chung RT, *et al*. IgG4-associated cholan-

gitis: a comparative histological and immunophenotypic study with primary sclerosing cholangitis on liver biopsy material. Mod Pathol 2009; 22: 1287-95.

9. Zen Y, Harada K, Sasaki M, et al. IgG4-related sclerosing cholangitis with and without hepatic inflammatory pseudotumor, and sclerosing pancreatitis-associated sclerosing cholangitis: do they belong to a spectrum of sclerosing pancreatitis? Am J Surg Pathol 2004; 28: 1193-203.

10. Hamano H, Kawa S, Uehara T, et al. Immunoglobulin G4-related lymphoplasmacytic sclerosing cholangitis that mimics infiltrating hilar cholangiocarcinoma: part of a spectrum of autoimmune pancreatitis? Gastrointest Endosc 2005; 62: 152-7.

11. Hamano H, Kawa S, Horiuchi A, et al. High serum IgG4 concentrations in patients with sclerosing pancreatitis. N Engl J Med 2001; 344: 732-8.

12. Kawano M, Saeki T, Nakashima H, et al. Proposal for diagnostic criteria for IgG4-related kidney disease. Clin Exp Nephrol 2011; 15: 615-26.

13. Novotný I, Dítě P, Trna J, Lata J, Husová L, Geryk E. Immunoglobulin G4-related cholangitis: a variant of IgG4-related systemic disease. Dig Dis 2012; 30: 216-9.

14. Deshpande V. IgG4-related disease of the gastrointestinal tract: a 21st century chameleon. Arch Pathol Lab Med 2015; 139: 742-9.

15. Miki A, Sakuma Y, Ohzawa H, et al. Immunoglobulin g4-related sclerosing cholangitis mimicking hilar cholangiocarcinoma diagnosed with following bile duct resection: report of a case. Int Surg 2015; 100: 480-5.

16. Graham RP, Smyrk TC, Chari ST, Takahashi N, Zhang L. Isolated IgG4-related sclerosing cholangitis: a report of 9 cases. Hum Pathol 2014; 45: 1722-9.

17. Cheuk W, Yuen HK, Chu SY, Chiu EK, Lam LK, Chan JK. Lymphadenopathy of IgG4-related sclerosing disease. Am J Surg Pathol 2008; 32: 671-81.

18. Ohara H, Okazaki K, Tsubouchi H, et al. Clinical diagnostic criteria of IgG4-related sclerosing cholangitis 2012. J Hepatobiliary Pancreat Sci 2012; 19: 536-42.

19. Lazaridis KN. Sclerosing cholangitis epidemiology and etiology. J Gastrointest Surg 2008; 12: 417-9.

20. Chung DT, Tang CN, Lai EC, Yang GP, Li MK. Immunoglobulin G4-associated sclerosing cholangitis mimicking cholangiocarcinoma. Hong Kong Med J 2010; 16: 149-52.

Intramuscular Tenosynovial Giant Cell Tumor, Diffuse-Type

Yoo Jin Lee · Youngjin Kang · Jiyoon Jung · Seojin Kim · Chul Hwan Kim

Department of Pathology, Korea University Anam Hospital, Seoul, Korea

Tenosynovial giant cell tumors (TSGCT), a group of tumors that originate in tendon sheaths, joints, bursae, or adjacent soft tissue, were first described in 1941 by Jaffe *et al*.[1] Diffuse-type TSGCT are known to be located in the periarticular soft tissue, while pure intramuscular tumors are rare. This case describes a diffuse-type TSGCT located in the hamstring muscle, which was determined to be a pure intramuscular type.

CASE REPORT

A healthy 52-year-old Korean woman presented with a 1-month history of right thigh pain and numbness with a palpable mass in the thigh. A T2-weighted magnetic resonance image showed a 7 cm × 5 cm-sized heterogeneous mass with distinct demarcation in the right hamstring muscle (Fig. 1A) that was suggestive of soft tissue sarcoma or nodular fasciitis. The patient was relatively healthy and had no history of previous surgery.

The patient underwent an operation to enucleate the entire mass, and a well-encapsulated yellowish round mass was dissected and removed. Grossly, the resected specimen was a 7 cm × 5 cm × 2 cm-sized mass and weighed 45 g. The cut surface showed a variegated brown- to yellow-colored appearance with dark reddish punctuated areas and focal myxoid portions (Fig. 1B). Upon microscopic examination, the tumor revealed a villonodular pattern with polygonal mononuclear cells, foamy macrophages and multinucleated giant cells (Fig. 2A, B). Differential

diagnosis included tenosynovial giant cell tumor, giant cell tumor of soft tissue, fibromas of the tendon sheath, epithelioid sarcoma, synovial sarcoma, and granulomatous lesions such as tendinous xanthoma. The immunohistochemical stains for CD68, S-100, desmin, epithelial membrane antigen (EMA), and CD34 were performed. The tumor cells showed granular cytoplasmic positivity for CD68 (Fig. 2C) and S-100 but were negative for desmin, EMA, and CD34. TSGCT was suggested based on histopathologic and immunohistochemical findings. A cytogenetic study was performed to confirm the diagnosis.

A nested polymerase chain reaction was performed, using the first and second round primer sets from a previous report (Fig. 2D).[2] When using the primer set COL6A3-2529F/CSF1-1752R in the first round and COL6A3-2588F/CSF1-1698R (exon 8) in the second round (lane 2), a 1.4-kbp fragment was amplified. Therefore, the cytogenetic result of this case indicated the fusion of colony stimulating factor-1 (CSF1) and collagen type VI alpha-3 (COL6A3), and the tumor was diagnosed as an intramuscular TSGCT diffuse type. This report was approved by the Institutional Review Board of Korea University Anam Hospital (AN15199-001).

DISCUSSION

TSGCT can be subtyped into diffuse and localized types, and intra-articular and extra-articular types, according to the growth pattern and location. This classification suggests different clinical behaviors.[3] Diffuse-type TSGCT presents as an extra-articular type in about 5% to 15% of cases.[4] It is a slow-growing lesion with a favorable prognosis, usually treated with complete excision. The tumor can be locally aggressive, even if benign in nature, and 33% to 50% can recur, although metastasis to other organs is rare after multiple recurrences.[4,5]

It is usually identified in periarticular tissue and can present

Corresponding Author
Chul Hwan Kim, MD
Department of Pathology, Korea University Anam Hospital, 73 Inchon-ro, Seongbuk-gu, Seoul 02841, Korea
Tel: +82-2-920-5595, Fax: +82-2-920-6576, E-mail: chkap@korea.ac.kr

as extra-articular extension of a primary intra-articular process. It can also reside completely outside of the joint, bursa or tendon sheath. Pure intramuscular type of the tumor has only been reported a few times. A previous study[4] showed only eight cases of diffuse-type TSGCT that had a clear origin in tendinous or synovial tissue. Six cases were located in a predominantly sub-
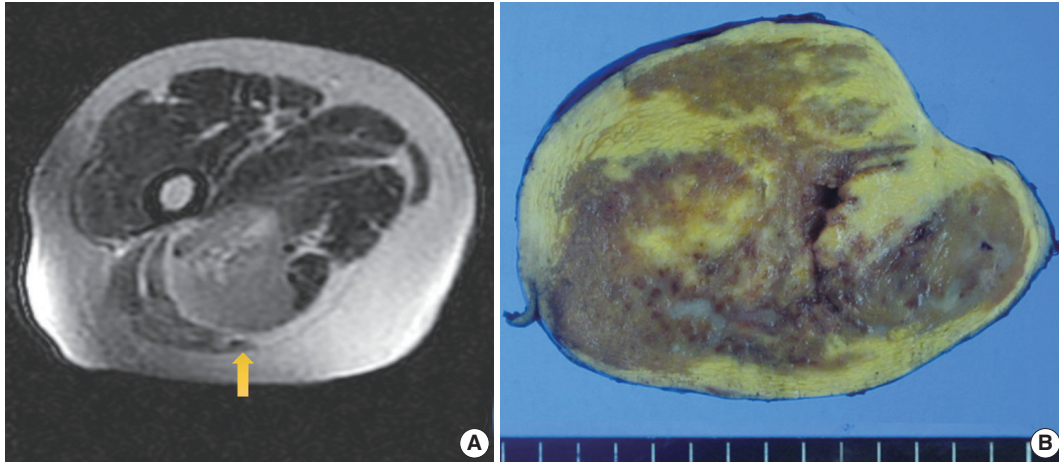
Fig. 1. (A) T2-weighted magnetic resonance image showing a well-marginated mass in the muscle of the right thigh (arrow). (B) The cut surface of the resected specimen shows a variegated brown to yellow colored mass with multifocal dark reddish punctuate areas and focal myxoid portions.
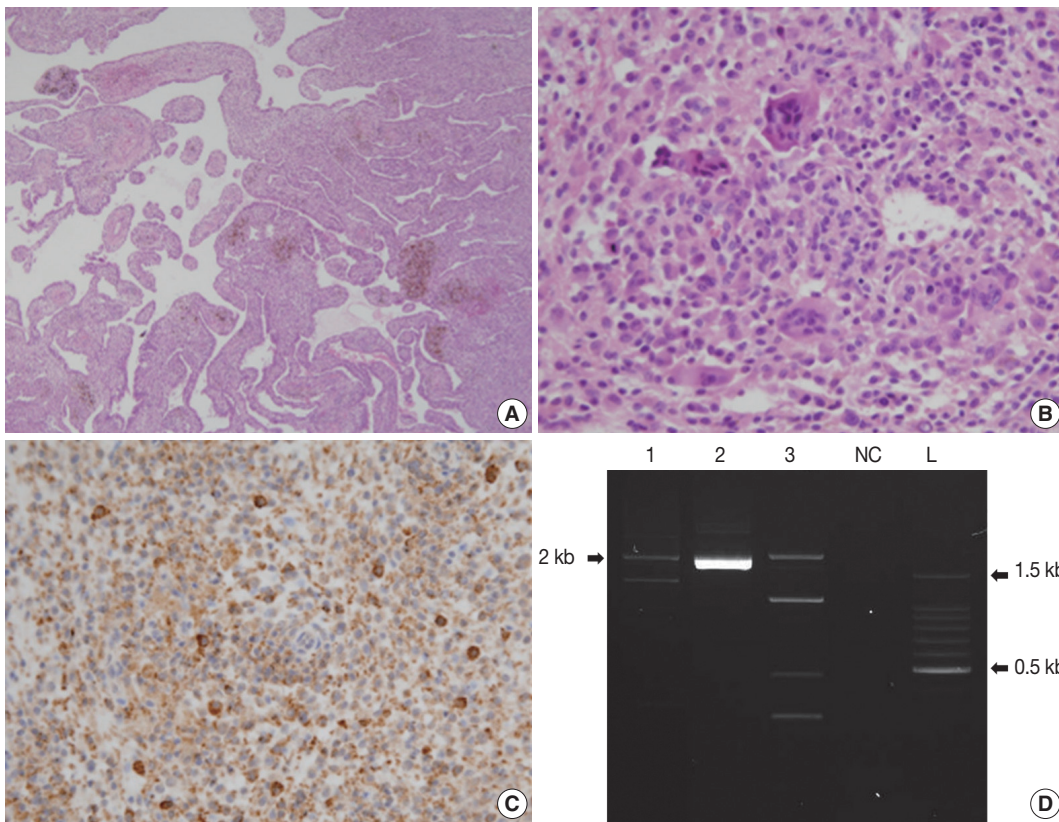
Fig. 2. (A) Hematoxylin-eosin stained slide of a diffuse-type tenosynovial giant cell tumor shows sheets of small histiocytes with a villonodular pattern and hemosiderin pigments. (B) Variable proportions of polygonal mononuclear cells and multinucleated giant cell are seen. (C) The tumor cells are positive for CD68 immunohistochemical staining. (D) Nested polymerase chain reaction to detect the COL6A3-CSF1 fusion transcript (lane 1 and lane 2) and CSF1 wild-type transcripts (lane 3). COL6A3, collagen type VI alpha-3; CSF1, colony stimulating factor-1; NC, negative control; L, ladder.

cutaneous area, and five cases were entirely intramuscular. The intramuscular type tumor can affect any muscle, but most were located in the lower extremities, including thigh, buttock, and lower leg,[4] which was similar to our case, while one case from another report[6] originated in an upper extremity, specifically the deltoid muscle.

This tumor was once regarded as a non-neoplastic condition, but their potential for recurrence and metastasis suggested the possibilities of neoplastic nature.[5,7] Furthermore, the cytogenetic studies identified clonal abnormalities, which suggested that this tumor was indeed a neoplasm.[5] An additional study[2] found a high expression of CSF1, localized to the 1p13q breakpoint, which is a hematopoietic growth factor that involves the proliferation and differentiation of macrophages and monocytes. CSF1 is often fused with COL6A3 on 2q35, which is thought to have a major oncogenic role in TSGCT. Due to the overexpression of CSF1, macrophages proliferate and become the main component of TSGCT. However, about 39% do not have CSF1 translocation, so the other alternative mechanism may affect CSF1 upregulation.

This case was an intramuscular soft tissue tumor without any connections to joints, tendons, or bursa and presented as a pure intramuscular type. The histologic features showed a villonodular pattern composed of histiocytes, foamy macrophages, multinucleated giant cells, and hemosiderin deposits. On cytogenetic study, this neoplasm was found to have clonal abnormalities, which are evidence for diffuse-type TSGCT. One report[6] suggested that the recurrence rate of intramuscular-type is lower than that of other types, as complete excision is easier for intramuscular masses than intra-articular lesions. However, the biologic behavior of intramuscular type tumors remains unclear

due to the small number of cases, which necessitates further studies to determine the prognostic significance of intramuscular lesions.

Conflicts of Interest

No potential conflict of interest relevant to this article was reported.

REFERENCES

1. Jaffe HL, Lichtenstein L, Sutro CJ. Pigmented villonodular synovitis, bursitis and tenosynovitis. Arch Pathol 1941; 31: 731-65.

2. Möller E, Mandahl N, Mertens F, Panagopoulos I. Molecular identification of COL6A3-CSF1 fusion transcripts in tenosynovial giant cell tumors. Genes Chromosomes Cancer 2008; 47: 21-5.

3. Ushijima M, Hashimoto H, Tsuneyoshi M, Enjoji M. Giant cell tumor of the tendon sheath (nodular tenosynovitis). A study of 207 cases to compare the large joint group with the common digit group. Cancer 1986; 57: 875-84.

4. Somerhausen NS, Fletcher CD. Diffuse-type giant cell tumor: clinicopathologic and immunohistochemical analysis of 50 cases with extraarticular disease. Am J Surg Pathol 2000; 24: 479-92.

5. Lucas DR. Tenosynovial giant cell tumor: case report and review. Arch Pathol Lab Med 2012; 136: 901-6.

6. Yun SJ, Hwang SY, Jin W, Lim SJ, Park SY. Intramuscular diffuse-type tenosynovial giant cell tumor of the deltoid muscle in a child. Skeletal Radiol 2014; 43: 1179-83.

7. Sanghvi DA, Purandare NC, Jambhekar NA, Agarwal MG, Agarwal A. Diffuse-type giant cell tumor of the subcutaneous thigh. Skeletal Radiol 2007; 36: 327-30.

IgG4-Related Sclerosing Mesenteritis

Seok Joo Lee · Cheol Keun Park · Woo Ick Yang · Sang Kyum Kim

Department of Pathology, Yonsei University Medical Center, Seoul, Korea

Sclerosing mesenteritis (SM) is a rare disease first described by Sulla[1] in 1924 under the name "retractile mesenteritis." SM shows fibrosis with fat necrosis and chronic inflammation on microscopic examination.[2] In particular, if the histologic and immunologic features are associated with IgG4-related disease (IgG4-RD), the condition is defined as IgG4-related sclerosing mesenteritis (IgG4-RSM).[3] Here, we report a case of a 70-year-old woman, who presented with a palpable intra-abdominal mass and vague abdominal pain, and was finally diagnosed with IgG4-RSM based on histology and immunohistochemistry. This case report was approved by the Institutional Review Board (IRB) of Yonsei University Medical Center (IRB No. 4-2015-0650).

CASE REPORT

A 70-year-old woman presented with a palpable intra-abdominal mass and pain for about 3 months. She had a history of hypertension and a total hysterectomy 10 years earlier. Radiologically, a 7.9 cm lobulated mass was found in her right lower abdomen with multiple calcifications (Fig. 1A), suggesting a mesenteric-origin tumor. Positron emission tomography–computed tomography revealed a mesenteric mass with calcification in the rihgt lower quadrant of abdomen which had intense fluorodeoxyglucose (FDG) uptake. A few satellite nodules were also present in the mesentery; however, no other abnormal FDG uptake was identified. The patient underwent segmental resection of the small bowel. Grossly, the mucosal surface was intact and a multilobulated mass with whitish fibrosis was noted in the mesentery (Fig. 1B). Light microscopy revealed fat necrosis and a sclerosing fibrotic lesion including lymphocytic aggregation with germinal center formation and spindle cell proliferation (Fig. 2A). The spindle cells had abundant cytoplasm, a vesicular nucleus, and prominent nucleoli (Fig. 2B). In the periphery, acute inflammatory cells and eosinophils were seen. Chronic inflammatory cell infiltration into the venular wall with obliteration of the lumen juxtaposed to an artery was also seen (Fig. 2C).

As a result, three histologic findings of storiform pattern of fibrosis, lymphoplasmacytic infiltration, and obliterative phlebitis were distinct features of the presented case. Based on these findings, the differential diagnoses included inflammatory malignant fibrous histiocytoma, inflammatory myofibroblastic tumor, and SM. We performed immunohistochemical staining using anaplastic lymphoma kinase (ALK, D5F3), smooth muscle actin (SMA), Ki-67, IgG, and IgG4 antibodies. The overall Ki-67 labeling index was low and was increased only in lymphoid follicles (Fig. 3A). ALK staining was negative and SMA staining revealed vascular obliteration (data not shown). Most of the plasma cells expressed IgG (Fig. 3B) and IgG4 (Fig. 3C), and the IgG4-positive cells/IgG-positive cells ratio was higher than 90%. Therefore, we concluded the lesion as IgG4-RSM. Immediately after the surgery, blood samples were taken to measure the patient's levels of IgG and IgG4. IgG4 level has greatly increased (2,130.0 mg/L; reference range, 39.2 to 864.0 mg/L), while IgG stayed within the normal range (1,318 mg/dL; reference range, 700 to 1,600 mg/dL). The patient was discharged without complication, received a clinical work-up for IgG4-RSM in an outpatient department, and started on steroid therapy.

DISCUSSION

SM is a rare benign condition that presents with fibrosis, inflammation, and fat necrosis and occurs idiopathically in the

Corresponding Author
Sang Kyum Kim, MD, PhD
Department of Pathology, Yonsei University Medical Center, 50-1 Yonsei-ro, Seodae-mun-gu, Seoul 03722, Korea
Tel: +82-2-2228-6751, Fax: +82-2-2227-7939, E-mail: nicekyumi@yuhs.ac

small bowel mesentery.[2] Clinically, patients with SM mostly complain of chronic severe pain and chronic non-specific problems such as nausea, vomiting, diarrhea, cramping, weight loss, and fever.[4] Histologically, SM shows fibrosis with fat necrosis, chronic inflammation especially around the vessels, and variable focal calcification. In particular, if the immunologic and histologic characteristics are consistent with the IgG4-RD, it is classified

as IgG4-RSM.[3] The histologic features of IgG4-RSM include more than two of the followings: lymphoplasmacytic infiltration, storiform fibrosis, and obliterative phlebitis. The immunologic criterion is IgG4-positive/IgG-positive cells >40%, but this ratio is considered secondary in importance to the histological appearance.

Kerdsirichairat *et al.*[3] conducted a systematic literature review
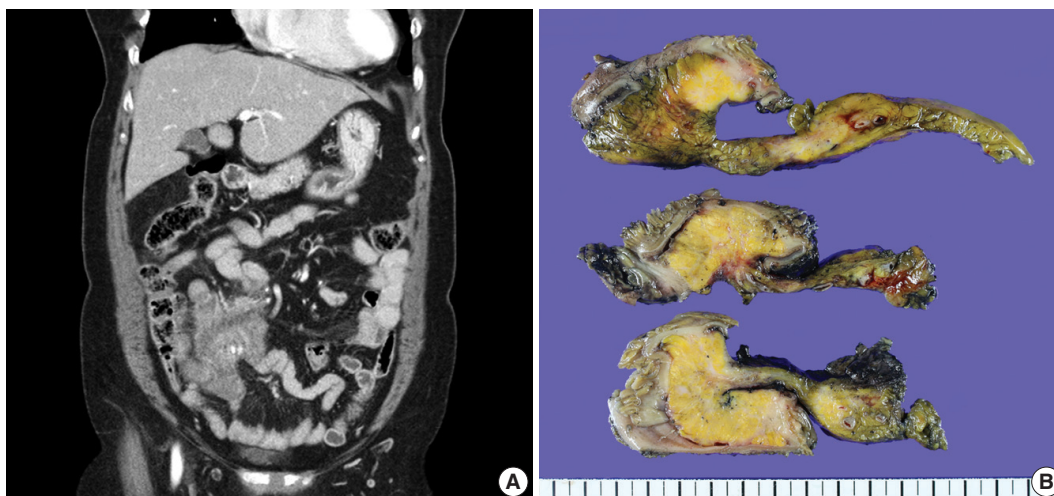
Fig. 1. (A) A 7.9 cm lobulated mass with multiple variable calcifications is seen in the right lower abdomen on abdominal computed tomography. (B) An ill-defined whitish fibrotic lesion is noted in the mesentery.
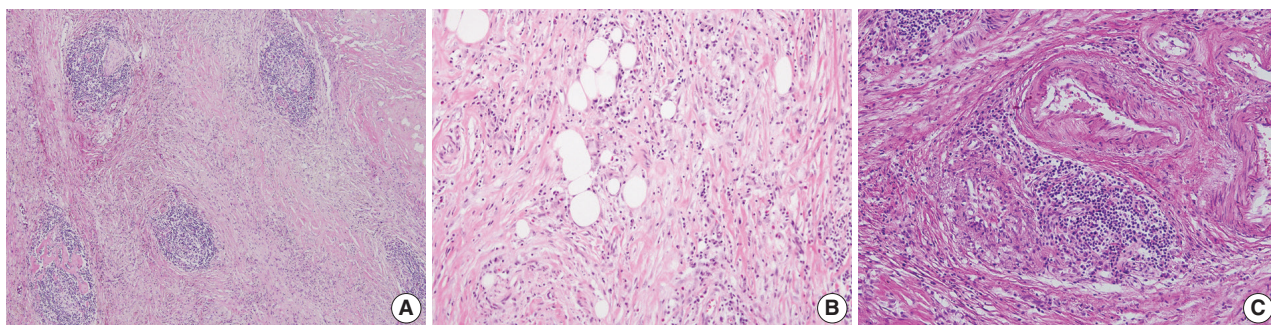
Fig. 2. (A, B) The microscopic findings show fat necrosis and a sclerosing fibrotic lesion (storiform fibrosis) with lymphocytic aggregation within the germinal center formation and spindle cell proliferation. (C) Obliterative phlebitis just next to an artery is also seen.
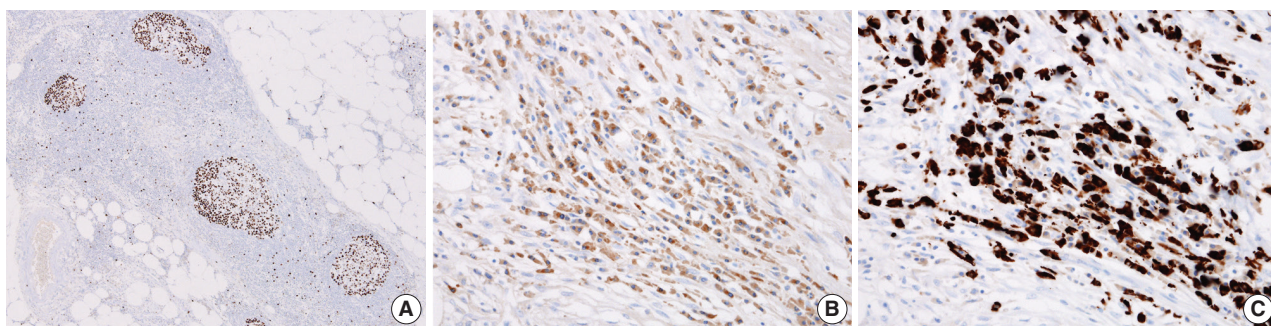
Fig. 3. (A) A low Ki-67–labeling index is shown with increase only in the lymphoid follicle. The IgG4-positive cells (C)/IgG-positive cells (B) ratio is higher than 90%.

of SM with IgG4 testing, and 11 out of 18 cases in total met the criteria for IgG4-RSM. The age of patients with IgG4-RSM ranges from 48 to 82. IgG4-RSM has a male predominance similar to SM. IgG4-RSM is known as a rare mesenteric disease of unknown etiology, although prior abdominal surgery can result in SM. Emory *et al.*[2] reviewed 84 cases of SM and a history of trauma or surgery was present in four of 84 patients. Two of four patients had hysterectomies 20 and 12 years earlier. Our patient has a history of total abdominal hysterectomy, which might be the cause of the IgG4-RSM.

There is no generalized consensus regarding the treatment of SM, including medical therapy, surgical therapy, and surgery with additional medical therapy. In one study, the response rates were shown to be good for all therapies (65%, 82%, and 71%, respectively),[3] but the limited number of cases made it difficult to determine a treatment of choice. Even, when patients with SM are not treated, they show a high rate of spontaneous resolution.[5] Therefore, therapy is needed when a patient displays symptoms.

In our case, the patient's differential diagnoses included inflammatory malignant fibrous histiocytoma and inflammatory myofibroblastic tumor, based on microscopic features. Inflammatory malignant fibrous histiocytoma shows neoplastic histiocyte-like cells mixed with neutrophils and other inflammatory cells. It has a high Ki-67 index, but in our patient's case, the overall Ki-67 index was low and was only increased in lymphoid follicles. Inflammatory myofibroblastic tumor shows spindle cell proliferation with myofibroblastic differentiation, a collagen stroma, and chronic inflammatory cell infiltrations. However, it rarely shows obliterative phlebitis.[6] It is immunoreactive for ALK in about half the cases and stains for SMA.[7,8] Also, the ratio of IgG4-positive/IgG-positive cells is markedly lower than that of IgG4-RD.[9] In our case, SMA staining was non-specific and only confirmed the obliterative phlebitis. The high ratio of IgG4-positive/IgG-positive cells also supported IgG4-RSM.

In summary, we present a case of IgG4-RSM, which is compatible with previously described cases. The condition is benign and has a self-limiting course, but the pathologic diagnosis is important to exclude malignant conditions, which can be mis-diagnosed on radiologic analysis. The rarity of the disease limits its clear characterization, and more cases and studies are needed.

Conflicts of Interest

No potential conflict of interest relevant to this article was reported.

REFERENCES

1. Sulla JV. Mesenterite e sclerosante. Policlinico Prat 1924; 31: 575-81.
2. Emory TS, Monihan JM, Carr NJ, Sobin LH. Sclerosing mesenteritis, mesenteric panniculitis and mesenteric lipodystrophy: a single entity? Am J Surg Pathol 1997; 21: 392-8.
3. Kerdsirichairat T, Mesa H, Abraham J, *et al.* Sclerosing mesenteritis and IgG4-related mesenteritis: case series and a systematic review of natural history and response to treatments. Immunogastroenterology 2013; 2: 119-28.
4. Parra-Davila E, McKenney MG, Sleeman D, *et al.* Mesenteric panniculitis: case report and literature review. Am Surg 1998; 64: 768-71.
5. Akram S, Pardi DS, Schaffner JA, Smyrk TC. Sclerosing mesenteritis: clinical features, treatment, and outcome in ninety-two patients. Clin Gastroenterol Hepatol 2007; 5: 589-96.
6. Minato H, Shimizu J, Arano Y, *et al.* IgG4-related sclerosing mesenteritis: a rare mesenteric disease of unknown etiology. Pathol Int 2012; 62: 281-6.
7. Cessna MH, Zhou H, Sanger WG, *et al.* Expression of ALK1 and p80 in inflammatory myofibroblastic tumor and its mesenchymal mimics: a study of 135 cases. Mod Pathol 2002; 15: 931-8.
8. Qiu X, Montgomery E, Sun B. Inflammatory myofibroblastic tumor and low-grade myofibroblastic sarcoma: a comparative study of clinicopathologic features and further observations on the immunohistochemical profile of myofibroblasts. Hum Pathol 2008; 39: 846-56.
9. Yamamoto H, Yamaguchi H, Aishima S, *et al.* Inflammatory myofibroblastic tumor versus IgG4-related sclerosing disease and inflammatory pseudotumor: a comparative clinicopathologic study. Am J Surg Pathol 2009; 33: 1330-40.

Carney Complex with Multiple Cardiac Myxomas, Pigmented Nodular Adrenocortical Hyperplasia, Epithelioid Blue Nevus, and Multiple Calcified Lesions of the Testis: A Case Report

Hyunchul Kim · Hyun-Yee Cho · Jeong Nam Lee[1] · Kook-Yang Park[2]

Departments of Pathology, [1]Surgery, and [2]Thoracic and Cardiovascular Surgery, Gachon University Gil Medical Center, Incheon, Korea

In 1985, Carney *et al*.[1] reported a syndrome composed of myxoid tumors, endocrine overactivity, and pigmented skin lesions. Myxoid tumors typically manifested as cardiac myxoma, cutaneous myxoma, and myxoid mammary fibroadenoma. Endocrine overactivity, such as acromegaly and Cushing's syndrome, presented with associated endocrine tumors, including pituitary adenoma, thyroid tumors, primary pigmented nodular adrenocortical disease (PPNAD), and testicular tumors.[2] Pigmented skin lesions include lentiginosis, conventional melanocytic nevus, and epithelioid blue nevus.[3]

Recently, a new concept of pigmented skin lesion called pigmented epithelioid melanocytoma, which has identical histological features to the epithelioid blue nevus, but lacks the associated Carney complex, was proposed.[4] We present a case of Carney complex with a brief introduction to the epithelioid blue nevi and pigmented epithelioid melanocytomas.

CASE REPORT

The publication of case information and materials was approved by the Institutional Review Board of The Gachon University Gil Medical Center (GAIRB2015-197).

A 31-year-old male patient visited our hospital with symptoms of recurrent rib fractures in the absence of physical trauma,

increased body hair, and central obesity. His evaluation showed Cushing's syndrome with bilateral adrenal cortical thickening, three calcified lesions on the left testis, and a pigmented skin lesion on the buttock. The patient and his sister had resection for familial cardiac myxomas 5 years ago, but did not have any other symptoms at that point; they were the subject of a previous case report.[5] The patient was diagnosed with Carney complex, and bilateral adrenalectomy and resection of the pigmented skin lesion were performed. A needle biopsy was done for the testicular tumor to preserve patient fertility.

The cardiac myxomas resected 5 years ago were located in both the right atrium and the ventricle, with sizes of 6.0×3.5 cm and 0.9×0.5 cm, respectively. The resected specimens were composed of hyperemic gelatinous soft tissue (Fig. 1A). Histologically, they showed fusiform to stellate cells with a moderate amount of eosinophilic cytoplasm embedded within the myxoid stroma (Fig. 1B). The patient was found to have a mutation in the protein kinase A type I-a regulatory subunit (*PRKAR1A*) gene when he had the resection of his cardiac myxoma.[5]

The bilateral adrenalectomy specimen showed multiple dark to light brown nodules measuring up to 1.2×1.2 cm throughout the cortex (Fig. 1C). Histologically, the nodules were composed of cells resembling those of normal zona reticularis and contained dark brown pigments (Fig. 1D). The histological features were consistent with those of PPNAD.

The resected skin showed dumbbell-shaped intradermal melanocytic proliferation with heavy pigmentation resembling blue nevus (Fig. 1E), but with epithelioid melanocytes (Fig. 1F). The cells were positive for S-100 protein (Fig. 1G) and human melanoma black 45 (Fig. 1H), based on immunohistochemical staining. The lesion was consistent with epithelioid

Corresponding Author
Kook-Yang Park
Department of Thoracic and Cardiovascular Surgery, Gachon University Gil Medical Center, 21 Namdong-daero 774beon-gil, Namdong-gu, Incheon 21565, Korea
Tel: +82-32-460-8413, Fax: +82-32-460-3117, E-mail: kkyypak@gilhospital.com

blue nevus.

The testicular needle biopsy from a 1.0-cm-sized lesion showed solid tubules composed of large polygonal cells with abundant eosinophilic cytoplasm and calcified bodies in collagenous stroma with lymphocytic infiltration (Fig. 1I). The histological findings raised the possibility of a large cell calcifying Sertoli cell tumor. However, due to the low possibility of malignancy and the patient's young age, no further invasive procedures were performed.

The patient's clinical and pathological manifestations were in accordance with those of Carney complex. The patient was discharged after the surgical resection, and follow up in outpatient clinic with medication for adrenal insufficiency is ongoing.

DISCUSSION

Carney complex is an autosomal dominant clinical syndrome, and many patients show germline mutations in the *PRKAR1A* gene.[2] In addition to the *PRKAR1A* mutation, some of the patients also show mutations in the *PDE11A* gene.[6] Among the
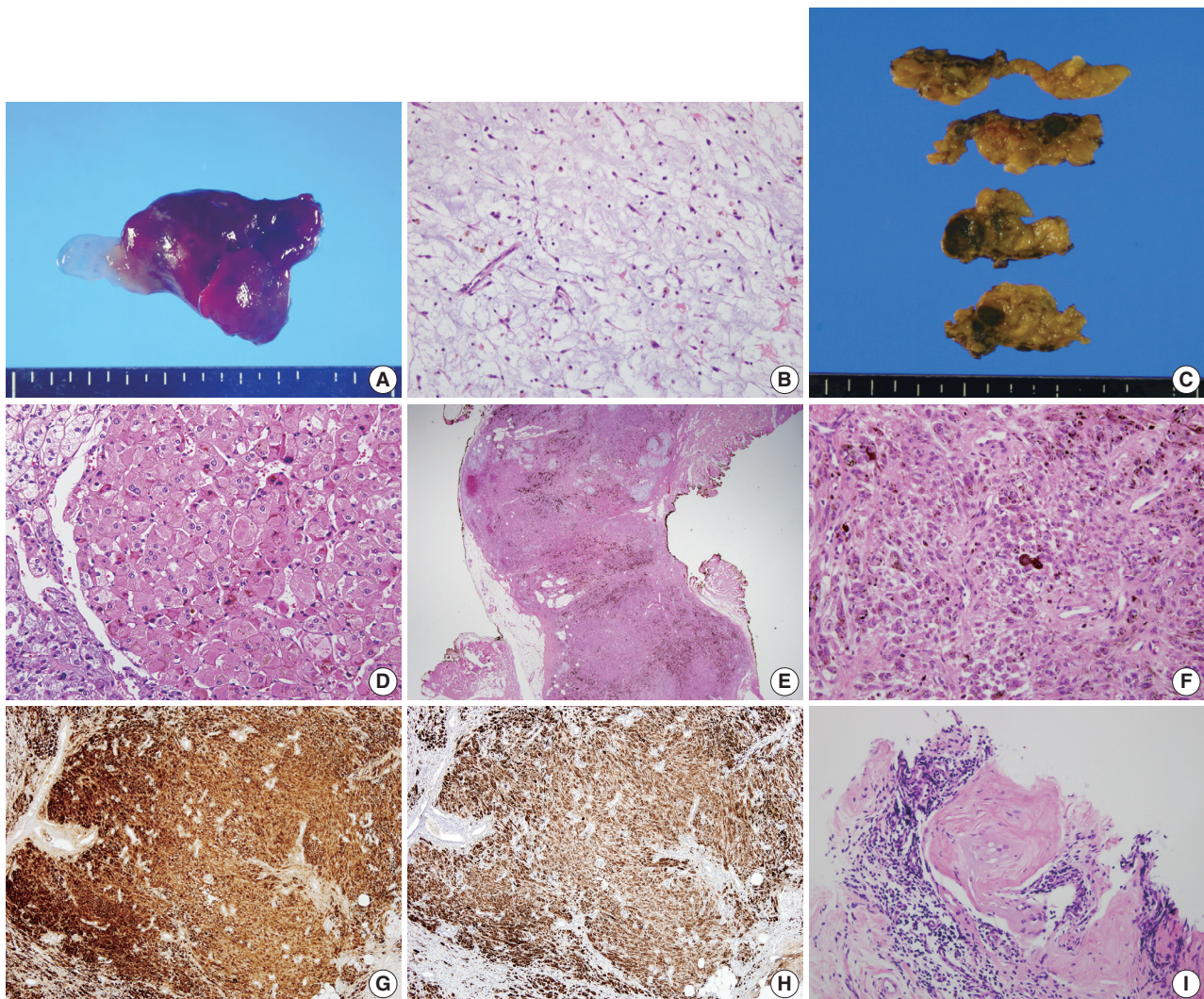
Fig. 1. Cardiac myxoma. (A) The gross photo of resected myxoma shows diffusely hyperemic and focally myxoid appearance. (B) Histologically, the tumor is composed of fusiform to stellate cells and surrounding blueish myxoid stroma. Primary pigmented nodular adrenocortical disease. (C) The gross photo of cut surface of resected adrenal glands show round to oval dark brown nodules throughout the cortex. (D) Histologically, the nodules are consisted of large polygonal cells with eosinophilic cytoplasm and granular brown pigments. Epithelioid blue nevus. (E) On low power view, the melanocytic lesion is in dumbbell-shaped and shows prominent dark pigmentation. (F) The tumor cells have relatively abundant eosinophilic cytoplasm and epithelioid appearance. The tumor cells are positive for S-100 protein (G) and human melanoma black 45 (H) immunostains. (I) The testicular biopsy showed large polygonal cells surrounded by hyalinized collagenous stroma and lymphocytic infiltration.

symptoms of Carney complex, cardiac myxoma is by far the most fatal, with a sudden death rate of over 10% in affected members with a familial Carney complex.[7] This high mortality requires regular screening in patients with Carney complex.[2] As in the current case, there can be multiple myxomas and they can be located in any heart chamber in patients with Carney complex, unlike myxomas in patients without Carney complex.[2]

PPNAD is unique in its clinical and histological features. It usually presents as bilateral adrenal hyperplasia.[2] Histologically, the affected adrenal glands show cortical nodules with dark pigmentation. PPNAD sometimes can be found in patients without Carney complex.[8]

The most recently established diagnostic entity related to the symptoms of the Carney complex is epithelioid blue nevus. Histologically, epithelioid blue nevus is similar to the original blue nevus due to heavy accumulation of melanin pigment is seen within the lesion, but it differs from the original blue nevus in that the melanocytes show epithelioid features. These lesions were first described in a report of 40 Carney complex patients and were named as such because of the histological features.[3] Later reports described melanocytic tumors showing identical histological features, potential for lymph node metastasis, and good prognosis after resection in patients without Carney complex.[4,9] The authors proposed the term "borderline pigmented epithelioid melanocytoma" as a provisional entity for the lesions, regardless of the presence or absence of Carney complex.[4]

This is a report on the rare Carney complex, which was diagnosed 5 years after its initial manifestation as familial cardiac myxoma. Isolated symptoms of Carney complex can be found outside of the syndrome, but their presentation is unique and such symptoms warrant clinical evaluation to enable early diagnosis and proper management.

Conflicts of Interest

No potential conflict of interest relevant to this article was reported.

REFERENCES

1. Carney JA, Gordon H, Carpenter PC, Shenoy BV, Go VL. The complex of myxomas, spotty pigmentation, and endocrine overactivity. Medicine (Baltimore) 1985; 64: 270-83.
2. Bertherat J. Carney complex (CNC). Orphanet J Rare Dis 2006; 1: 21.
3. Carney JA, Ferreiro JA. The epithelioid blue nevus: a multicentric familial tumor with important associations, including cardiac myxoma and psammomatous melanotic schwannoma. Am J Surg Pathol 1996; 20: 259-72.
4. Zembowicz A, Carney JA, Mihm MC. Pigmented epithelioid melanocytoma: a low-grade melanocytic tumor with metastatic potential indistinguishable from animal-type melanoma and epithelioid blue nevus. Am J Surg Pathol 2004; 28: 31-40.
5. Lee HL, Park KY, Kim KH, *et al*. Familiar myxoma with a positive genetic test: a case report. Korean J Thorac Cardiovasc Surg 2010; 43: 67-72.
6. Park KU, Kim HS, Lee SK, Jung WW, Park YK. Novel mutation in *PRKAR1A* in Carney complex. Korean J Pathol 2012; 46: 595-600.
7. Stratakis CA, Carney JA, Lin JP, *et al*. Carney complex, a familial multiple neoplasia and lentiginosis syndrome: analysis of 11 kindreds and linkage to the short arm of chromosome 2. J Clin Invest 1996; 97: 699-705.
8. Almeida MQ, Stratakis CA. Carney complex and other conditions associated with micronodular adrenal hyperplasias. Best Pract Res Clin Endocrinol Metab 2010; 24: 907-14.
9. Mandal RV, Murali R, Lundquist KF, *et al*. Pigmented epithelioid melanocytoma: favorable outcome after 5-year follow-up. Am J Surg Pathol 2009; 33: 1778-82.

■ BRIEF CASE REPORT ■

Tailgut Cyst in a Neonate: A Case Report

Ji Hyen Lee · Yun Suk Lee · So Yeon Shim · Su Jin Cho · Eun Ae Park · Soon Sup Chung[1] · Sanghui Park[2]

Departments of Pediatrics, [1]Surgery, and [2]Pathology, Ewha Womans University School of Medicine, Seoul, Korea

A tailgut cyst is a congenital anomaly located in the retrorectal space. This cyst is usually detected in adult patients, and is rarely diagnosed in the neonatal period.[1,2] These retrorectal cystic masses are believed to originate from the embryonic hindgut.[1,3] Following a literature review, we report a case of tailgut cyst in a neonate that was removed entirely through surgical excision.

CASE REPORT

A 3.3-kg baby girl was born at 37 weeks gestation by Cesarean section. During prenatal ultrasonography, a large mass was found in the pre-sacrococcygeal space. Local examination showed a 4×5-cm-sized swelling in the gluteal region, and laboratory tests were within normal limits. An X-ray of the lumbosacral spine indicated a soft mass in the coccygeal area without calcification (Fig. 1A). Ultrasonography showed a multiloculated cystic lesion with some echogenic portions at the pelvis that were located lateral and posterior to the rectosigmoid colon and anterior to the sacrococcygeal area (Fig. 1B). Magnetic resonance imaging (MRI) was performed and showed a large, well-demarcated mass with a small septated cyst within. There were calcifications within the upper portion of the cystic mass (Fig. 1C). When the infant was five days old, given concern for a possible sacrococcygeal cystic teratoma, a complete excision up to the coccyx was done through a posterior approach. The histopathology report showed a well-circumscribed, gray, soft mass ($4.7 \times 4.5 \times 3.5$ cm) with an attached ellipse of skin (2.3×1.9 cm), and the

cut section revealed a multilocular cyst. Microscopically, the cyst walls were lined by various epithelia: mucinous, low cuboidal, and pseudostratified columnar cells (Fig. 2). Additionally, dotted bundles of smooth muscle fibers and fibrous tissues were present between the cystic walls. No specific tissue fragments of significance such as skin adnexal elements, neural elements, or heterologous mesenchymal tissue (e.g., cartilage or bone) were found. The patient was discharged after 12 days and followed up as an outpatient with no postoperative complications.

This study was approved by the Institutional Review Board (IRB) of Ewha Womans University Mokdong Hospital (IRB No. 2015-08-002).

DISCUSSION

Tailgut cysts are uncommon congenital masses in the neonate, and they are commonly located in the retrorectal space; embryonically, they are believed to arise from vestigial remnants of the embryonic hindgut. Normally, at 35 days of gestation, the embryo has a true tail during early human development that reaches a maximum of 8 mm in length.[1] The primitive hindgut extends into this embryonic true tail, which is located at the site of the formation of the anus. During the eighth week of embryonic development, the tailgut usually atrophies, but occasionally can fail to regress completely. Some investigators have suggested that these remnants give rise to tailgut cysts.[1]

Tailgut cysts are more common in middle-aged women, and neonatal cases are considerably rare. The cyst usually occurs between the ages of 4 to 73 years, with an average presentation at 35 years, and the female-to-male ratio is 3:1.[3] Typical symptoms of tailgut cysts are closely associated with their region. Most adult patients complain of lower back pain or rectal pain while sitting or after falling on their buttocks, and other symptoms include urinary retention, dysuria, changes in stool caliber, and rec-

Corresponding Author
Eun Ae Park, MD
Department of Pediatrics, Ewha Womans University School of Medicine, 1071
Anyangcheon-ro, Yangcheon-gu, Seoul 07985, Korea
Tel: +82-2-2650-5574, Fax: +82-2-2650-3718, E-mail: pea8639@ewha.ac.kr

tal bleeding.

Developmental cysts can be classified according to their morphology and pathological features into sacrococcygeal teratomas, epidermoid cysts, dermoid cysts, enteric duplication cysts, gland cysts, anterior meningocele, and tailgut cysts.[1,2] Sacrococcygeal teratomas are the most common mass in newborns and consists of mixed elements of three germ cell layers, such as skin adnexa and neural elements. Epidermoid cysts are lined by a stratified squamous epithelium with lack smooth muscle fibers in the walls. In our study, skin appendages such as hair follicles and
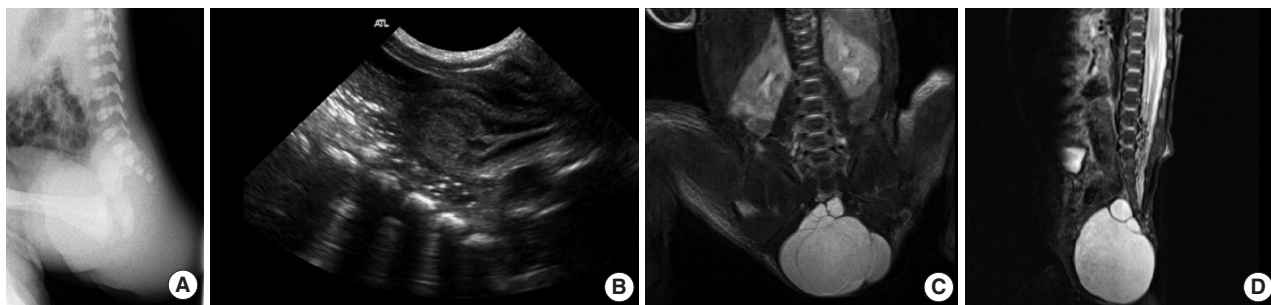
Fig. 1. Lumbosacral spinal X-ray shows a soft mass in the coccygeal area without calcification. (A) The cystic mass in the sacococcygeal area with intrapelvic and extrapelvic components (type II) is shown by abdominal sonography. (B) Sagittal magnetic resonance image shows a large cystic mass (6.2 × 4.2 × 5.6 cm) with a few small septae. This cystic mass is shown with low signal intensity in a T1W1 image and high signal intensity in a T2W1 image. (C, D) There are calcifications within the upper portion of the cystic mass with dark signal intensity.
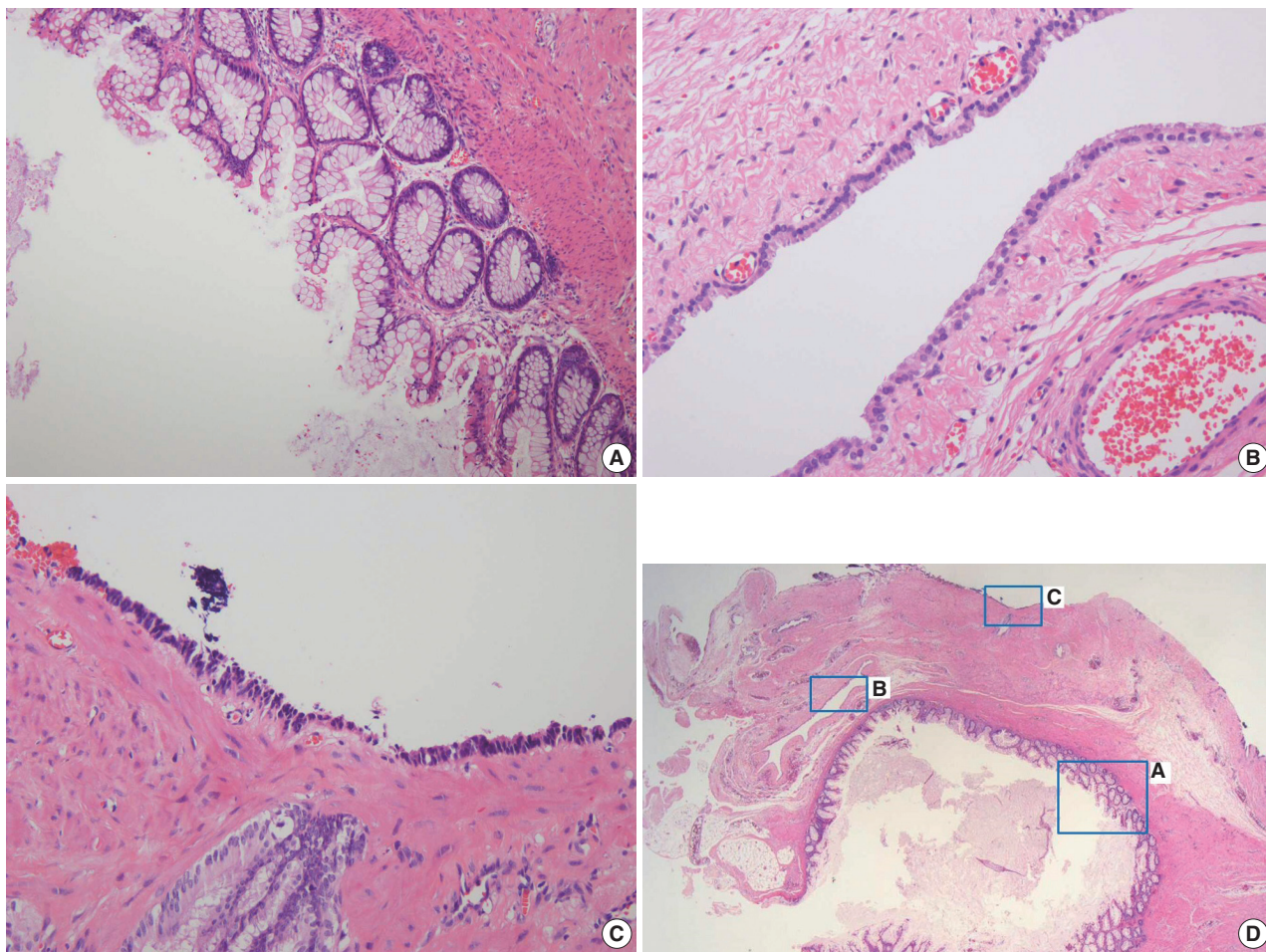
Fig. 2. On scanning view, different types of epithelia lining the cyst walls are identified (D). The cyst walls are lined by mucinous epithelium (A), low cuboidal epithelium (B), and pseudostratified columnar epithelium (C).

sweat glands were found, similar to dermoid cysts. Enteric duplication cysts are lined with intestinal epithelia with typical villi and crypts, and contain well-defined layers of smooth muscle and the myenteric plexus. Gland cysts can be differentiated through their lower region, usually closer to the anal sphincter rather than the retrorectal space. Anterior meningoceles are related to a sacral defect.[4]

The diameter of tailgut cysts varies from 1 to 22 cm, and they contain debris such as keratinous and mucinous material. According to Hjermstad and Helwig,[3] tailgut cysts are usually multiloculated and lined by squamous transitional and glandular epithelia. Squamous epithelium, present in 75% of cysts, is the most common type, and 50% of the cysts were covered with ciliated columnar epithelia. Some cysts also have a metaplastic process secondary to inflammation.[5] Malignant transformation is a rare complication of tailgut cysts. Only a few cases of adenocarcinomas, carcinoid tumors, neuroendocrine carcinomas, endometrioid carcinomas, adenosquamous carcinomas, squamous cell carcinomas and sarcomas have been reported.

To evaluate retrorectal masses, rectal examination, barium enema, transrectal sonography, computed tomography (CT), and MRI could be considered. Barium enemas and transrectal sonography are useful for initial viewing of the cystic nature of the masses. In particular, transrectal sonography demonstrates the unity of the layers of the rectum, whether cystic lesions are unilocular or multilocular, and also any internal echoes from mucoid materials or inflammatory debris. CT images of the tailgut cysts show well-defined, thin-walled, uni- or multilocular masses in the retrorectal region.[6] Calcification is not a characteristic of these cysts, and if present, should prompt consideration of malignancy. MRI is the best modality for imaging tailgut cysts because of its good soft tissue contrast and multiplanar imaging capability, which are useful for determining surgical techniques.

Entire surgical excision of tailgut cysts is strongly recommended because of the possibility of recurrence, infection, and local dissemination of malignant cells.[7] Various surgical approaches have been elaborated for removing tailgut cysts, including posterior, abdominal, and combined posterior and abdominal.[8] The best excisional approach is dependent on the size and location of the mass, possibility of infection, and adherence to the sacral or pelvic walls. Usually, the posterior approach is recommended for small benign tailgut cysts below the level of the S3 vertebrae. If the lowest level of the tailgut cyst is at the S4 vertebra, the mass should be approached through a transabdominal incision.

In conclusion, this rare case highlights that a tailgut cyst should be considered in the differential diagnosis of a sacrococcygeal mass in a neonate. Preoperative MRI is essential for planning the most appropriate surgical approach, and complete surgical excision is the treatment of choice for all tailgut cysts, as it provides definitive diagnosis, relieves symptoms, and prevents complications such as infection, fistula formation, and malignant degeneration.

Conflicts of Interest

No potential conflict of interest relevant to this article was reported.

REFERENCES

1. Prasad AR, Amin MB, Randolph TL, Lee CS, Ma CK. Retrorectal cystic hamartoma: report of 5 cases with malignancy arising in 2. Arch Pathol Lab Med 2000; 124: 725-9.

2. Al-Khuzaie J, Al-Hindi S, Hassan A, Al-Youssif R. Tailgut cyst in a newborn: report of a case and literature review. Bahrain Med Bull 2002; 24: 108-9.

3. Hjermstad BM, Helwig EB. Tailgut cysts: report of 53 cases. Am J Clin Pathol 1988; 89: 139-47.

4. Raisolsadat SM, Zabolinejad N, Tabrizian-Namini F, Faraji P. Tailgut cyst in an infant with imperforate anus: a case report. Iran J Pediatr 2013; 23: 597-600.

5. Mathieu A, Chamlou R, Le Moine F, Maris C, Van de Stadt J, Salmon I. Tailgut cyst associated with a carcinoid tumor: case report and review of the literature. Histol Histopathol 2005; 20: 1065-9.

6. Raje V, Raje V, Patil RK, et al. Tailgut cyst: a case report in a 9-month-old infant. Int J Surg Case Rep 2013; 4: 272-5.

7. Oh JT, Son SW, Kim MJ, Kim L, Kim H, Hwang EH. Tailgut cyst in a neonate. J Pediatr Surg 2000; 35: 1833-5.

8. Joyce EA, Kavanagh DO, Winter DC. A rare cause of low back pain: report of a tailgut cyst. Case Rep Med 2012; 2012: 623142.

Gastric Mixed Adenoneuroendocrine Carcinoma with Squamous Differentiation: A Case Report

Han-Ik Bae · Chaeyoon Lee[1] · Young-Min Jo · Ohkyung Kwon[1] · Wansik Yu[1] · Mee-Seon Kim[2] · An Na Seo

Department of Pathology, Kyungpook National University Hospital, Kyungpook National University Medical Center, Kyungpook National University School of Medicine, Daegu;
[1]Department of Surgery, Gastric Cancer Center, Kyungpook National University Medical Center, Kyungpook National University School of Medicine, Daegu;
[2]Department of Pathology, Samsung Changwon Hospital, Sungkyunkwan University School of Medicine, Changwon, Korea

The occurrence of gastric mixed adenoneuroendocrine carcinoma (MANEC) is relatively rare, although a few cells of gastric adenocarcinoma frequently show neuroendocrine differentiation.[1]

We herein present one of only a few reported cases of gastric MANEC with trilineage histologic differentiation, composed of adenocarcinoma, large cell neuroendocrine carcinoma (NEC), and squamous cell carcinoma (SqCC).

CASE REPORT

A 60-year-old woman presented with generalized weakness, anorexia, weight loss, and fasting epigastric pain over a 5-month period. The patient had suffered from allergic urticaria for several years, but this had been treated and subsequently controlled with standard medication. She denied any previous alcohol or herbal medication intake and had no significant family history. Esophagogastroduodenoscopy revealed an 8.5×7.0-cm-sized ulcerofungating mass in the anterior wall of the lower body. Biopsy of the mass was diagnosed as moderately differentiated adenocarcinoma. Preliminary laboratory test results were within normal limits, whereas a tumor marker level test revealed elevated carbohydrate antigen 19-9 (98.8 U/mL). Computed tomography demonstrated a large hypodense ulcerofungating mass in the gastric anterior wall along with multiple perigastric lymphadenopathies (Fig. 1A). The patient underwent D2 subtotal gastrectomy and early postoperative intraperitoneal chemotherapy. Gross examination of the resected stomach showed a smooth serosal surface and a large ulcerofungating mass measuring 8.5 $\times$ 7.0 cm, consistent with Borrmann type 2, in the lower anterior wall (Fig. 1B). On sectioning, the tumor had a heterogeneous appearance with a mixture of white and yellow lesions with infiltrative boundaries, invading to the serosal layer (Fig. 1C). Microscopically, the tumor comprised 55% large cell NEC, 35% moderately differentiated adenocarcinoma, and 10% well differentiated SqCC. The adenocarcinoma component was in the upper portion of the tumor, whereas the NEC component presented in the deep portion, with a small proportion in the upper portion, up to the mucosal layer (Fig. 1D). In particular, the collision between the adenocarcinoma and NEC components was found in the ulcerated tumor area (Fig. 2A). Additionally, transition from NEC to SqCC was found in some areas (Fig. 2C). As expected, immunohistochemical staining for synaptophysin and chromogranin A were positive in the NEC component but negative in the adenocarcinoma and SqCC components (Fig. 2B, D). The SqCC component but not the NEC or adenocarcinoma component revealed strong nuclear expression for p63 (Fig. 2E). The tumor mitotic count was 95 mitoses per 10 high-power fields, and the Ki-67 labeling index was 96%. The tumor penetrated the serosa, and 14 of the 48 regional lymph nodes showed metastasis, which, interestingly, was composed of only the adenocarcinoma component (Fig. 2F), but distant metastasis was not detected. Interestingly, for c-erbB2, the NEC com-

Corresponding Author
An Na Seo, MD, PhD
Department of Pathology, Kyungpook National University Hospital, Kyungpook National University Medical Center, Kyungpook National University School of Medicine, 807 Hoguk-ro, Buk-gu, Daegu 41404, Korea
Tel: +82-53-200-3403, Fax: +82-53-200-3399, E-mail: san_0729@naver.com

Mee-Seon Kim, MD
Department of Pathology, Samsung Changwon Hospital, Sungkyunkwan University School of Medicine, 158 Paryong-ro, Masanhoewon-gu, Changwon 51353, Korea
Tel: +82-55-290-1332, Fax: +82-55-290-6148, E-mail: kimm23@naver.com
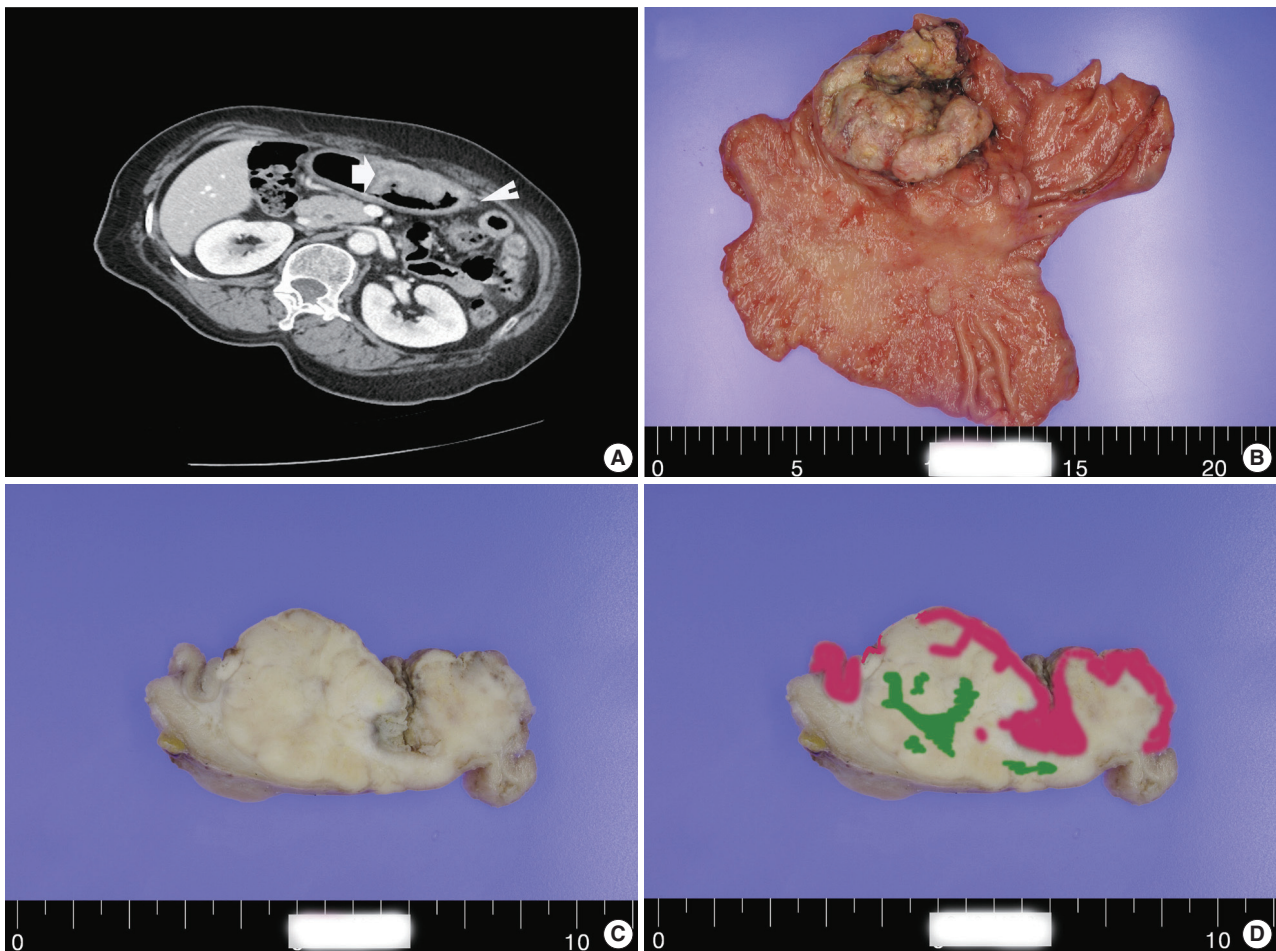
Fig. 1. (A) A computed tomography scan demonstrating a large ulcerofungating hypodense mass in the anterior gastric wall (arrow) and enlargement of multiple perigastric lymph nodes (arrowhead). Macroscopic findings (B) and cross-section of gastric cancer (C). (D) Mapping of the gastric mixed adenoneuroendocrine carcinoma with trilineage histologic differentiation composed of adenocarcinoma (pink color), large cell neuroendocrine carcinoma, and squamous cell carcinoma (green color).

ponent revealed negativity, whereas the adenocarcinoma component showed complete membranous staining of strong intensity in primary gastric cancer and in its corresponding metastatic regional lymph nodes (Fig. 3). During seven cycles of adjuvant chemotherapy, the patient experienced sudden abdominal pain due to mechanical obstruction by an adhesion at the operation site. Since then, she has stopped receiving chemotherapy and is currently receiving supportive care. The patient has been monitored for 18 months post-surgery and remains alive without evidence of disease recurrence.

The study was performed in accordance with the guidelines of the Institutional Review Board of Kyungpook National University Medical Center and was exempt from written informed consent. The information of this case was retrospectively obtained from medical records in the database of Kyungpook National University Medical Center.

DISCUSSION

Gastric MANECs are mixed exocrine and endocrine carcinomas, with one component exceeding at least 30% of the tumor lesion.[1,2] The exocrine component is characterized by adenocarcinoma with various differentiated grades, and the neuroendocrine component is usually represented by NEC.[1] To our knowledge, there have been only four reported cases of gastric MANEC containing a SqCC component.[3-5] Pericleous et al.[5] reported a case of MANEC with a SqCC component where only the NEC component metastasized to the liver. In addition, Shibuya et al.[4] reported a small cell undifferentiated carcinoma with adenocarcinoma and SqCC components, and hepatic nodules showed an atypical carcinoid component. In contrast, in the current case, only the adenocarcinoma component metastasized to the regional lymph nodes, with no distant metastasis detected.

The pathogenesis of gastric NEC is unclear. Based on the presence of NEC with other glandular or squamous cell components, the proposed origin of gastric MANEC is pluripotent stem cells that have the potential to differentiate into other cell types producing mucin or keratin.[6,7] Owing to the heterogeneous composition of MANEC, treatment approaches should focus on the
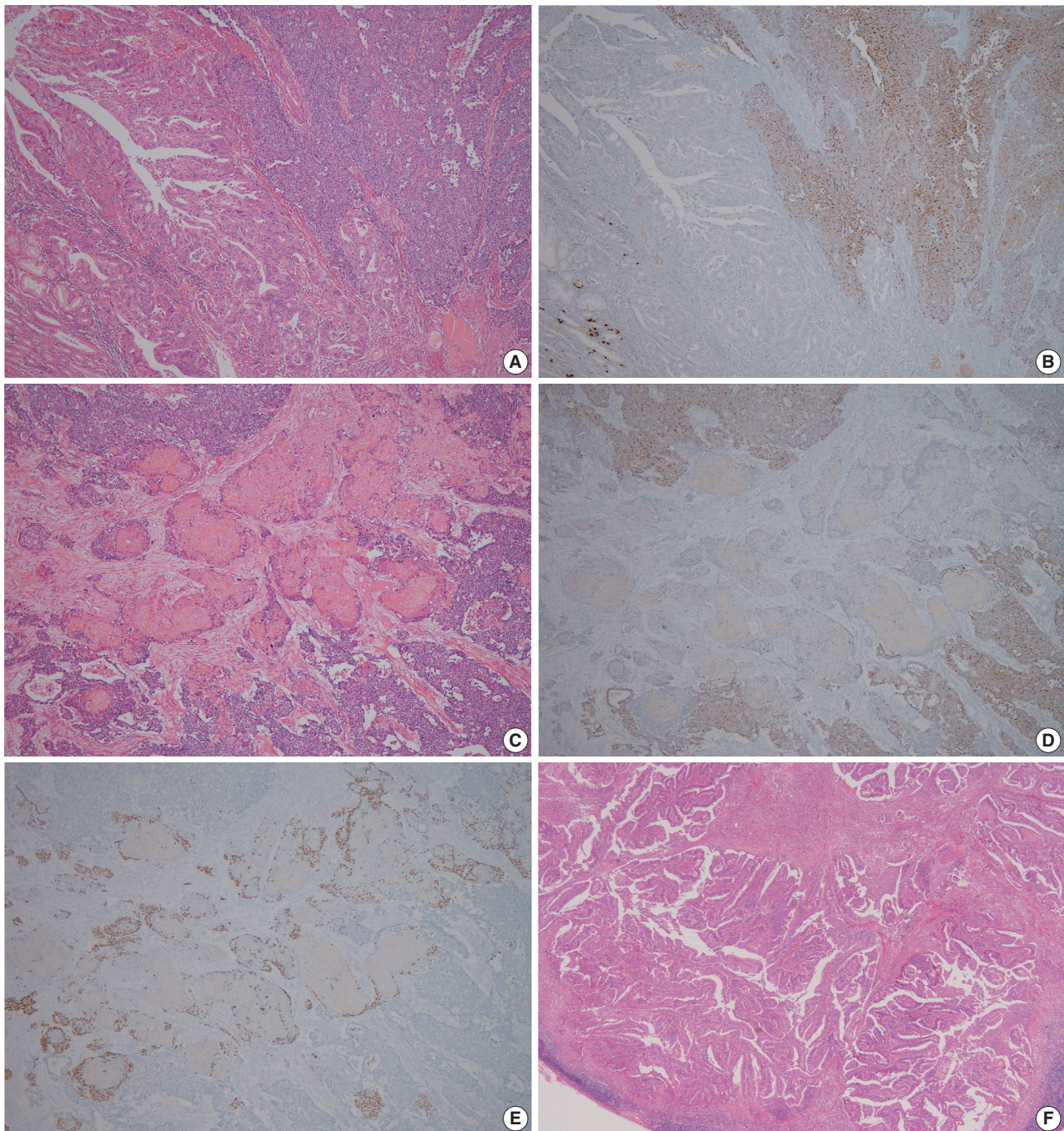
Fig. 2. Representative microscopic findings of mixed adenoneuroendocrine carcinoma with trilineage histologic differentiation. (A) Moderately differentiated adenocarcinoma admixed with large cell neuroendocrine carcinoma (NEC). (B) The NEC component demonstrates positive staining for chromogranin A, whereas the adenocarcinoma component shows negativity. (C) Squamous cell carcinoma (SqCC) component admixed with the NEC component, and (D) the NEC component presented positivity for chromogranin A, but not the SqCC component. (E) The cells with squamous cell differentiation are identified by expression of p63. (F) Metastasis of only the adenocarcinoma component to the gastric regional lymph nodes.
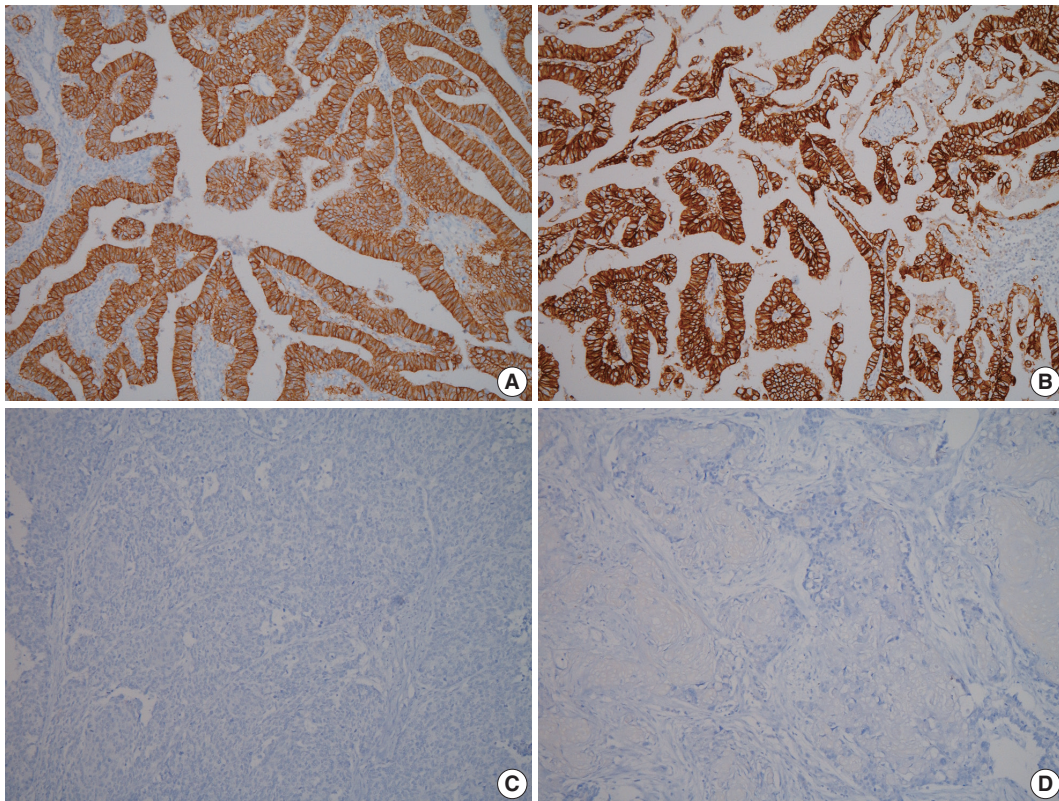
Fig. 3. Photomicrographs of immunohistochemistry (IHC) for c-erbB2 in mixed adenoneuroendocrine carcinoma with trilineage histologic differentiation. IHC for c-erbB2 shows strong positivity in the adenocarcinoma component (A), and in the metastatic regional lymph nodes (B), whereas IHC for c-erbB2 is negative in neuroendocrine carcinoma (C) and squamous cell carcinoma component (D).

most aggressive tumor components. However, the prognosis and behavior of gastric MANEC with trilineage histologic differentiation are unknown because of its rarity. Therefore, collaborative multicenter studies including such patients are required to determine optimal treatment regimens, prevent relapse, and improve prognosis.

Herein, we report a gastric MANEC with trilineage histologic differentiation including large cell NEC, adenocarcinoma, and SqCC, of which only the adenocarcinoma component metastasized to the regional lymph nodes, without distant metastasis.

Conflicts of Interest

No potential conflict of interest relevant to this article was reported.

REFERENCES

1. Bosman FT, Carneiro F, Hruban RH, Theise ND. WHO classification of tumours of the digestive system. 4th ed. Lyon: IARC Press, 2010.

2. Volante M, Rindi G, Papotti M. The grey zone between pure (neuro)endocrine and non-(neuro)endocrine tumours: a comment on concepts and classification of mixed exocrine-endocrine neoplasms. Virchows Arch 2006; 449: 499-506.

3. Haratake J, Horie A, Inoshita S. Gastric small cell carcinoma with squamous and neuroendocrine differentiation. Pathology 1992; 24: 116-20.

4. Shibuya H, Azumi N, Abe F. Gastric small-cell undifferentiated carcinoma with adeno and squamous cell carcinoma components. Acta Pathol Jpn 1985; 35: 473-80.

5. Pericleous M, Toumpanakis C, Lumgair H, *et al*. Gastric mixed adenoneuroendocrine carcinoma with a trilineage cell differentiation: case report and review of the literature. Case Rep Oncol 2012; 5: 313-9.

6. Bartley AN, Rashid A, Fournier KF, Abraham SC. Neuroendocrine and mucinous differentiation in signet ring cell carcinoma of the stomach: evidence for a common cell of origin in composite tumors. Hum Pathol 2011; 42: 1420-9.

7. Kim KM, Kim MJ, Cho BK, Choi SW, Rhyu MG. Genetic evidence for the multi-step progression of mixed glandular-neuroendocrine gastric carcinomas. Virchows Arch 2002; 440: 85-93.

Primary Cutaneous Adenoid Cystic Carcinoma Arising in Umbilicus

Seok Joo Lee · Woo Ick Yang · Sang Kyum Kim

Department of Pathology, Yonsei University College of Medicine, Seoul, Korea

Primary cutaneous adenoid cystic carcinoma (PCACC) is a rare adnexal tumor, first described by Boggio in 1975.[1] Fewer than 70 cases have been reported in the English literature. It has an indolent course and a high tendency to recur but manifests low potential for distant metastases.

Herein, we report a case of 66-year-old male who presented with a slow-growing erythematous lesion in the umbilicus. Upon histopathological examination, the tumor exhibited features of PCACC. The patient was treated with Mohs micrographic surgery. To our knowledge, this is the first reported case of a PCACC in the umbilicus. We discuss the clinicopathological characteristics of PCACC and include review of the literature.

CASE REPORT

A 66-year-old man with a medical history of congestive heart failure presented with a single, ill-defined, bean-sized erythematous lesion with tenderness in the umbilicus (Fig. 1A). Because the lesion had been nearly asymptomatic, except for mild tenderness, the patient had not sought a medical treatment. He eventually became concerned about the abnormal appearance of it and visited an outpatient clinic. An incisional biopsy was done and the patient was referred to our institution. Mohs micrographic surgery was performed. The cut surface of the specimen revealed a firm infiltrative mass involving dermis and subcutis (Fig. 1B). Hematoxylin and eosin stained slides were reviewed by three pathologists (S.K.K., S.J.L., and W.I.Y.). Microscopic examination revealed infiltrative nests and cords of basaloid tu-

Corresponding Author
Sang Kyum Kim, MD, PhD
Department of Pathology, Yonsei University College of Medicine, 50-1 Yonsei-ro,
Seodaemun-gu, Seoul 03722, Korea
Tel: +82-2-2228-6751, Fax: +82-2-2227-7939, E-mail: nicekyumi@yuhs.ac

mor cells with cribriform or tubular architecture in the dermis and subcutaneous tissue without connection to the epidermis (Fig. 2A). Abundant mucin was present and perineural invasion by the tumor cells was often observed (Fig. 2B, C). Based upon these histologic findings, primary or metastatic adenoid cystic carcinoma (ACC), adenoid cystic variant of basal cell carcinoma, and microcystic adnexal carcinoma entered in the differential diagnoses. Immunohistochemistry with antibodies against type III receptor tyrosine kinase KIT (CD117, catalog #A4502, Dako, Carpinteria, CA, USA) and epithelial membrane antigen (EMA; catalog #M0613, Dako) was performed with an automated immunohistochemical staining instrument (VentanaDiscovery XT, Ventana Medical System Inc., Oro Valley, AZ, USA). The tumor cells showed strong expressions of EMA (Fig. 3A) and KIT (Fig. 3B). The histological findings and immunohistochemical results indicated that the tumor was ACC. There was no other palpable mass on physical examination and there was no evidence of metastasis in the imaging study. Therefore, the tumor was diagnosed as a PCACC. The patient was discharged without complication. At postoperative follow-up after 6 months, he was healthy without evidence of local recurrence.

This retrospective study was approved by the Institutional Review Board of Yonsei University Medical Center (approval No. 4-2015-0695).

DISCUSSION

ACC is a rare type of cancer that usually occurs in the head and neck, particularly in the salivary glands. However, it may develop in any site where secretory glands are present. It has been reported in the breast, lacrimal gland, lung, brain, uterine cervix, trachea, paranasal sinus, and skin.[1] The etiology of PCACC is not entirely clear. However, the World Health Organization (WHO) recently concurred with the prevailing view that the

tumor originates from the apocrine glands. In the *WHO Classification of Skin Tumors*, ACC is classified as an adnexal neoplasm.[2]

Clinically, the tumor is a firm, poorly circumscribed, slowly growing nodule that is flesh-colored or red, and may or may not be accompanied by pain and tenderness.[3] Tumors that occur on the head and neck represent 46% of PCACCs and many of these are on the scalp. Of the remaining tumors that have been reported, 15% occur on the trunk, 17% on the upper limbs or in the area of the pectoral girdle, and 13% on the lower limbs or in the area of the pelvic girdle.[4] To our knowledge, this is the first reported case of a PCACC in the umbilicus.

For the diagnosis of PCACC, it is essential to rule out the possibility that the tumor has metastasized from elsewhere, particularly from the salivary glands. ACC of the salivary glands is aggressive and highly metastatic, with a high rate of local recurrence, while PCACC rarely metastasizes: metastases of PCACC
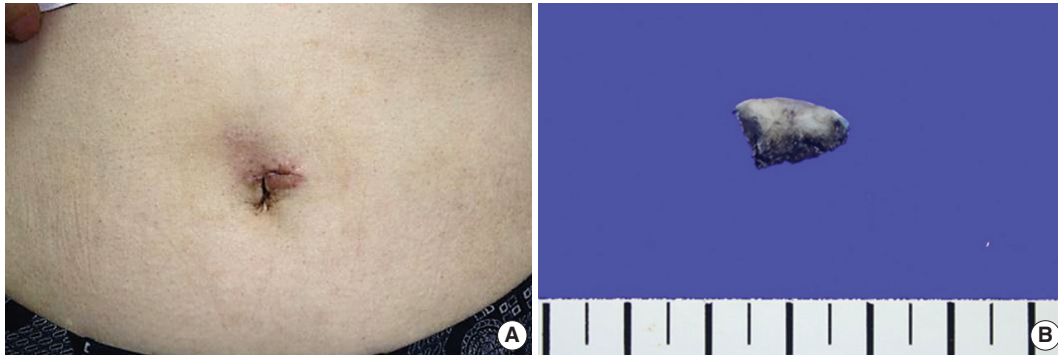
Fig. 1. Macroscopic findings of tumor arising in umbilicus. (A) An ill-defined bean-sized erythematous lesion on the umbilicus. (B) In sections of the specimen from the Mohs micrographic surgery, cut surfaces had an infiltrative firm mass.
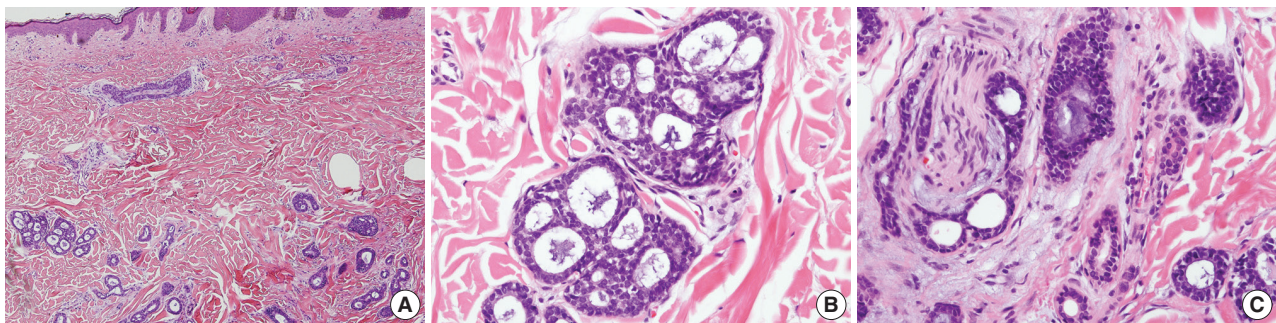
Fig. 2. Microscopic findings of primary cutaneous adenoid cystic carcinoma. (A) Images of basaloid cells that have infiltrated the dermis and the subcutaneous layer, but not the epidermis. Note the tumor cells' arrangement in nests and their cribriform pattern. (B) Images showing the cribriform and tubular growth patterns of the tumor, which also have a solid portion. (C) Perineural invasion by the tumor.
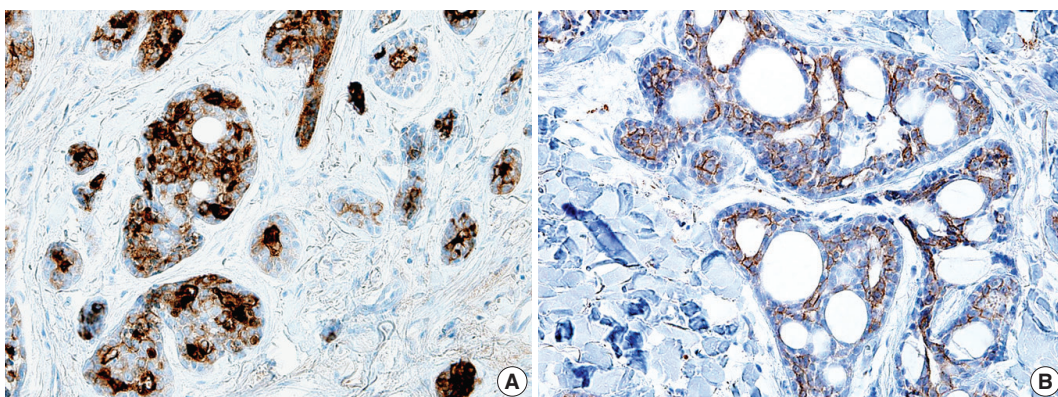
Fig. 3. Immunohistochemical staining results of primary cutaneous adenoid cystic carcinoma. Immunohistochemical staining images showing strong expression of epithelial membrane antigen (A) and KIT (B) in tumor cells.

to lymph nodes and the lungs have been reported in five and six cases, respectively.[3] In our case, there was no evidence of metastasis on chest computerized tomography scan.

Histologically, PCACC consists of basaloid cells arranged in a solid, tubular, or cribriform pattern. The tumor usually involves mid-to-reticular dermis, lying in a hyalinized fibrous stroma. It is usually not associated with the overlying epidermis and rarely invades underlying tissues. Cystic spaces are filled with mucin. The histologic findings of our case were compatible with these characteristics of PCACC.

It has been suggested that KIT (CD117) is a useful ancillary marker for ACC, distinguishing ACCs from other carcinomas with high sensitivity and specificity.[5-8] In our case, EMA and KIT were strongly immunoreactive in the tumor, thus rendering the diagnosis of ACC. In contrast, basal cell carcinoma does not express EMA,[5,9] and it shows palisading of the nuclei, stromal retraction, and continuity with the epidermis. These histological and immunohistochemical features were not detectable in our case, and thus we were able to rule out the possibility of basal cell carcinoma with features of adenoid cystic growth pattern.

The standard treatment of PCACC is a wide surgical excision with at least a 2 cm safety margin around the tumor, due to its frequent recurrence.[10] In recent years, several cases of PCACC have been treated with Mohs micrographic surgery.[9] The authors consider Mohs surgery to be superior to the traditional wide-excision method. However, considering the limited number of cases and follow-up period, we cannot make definitive conclusions at this point.

In summary, we described a rare adnexal tumor, a PCACC arising in the umbilicus. The PCACC is typical of its type, with features similar to other reported PCACCs. PCACCs are rare in general, regardless of their location, and this is the first reported case arising in the umbilicus. Medical caution with regards to the treatment options is required, as the recurrence rate of this tumor is not certain, and a long-term follow-up is warranted due to the possibly prolonged period before recurrence.

Conflicts of Interest

No potential conflict of interest relevant to this article was reported.

REFERENCES

1. Boggio R. Letter: adenoid cystic carcinoma of scalp. Arch Dermatol 1975; 111: 793-4.

2. Rocas D, Asvesti C, Tsega A, Katafygiotis P, Kanitakis J. Primary adenoid cystic carcinoma of the skin metastatic to the lymph nodes: immunohistochemical study of a new case and literature review. Am J Dermatopathol 2014; 36: 223-8.

3. Naylor E, Sarkar P, Perlis CS, Giri D, Gnepp DR, Robinson-Bostom L. Primary cutaneous adenoid cystic carcinoma. J Am Acad Dermatol 2008; 58: 636-41.

4. Ramakrishnan R, Chaudhry IH, Ramdial P, *et al*. Primary cutaneous adenoid cystic carcinoma: a clinicopathologic and immunohistochemical study of 27 cases. Am J Surg Pathol 2013; 37: 1603-11.

5. Holst VA, Marshall CE, Moskaluk CA, Frierson HF Jr. KIT protein expression and analysis of c-kit gene mutation in adenoid cystic carcinoma. Mod Pathol 1999; 12: 956-60.

6. Jeng YM, Lin CY, Hsu HC. Expression of the c-kit protein is associated with certain subtypes of salivary gland carcinoma. Cancer Lett 2000; 154: 107-11.

7. Penner CR, Folpe AL, Budnick SD. C-kit expression distinguishes salivary gland adenoid cystic carcinoma from polymorphous low-grade adenocarcinoma. Mod Pathol 2002; 15: 687-91.

8. Mino M, Pilch BZ, Faquin WC. Expression of KIT (CD117) in neoplasms of the head and neck: an ancillary marker for adenoid cystic carcinoma. Mod Pathol 2003; 16: 1224-31.

9. Xu YG, Hinshaw M, Longley BJ, Ilyas H, Snow SN. Cutaneous adenoid cystic carcinoma with perineural invasion treated by mohs micrographic surgery-a case report with literature review. J Oncol 2010; 2010: 469049.

10. van der Kwast TH, Vuzevski VD, Ramaekers F, Bousema MT, Van Joost T. Primary cutaneous adenoid cystic carcinoma: case report, immunohistochemistry, and review of the literature. Br J Dermatol 1988; 118: 567-77.

Notice of Retraction: Therapeutic Effects of Umbilical Cord Blood Derived Mesenchymal Stem Cell-Conditioned Medium on Pulmonary Arterial Hypertension in Rats

Jae Chul Lee[1,2,3] · Choong Ik Cha[3] · Dong-Sik Kim[2] · Soo Young Choe[1]

[1]Department of Biology, School of Life Sciences, Chungbuk National University, Cheongju;
[2]Department of Surgery, Brain Korea 21 PLUS Project for Medical Sciences and HBP Surgery and Liver Transplantation, Korea University College of Medicine, Seoul;
[3]Department of Anatomy, Seoul National University College of Medicine, Seoul, Korea

J Pathol Transl Med 2015; 49(6): 472-480. http://dx.doi.org/10.4132/jptm.2015.09.11

Editors, Journal of Pathology and Translational Medicine

Several issues related to the authorship, research materials, and protocols have been raised with the above article published in the Journal of Pathology and Translational Medicine (2015; 49: 472-80).[1] The first author of the article has duely admitted that he is mainly responsible for the misconduct. Thus, the editors and publication board of the JPTM have decided to retract the article.

REFERENCE

1. Lee JC, Cha CI, Kim DS, Choe SY. Therapeutic effects of umbilical cord blood derived mesenchymal stem cell-conditioned medium on pulmonary arterial hypertension in rats. J Pathol Transl Med 2015; 49: 472-80.